ION TRANSPORT MECHANISMS OF BOLA-AMPHIPHILES IN PLANAR BILAYER MEMBRANES

by

Daniela Loock
Dipl.-Ing.Technische Hochschule Darmstdt, 1993

A Dissertation Submitted in Partial Fulfillment of the
Requirements for the Degree of

DOCTOR OF PHILOSOPHY

in the Department of Chemistry

We accept this thesis as conforming
to the required standard

[redacted]

Dr. T. M. Fyles, Supervisor (Department of Chemistry)

[redacted]

Dr. C. Bohne, Departmental Member (Department of Chemistry)

[redacted]

Dr. D. A. Harrington, Departmental Member (Department of Chemistry)

[redacted]

Dr. C. J. Pritchet, Outside Member (Department of Physics and Astronomy)

[redacted]

Dr. G. W. Gokel, External Examiner (Washington University School of Medicine)

© DANIELA LOOCK, 1997
University of Victoria

All rights reserved. Dissertation may not be reproduced in whole or in part, by photocopying or other means, without the permission of the author.

Supervisor: Dr. Thomas M. Fyles

ABSTRACT

The bilayer clamp technique was used as an investigative tool to explore the ion transport activity of bola-amphiphiles across planar lipid bilayers. It was demonstrated that 'small' synthetic molecules can transport ions across lipid bilayer membranes with mechanisms that have not been reported for natural protein ion channels. In addition to the step conductance changes that are typical for natural ion transporters a variety of signal shapes were observed. The overall transport behaviour could be controlled by influencing specific steps in the mechanism *via* small structural alterations of the bola-amphiphiles. This approach was analogous to the introduction of point mutations in proteins.

Transporter aggregates were assumed as the ion conducting structure of most bola-amphiphiles investigated. It has been demonstrated that controlling the forces that lead to the stabilization and destabilization of aggregates will lead to control of the observed transport mechanism which was reflected in the signal shapes observed. Head group repulsion, the hydrophilic/hydrophobic balance in the wall units, and the flexibility of the molecule offer possibilities for the regulation of ion transport.

Charge selectivity could be controlled *via* the introduction of charged head groups and *via* the degree of hydration of the wall units. 'Dryer' pores led to perfect cation:anion selectivity which in turn gave rise to an unusual signal shape. The development of a local Donnan-potential was invoked in the transport mechanism of these bola-amphiphiles.

Rectifying current-voltage responses were achieved by the introduction of asymmetry into the mechanism. Two different classes of transporters displayed voltage-gated behaviour in planar bilayer membranes. In one case the asymmetry was introduced

into the structure of the bola-amphiphile itself. In a second case the unequal distribution of symmetric transporter molecules in the two bilayer leaflets led to the observed non-ohmic current-voltage relationship.

The activity of eleven transporter molecules was studied in planar lipid bilayers and was compared to results previously obtained for these compounds in vesicles. In some cases different conclusions were reached from the two experiments.

Examiners:

[redacted]

Dr. T. M. Fyles, Supervisor (Department of Chemistry)

[redacted]

Dr. C. Bohne, Departmental Member (Department of Chemistry)

[redacted]

Dr. D. A. Harrington, Departmental Member (Department of Chemistry)

[redacted]

Dr. C. J. Pritchet, Outside Member (Department of Physics and Astronomy)

[redacted]

Dr. G. W. Gokel, External Examiner (Washington University School of Medicine)

Table of Contents

List of Tables

List of Figures

List of Abbreviations

A/D	analog to digital
ASP	analog signal processing device
CAChe	computer aided chemistry
CF	5[6]-carboxyfluorescein
Chol	cholesterol
diPhyPC	diphytanoyl phosphatidiylcholine
DMA	direct memory access
egg-PA	egg phosphatidic acid
FCCP	carbonyl cyanide 4-(trifluoromethoxy)phenylhydrazone
FET	field-effect transistor
MES	4-morpholine ethane sulfonic acid
NMR	nuclear magnetic resonance
THF	tetrahydrofuran
VB	visual basic

Acknowledgements

Many people contributed to this dissertation. I am especially grateful to

• my supervisor Dr. Tom Fyles for his continuous interest and advice, many discussions, his support and encouragement.

• All the people in our group who went through the feat of actually synthesizing all the compounds I studied and without whom this dissertation would not have been possible. Many thanks to the two persons who experienced the joys of 8Trg: Xin Zhou for the great collaboration, many stimulating discussions, his vesicle work, and sharing some of his data with me. Pedro Montaya-Pelaez for re-synthesizing the unimolecular ion transporter, his inquisitive mind, and his very special sense of humour. Thanks to Binqi Zeng for synthesizing the bis-crown ethers.

• David Robertson for writing the 'ai' program and teaching me about programming

• Dr. David Harrington for introducing me to the art of electronics and for his help during the creation of the analog signal processor.

• Wilma Nijenhuis for getting me started on the bilayer clamp technique, sharing some of her data with me, and her encouragement.

• Terry Davies, Bob Dean, and Terry Wiley for their excellent technical assistance over the past years and their patience while I was building the analog signal processor.

• Dr. George Gokel for generously sharing information prior to publication.

• Lynn Cameron, Blair King, David Lycon, Mark Pawluk, and Chiwei Hu for discussions and the friendly atmosphere they created in the lab.

• Dr. Cornelia Bohne for her interest, instructive discussions, advice, and for her thoughtfulness when it came to not banging the door while I was doing experiments.

• The staff of the Department of Chemistry and Fellow Graduate students who created a wonderful workplace.

• Last but not least my husband Hans-Peter Loock for proofreading this dissertation, his patience, support, interest, and countless discussions.

1. Introduction

Biological membranes are life's boundary. These sheetlike structures, only a few molecules thick consist mainly of proteins and lipids and are held together by noncovalent forces. Plasma membranes give cells their individuality by separating them from their surroundings. While the lipids serve as a permeability barrier for ions and most polar molecules, it is the proteins that mediate the distinctive functions of the membrane. Natural ion channels, one class of membrane proteins, are large protein aggregates that contain multiple transmembrane segments which act in concert to regulate the cell volume and maintain the intracellular pH and ion composition within a narrow range. They extract and concentrate metabolic fuels and building blocks from the environment, and generate ionic gradients that are essential for the excitability of nerve and muscle.[1] The investigation of ion channels is aggravated by the fact that the activity of these proteins can only be expressed in a membrane. To date, the crystal structure of very few transmembrane proteins has been determined[2-5] but structural information is slowly evolving from molecular biology.[6-8]

However, the Nobel-Prize-winning patch clamp technique allows the measurement of electric currents arising from the ionic fluxes due to the activity of a single channel molecule.[9] A thin glass pipette of appropriate dimensions is tightly sealed against a cell membrane and thereby isolates a small patch of the membrane. The ion channels contained in this patch can then be chemically or electrically manipulated and their properties deduced.[9] All natural ion channels display discrete conductance changes in the current-time records obtained by the patch clamp technique. Thus, the proteins seem to alter between two defined states, a closed state with no current flow, and an open state during which ions flow from one side of the membrane to the other.[1,9,10] Since natural ion channel proteins are difficult to isolate and handle due to their limited quantities and their association with the membrane, abundant and naturally occurring peptides have been employed as simple model systems for these proteins.[11,12] The development of small,

chemically defined systems for the study of ion selectivity, and the role of the electric field in triggering changes in the ion conduction have also been motivations for the investigation of these peptides. While the channel forming ability of peptides has been studied for almost 30 years[9,11,13,14] it is only for the last 15 years that chemists have tried to mimic the ion transport *function* by artificial molecules.[15,16] In the following paragraphs examples of both naturally occurring peptides and artificial ion channels will be presented. Two well defined synthetic membrane systems, lipid vesicles and planar bilayers, are generally employed to evaluate the ion transport function of these molecules.

Lipid vesicles are aqueous compartments enclosed by a bilayer. They can have diameters of 0.3-1 μm and are nearly spherical in shape. Thus, the membranes are curved and the lipid packing density varies between the two bilayer leaflets. Ions or molecules can be trapped in the aqueous compartment by forming the vesicles in the presence of these substances. The activity of ion transporters can then be followed by the collapse of gradients that were imposed across the membrane, the release of dyes, or the exchange of labeled substances under equilibrium conditions, to name only a few possibilities. Thus, the average behaviour of a large number of molecules is observed and the transport mechanism is generally inferred by comparison with known ion channels.[17]

Planar bilayer membranes are well suited for electrical studies because in principle the activity of a single transporter molecule can be observed and access to both sides of the membrane is possible. These membranes can be formed across holes of 0.25-1 mm diameter in a partition between two aqueous compartments. The electrical conduction properties of single ion channels can be studied by inserting electrodes into the aqueous compartments. With this technique the ion translocation step can be observed directly and ion channels can be easily identified.[1]

1.1 Peptide models

1.1.2 Naturally occurring peptides

Two of the most studied, naturally occurring peptide models for ion channels are gramicidin and alamethicin. Both peptides display behaviour characteristic for ion channels such as ion selectivity, voltage dependence, subconductance states and blocking of the channel pore.[18,19]

Gramicidin is a hydrophobic peptide antibiotic produced by *Bacillus brevis*, that consists of 15 alternating L- and D-amino acid residues and occurs as a mixture of gramicidin A, B, and C. The primary sequence of gramicidin A, which constitutes 80 % of the mixture, is shown as part of Figure 1.1. Gramicidin B and C are natural sequence variants with substitution at position 11.[18] A large body of evidence indicates that gramicidin forms a head-to-head single-helix dimer in the membrane.[18]

(HCO)HN-L-Val-Gly-L-Ala-D-Leu-
L-Ala-D-Val-L-Val-D-Val-L-Trp-D-Leu-
L-Trp-D-Leu-L-Trp-D-Leu-L-Trp-
$CO(NHCH_2CH_2OH)$

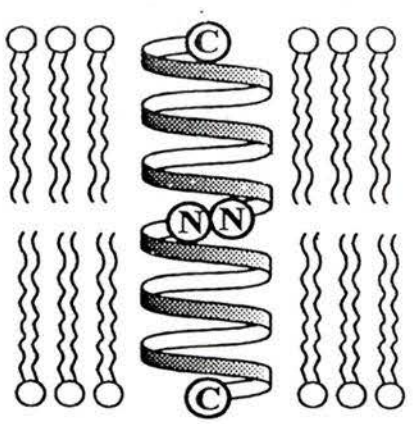

Figure 1.1: Gramicidin A

Each gramicidin monomer adopts a β-helical conformation that spans about half a bilayer and contains a central cavity of about 4 Å diameter. This aqueous pore is lined by the peptide backbone while the side-chains are on the outside of the helix in contact with

the lipid environment. Dimerization of monomers from each bilayer leaflet was proposed to result in an active channel structure.[18] Mean channel lifetimes of seconds have been observed which presumably reflects the high activation energy involved in breaking the six hydrogen bonds that hold the N-termini together.[18] Gramicidin channels are impermeable to anions and divalent cations and show alkali cation selectivity in the order $Cs^+ > Rb^+ > K^+ > Na^+ > Li^+$.[20,21] This Eisenmann I sequence indicates that the cation selectivity is mainly determined by ion dehydration energies.[22] Divalent cations such as Ca^{2+} or Ba^{2+} block the gramicidin channel which is reflected in lower specific single channel conductances in the presence of these ions.[13] Despite the fact that the side-chains of gramicidin are not in contact with the permeating ions, their modification can alter the conductance properties of the channel.[18] The changes in channel properties can be due to conformational or electrostatic effects and experiments have been performed to investigate and distinguish both possibilities.[23,24] More recently, the interest has shifted to changing the amino acid sequence in order to obtain new functional properties.[25] Regulatory elements have been introduced at the C-terminus of gramicidin monomers which lead to reversible blocking of the channel either *via* thermal isomerization of the carbamate bond[26,27] or *via* photoisomerization of an attached azobenzene moiety.[28]

The voltage-gated channel-forming peptide alamethicin is produced by the fungus *Trichoderma viride*. It is a member of a class of peptaibol channel forming *pep*tides that are rich in the helix-promoting α-amino isobutyric acid (*Aib*) and are usually terminated in an alcoh*ol*.[19] The amino acid sequence of alamethicin is shown below:

Ac-Aib-Pro-Aib-Ala-Aib-Ala-Gln-Aib-Val-Aib-Gly-Leu-Aib-Pro-Val-Aib-Aib-Gln-Gln-Pheol

Alamethicin assumes a predominantly α-helical structure in the membrane where the helices can adopt a transmembrane conformation.[18,19,29] The helix is laterally amphipathic where one face is more hydrophobic than the other.[19] Ion-conducting channels are assumed to be composed of a bundle of helices that surround an aqueous

pore (barrel-stave model).[18,19,29] The size of the pore formed from this type of aggregate increases with the number of monomers in the aggregate. Single-channel measurements of alamethicin show bursts of channel activity where each burst contains five or more well defined step conductance changes. These conductance states are not integral multiples of each other which supports the barrel-stave model.[18,19] Macroscopic currents induced by high concentrations of alamethicin are rectifying. The conductance increases *e*-fold for every 4-5 mV increase in voltage.[18] Greater currents are observed when the side of alamethicin addition is held at positive potentials. The transmembrane segments of the voltage-gated ion channels of excitable membranes are assumed to be α-helices where five or seven of these helices form the aqueous channel.[10] Thus, its rectifying behaviour made alamethicin an attractive model for these channels.[29] Several models for the voltage-dependent mechanism of alamethicin have been proposed all of which involve the interaction of a helix dipole with the membrane electric field.[19,29] However, the mechanism has not been resolved yet.

1.1.2 Synthetic peptides

Two examples for the use of synthetic peptides as models for ion channels should be mentioned here. Montal and coworkers[30,31] designed synthetic peptide sequences that correspond to the putative pore-lining or voltage-sensing segments of natural proteins. This allowed the investigation of structure-function relationships of these segments in the absence of the rest of the protein.[32] A different approach was taken by DeGrado and coworkers who designed and studied simple peptides that do not directly resemble natural sequences but incorporate features believed to be essential for ion transport.[12] These α-helical peptides consist of 21 amino acid residues and are rich in serine and leucine. The transport and aggregation behaviour of these transporters has been studied extensively.[12,33-35] Planar bilayer studies revealed discrete conductance states, ion selectivity and voltage-dependent gating behaviour for these peptides.[12] Modification of

the peptides allows the investigation of the effect of specific residues on the ion transport behaviour.[34]

1.2 Polyene antibiotics: Amphotericin B

The first non-peptide ion channel model used was amphotericin B.[36] It is a polyene macrolide antibiotic produced by *Streptomyces* species, a group of gram-positive bacteria. Amphotericin B consists of a large lactone ring containing a rigid, hydrophobic heptaene unit and a more flexible hydrophilic polyol region. In aqueous solutions the structure is zwitterionic due to the presence of a mycosamine residue and a carboxylate group at one end of the molecule. The overall length of the molecule is about 25 Å, nearly half the thickness of the bilayer. The mode of action of these antibiotics has been investigated using a variety of model bilayer membranes. Depending on the model system used, however, seemingly contradictory results have been obtained. It now seems to be accepted that there is not only one mechanism present but several ones.[36] Based on bilayer clamp experiments the formation of a barrel-like structure, comprised of 8 to 12 amphotericin B monomers, has been proposed.[37] The barrel would be lined by the hydrophilic polyol segments while the more hydrophobic heptaene units would interact with the lipid environment. In contrast to alamethicin the number of monomers in the barrel seems to be constant, yielding pores with defined diameter.[36,37]

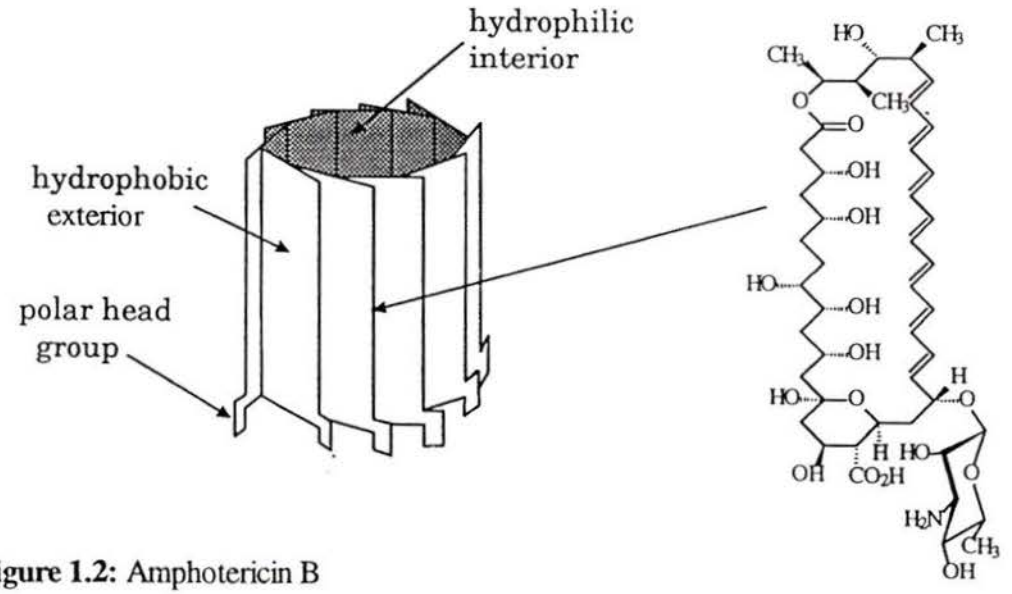

Figure 1.2: Amphotericin B

Dimeric pores that are formed from two barrels have also been shown.[36,38] Interestingly, the 'monomeric' pore is cation selective while the channel formed from two barrels is anion selective.[37,39] Pore-formation seems to be also dependent on the sterol content of the cellular membrane, which seems to be responsible for the antibiotic's specificity towards fungal membranes.[36] The active structures of amphotericin B are intimately related to the properties of the bilayer membrane with which it interacts. However, the actual structure of the different pores is still unknown. Amphotericin B has proven an instructive case for the complexity of the process investigated. Nevertheless, it demonstrated the basic requirements that non-peptide-based ion transporters need to fulfill in order to mimic the function of natural ion channels.

1.3 Ion transport by non-peptidic ion channels

Ion transport across bilayer membranes can occur by different mechanisms as depicted in Figure 1.3. Valinomycin[40] is a typical natural example for an ion carrier where a transporter-ion complex is formed at one membrane interface and the whole complex diffuses through the membrane and releases the ion at the opposite interface. On the other end, detergents or certain toxins such as melittin[41] induce temporary defects in the bilayer that allow ions to cross the membrane. These defects are generally not well structured and of short duration. An ion channel provides a membrane-spanning molecular structure that facilitates ion translocation along or through the transporter.[15] This structure can be either a long tubular or helical structure, as exemplified by gramicidin, or it can be an aqueous pore that is formed by the aggregation of several amphiphilic monomers such as alamethicin or amphotericin B.

Some general criteria for the design of pores and channels emerged from studies on the peptides mentioned in the previous paragraphs. A membrane-spanning structure is required which can be achieved by a single molecule or by end-to-end interactions between subunits. The overall structure has to be amphiphilic to orient and anchor the transporter in the membrane. A roughly columnar shape to facilitate insertion into the bilayer was required in addition to an inward-facing functionality for ion stabilization.[15]

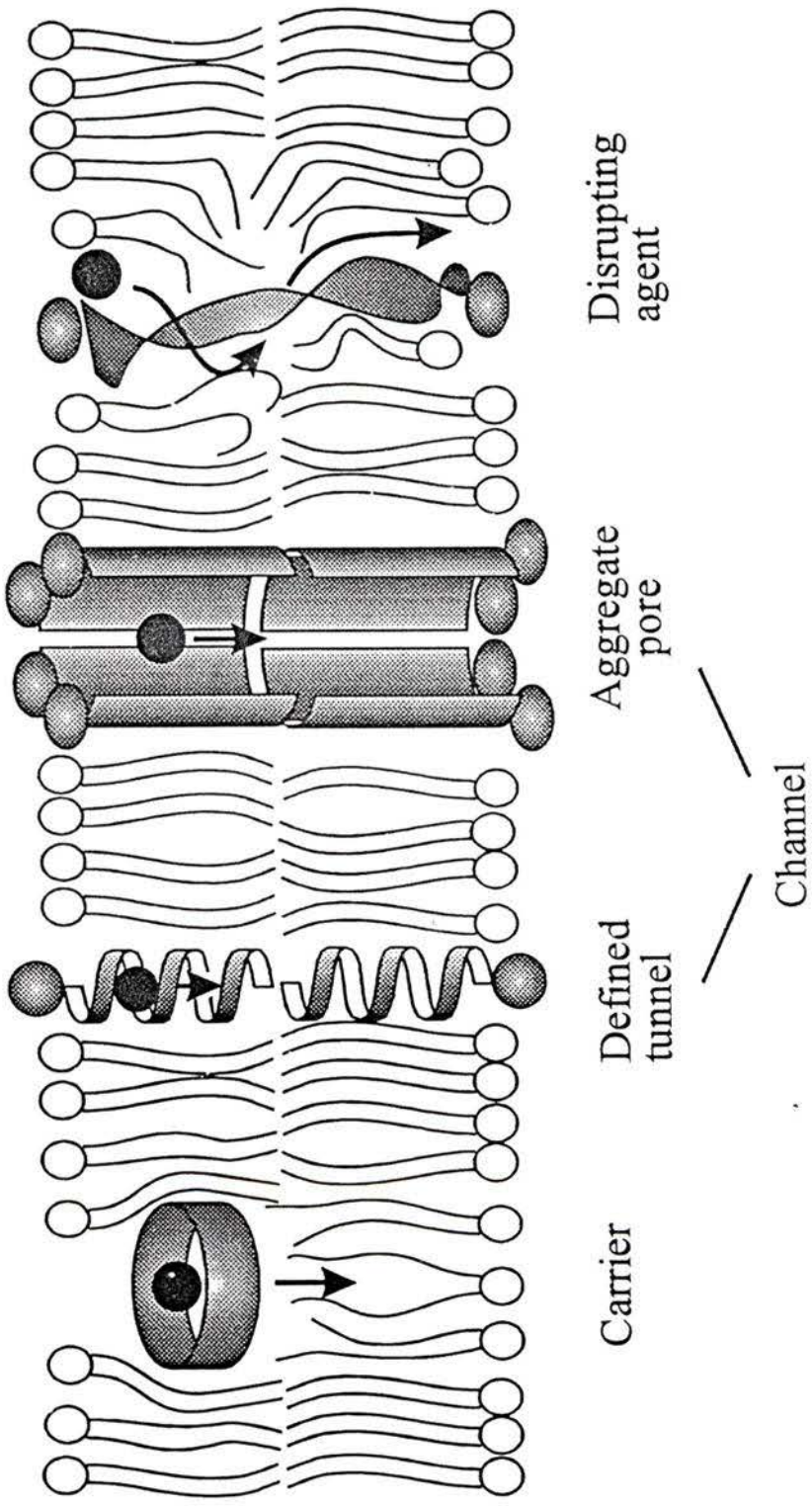

Figure 1.3: Schematic mechanisms for ion transport

Over the past 15 years many groups have explored these design principles and synthesized a variety of different ion transporters. The transport behaviour of all systems has been evaluated by vesicle experiments. However, the ion transport mechanism has to be inferred from comparison to known ion channels and cannot be determined directly. Therefore only the compounds that have been characterized by the bilayer clamp technique will be described in detail, as their behaviour can be directly related to the studies presented in this thesis. The other systems will only be briefly mentioned in the following paragraph.

1.3.1 Artificial ion channels

The earliest work was described by Tabushi and co-workers.[40] Their system used β-cyclodextrin as the backbone of the target to which four hydrophobic chains were attached to anchor the amphiphile in the membrane. The ion-conducting structure was proposed to be a dimeric transporter. Lehn and coworkers[42,43] reported the synthesis and activity of 'bouquet' molecules. Poly(ethyleneoxide) or polyalkyl chains were attached to a central 18-crown-6 or a cyclodextrin derivative. A unimolecular structure was proposed as the active channel. Two series of compounds were synthesized by Regen and co-workers. Double-headed single-chain surfactants based on a homologous series of linear saturated, olefinic, and acetylenic α,ω-dicarboxylic acids fused to hexaethylene glycol had membrane-disrupting properties.[44] A second transporter was designed to mimic the activity of amphotericin B. This sterol-polyether conjugate was shown to induce ion permeation *via* the formation of aggregates in vesicle membranes.[45]

1.3.2 Artificial ion channels characterized in planar bilayer membranes

Kobuke and co-workers reported two different ion channel systems. Condensation of resorcinol with octadecanal afforded an amphiphilic cyclic tetramer shown in Figure 1.4.[46] Only one type of step conductance change was observed after incorporation of the transporter into planar bilayers, suggesting a well-defined aqueous pore. The channel favored potassium over sodium ions and could be blocked by rubidium ions. A dimer was proposed as the ion conducting structure.

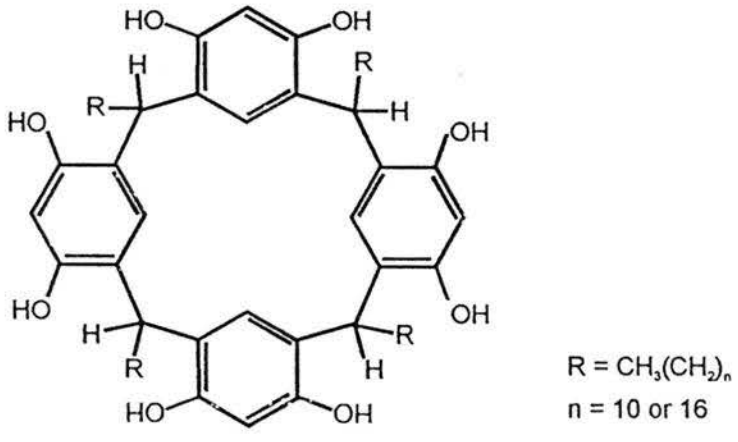

Figure 1.4: Calixarene ion channel

Another system synthesized by this group and shown in Figure 1.5 consists of an oligoether amphiphile that was terminated either in a carboxylate[47] or in a phosphate group.[48] This amphiphile was combined with mono- or dioctadecylammonium cations yielding an ion pair that resembled a lipid molecule. Both types of amphiphiles exhibited properties characteristic for single ion channels. Step conductance changes induced by these molecules varied in amplitude between experiments, indicating the formation of aggregates. While the current-voltage relationship of the step conductance changes was ohmic, the open probability of the channels induced by the phosphate-terminated amphiphile was dependent on the applied transmembrane potential. The sign of this voltage dependence was variable between experiments. The channels were selectively permeable to cations but showed no discrimination between monovalent cations. The open-closed transition might be explained by the association-dissociation of the half-channels on opposite sides of the membrane.

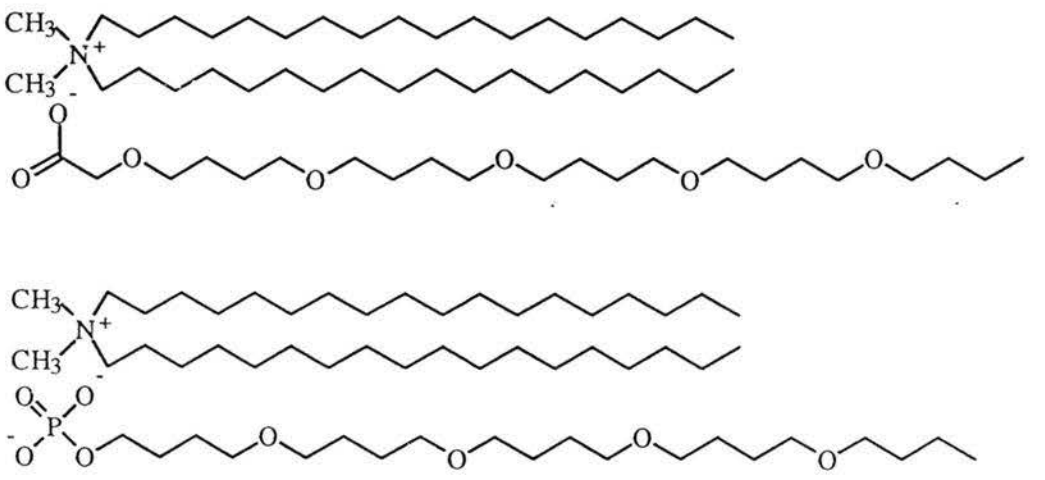

Figure 1.5: Ion pair system synthesized by Kobuke *et al.*[47,48]

Seebach *et al.* reported the synthesis of monodisperse poly[(R)-3-hydroxybutanoates] of the general formula X-[OOC-CH_2-$CHCH_3$]$_n$-O-Y.[49] These polymers occur ubiquitously in procaryotic and eucaryotic cells in a polydisperse form. Of the synthetic molecules, polymers with $n \geq 16$ and X and Y = H, induced step conductance changes in planar bilayer membranes when combined with calcium polyphosphate. The observed specific conductances were variable between experiments for the same molecule and between different polyesters, indicating that aggregates are responsible for the observed activity. The formation of 'islands' of polymer within the lipid membrane was proposed. The observed current fluctuations would then be due to defects induced at the interfacial region between these islands and the bilayer. This work suggested a new role for these polymers as channels for the uptake of Ca^{2+}, polyphosphate, or even DNA by cells.

Voyer and co-workers[50,51] synthesized a 21-amino acid peptide bearing six 21-crown-7 moieties. Conformational studies revealed that the peptide preferentially occurs in an α-helical structure with all crown ether units aligned on one side of the helix. The transporter showed poor partitioning to the bilayer, probably due to its high tendency to self-aggregate in aqueous solution. Once incorporated however, discrete step conductance changes were observed. Vesicle experiments revealed a lack of cation selectivity.

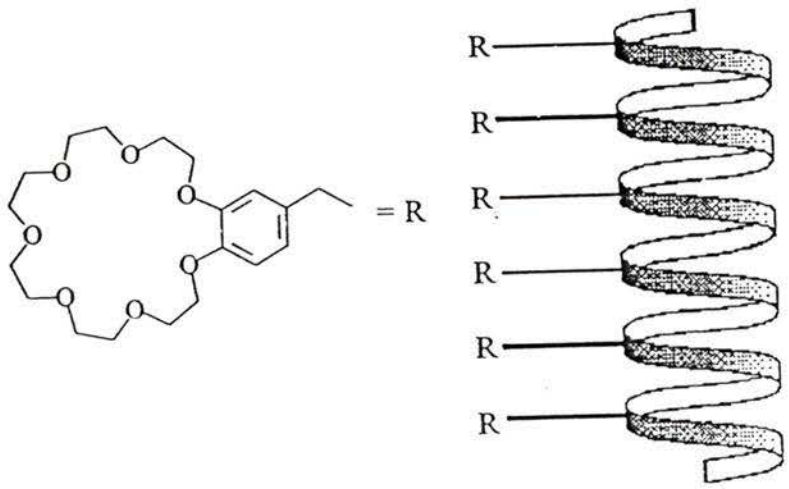

Figure 1.6: Crown ether derivatized peptide synthesized by Voyer *et al.*[50,51]

Oligo(tetrahydrofuran)-peptides have been synthesized and characterized by Wagner *et al.*.[52] The compound with ten ter-(THF)amino acid units induced an increase in the conductance of the bilayer membrane. Instead of step-conductance changes current peaks of varying intensity and milliseconds duration were reported. This transport behaviour is indicative of defects rather than well defined channels. Interestingly, while the N-protected decapeptide showed voltage-symmetric increases in conductance, deprotection led to smaller current peaks when the side of addition was held at negative potentials than at positive potentials.

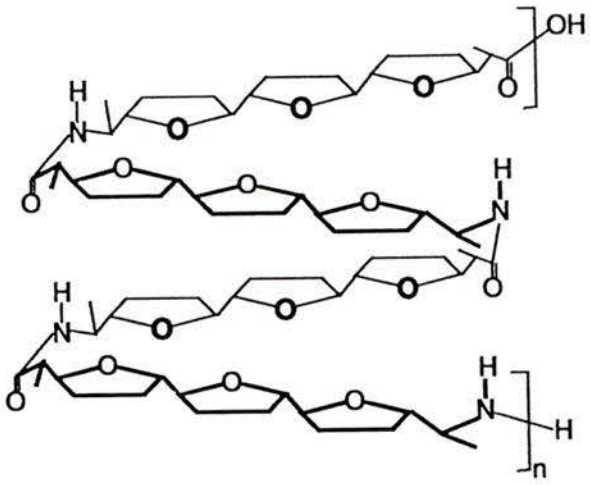

Figure 1.7: Schematic illustration of an oligo(tetrahydrofuran)-peptide

Ghadiri *et al.* reported the synthesis of peptide nanotubes.[53] These tubular structures that encircle an aqueous pore of about 7.5 Å were made up of stacks of 8 to 10 cyclic peptides held together by hydrogen bonds. Even numbers of alternating L- and D-amino acid residues in a cyclic peptide can adopt a flat ring conformation where the side-chains are directed away from the center. The driving forces for aggregation in the bilayer are the formation of multiple intermolecular hydrogen bonds and the interaction between the side chains and the lipid. These nanotubes displayed step conductance changes in planar bilayers that showed ohmic current-voltage response. The conductivity was almost three times higher than for gramicidin under similar conditions which reflects the larger pore diameter. The gating mechanism was ascribed to structural flexibility or rapid assembly-disassembly of the tubular structure.

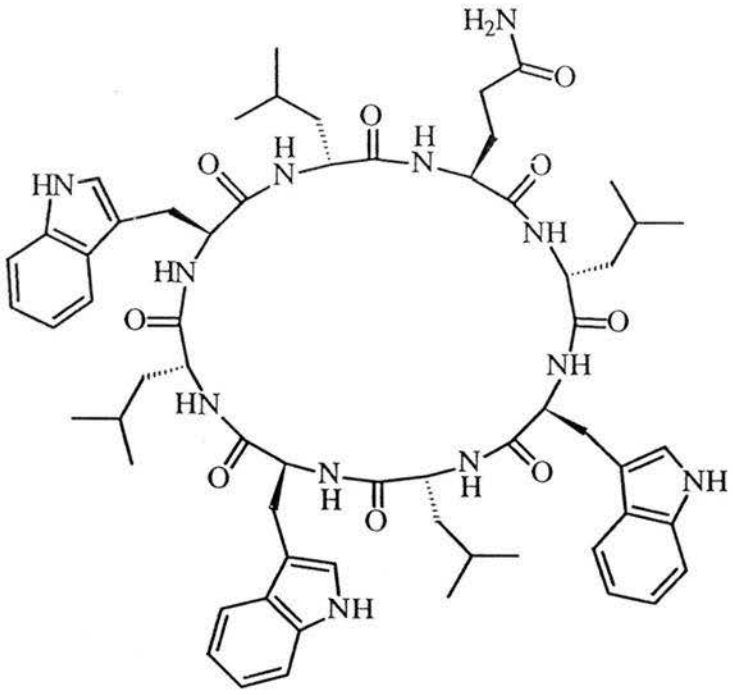

Figure 1.8: Chemical structure of the cyclic peptide subunit synthesized by Ghadiri *et al.*[53]

A more flexible tris-macrocyclic system has been synthesized by Gokel and co-workers.[16,54-57] In the initial design three diaza-18-crown-6 units were linked and terminated by dodecyl chains as shown in Figure 1.9. The distal crown ethers served as hydrophilic head

groups while the central macrocycle was needed as an ion relay and to give the molecule more rigidity. More recently the terminal dodecyl chains have been replaced by substituted benzyl groups[56,57] which allows spectroscopic access to these molecules. Thus, for the first time, octanol-water partition coefficients for non-peptidic ion transporters could be determined.[56] Bilayer clamp experiments for the benzyl channels were reported.[56,57] Step conductance changes that displayed ohmic current-voltage relationships with specific conductances of about 13 pS for sodium ions were observed for the three compounds investigated. This similarity in conductance was in contrast to the substituent-dependent cation fluxes that were observed using a dynamic ^{23}Na-NMR method with vesicle membranes.[56] However, the mean duration of the open states appeared to vary between about 5 seconds for the H-substituted channel and about 30 seconds for the methoxybenzyl channel.[57]

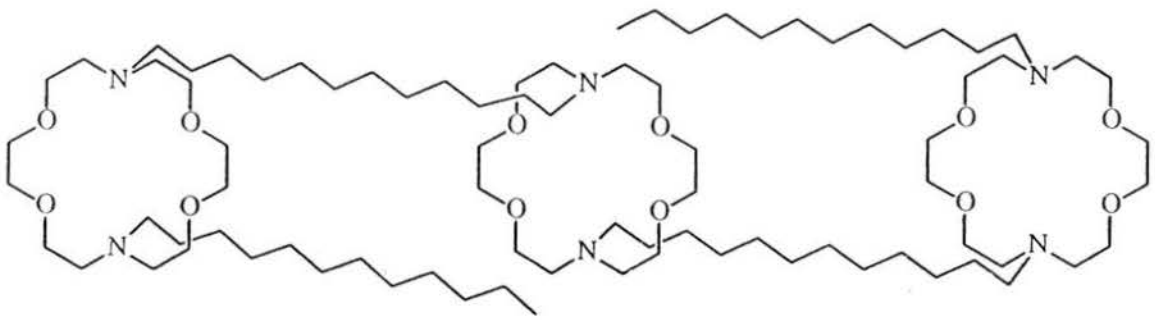

Figure 1.9: Tris-macrocyclic ion channel synthesized by Gokel *et al.*[55]

1.4 Ion channels synthesized in the Fyles group

Our group used a modular approach for the synthesis of a large number of ion transporters which allowed structure-activity studies. The transport activity of these compounds has been evaluated by the pH-stat technique. Briefly, predominantly unilamellar vesicles were prepared by reverse-evaporation in a buffered choline sulfate/mannitol solution at pH 6.6. The outside pH was then adjusted to 7.6 through the addition of choline hydroxide.

The proton carrier FCCP (carbonyl cyanide 4-(trifluoromethoxy)phenylhydrazone), and alkali metal ion sulfates were added. Release of protons from the vesicle *via* electroneutral cation-proton antiport was provoked by the addition of transporter molecules, and the proton efflux was quantified by the addition of choline hydroxide to maintain a set pH.[58] A schematic description of the pH-stat experiment is given in Figure 1.10.

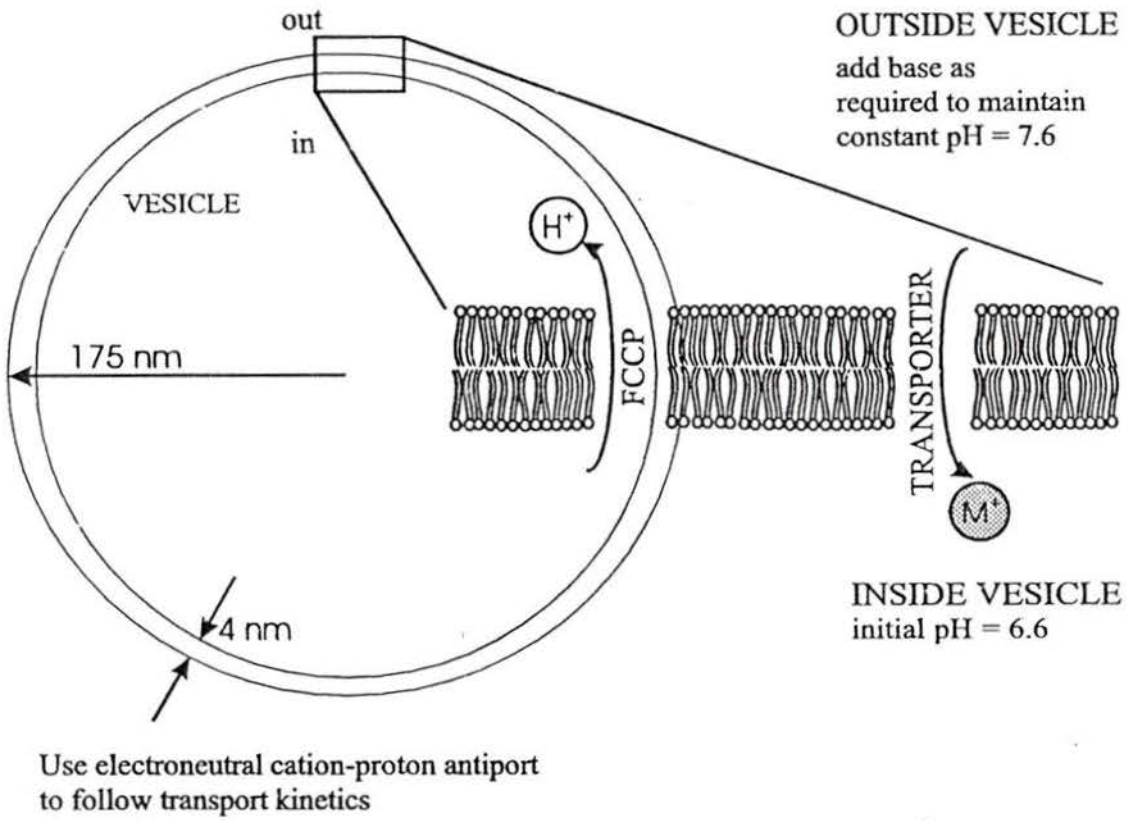

Figure 1.10: Schematic description of a pH-stat experiment

Two different classes of ion transporters were developed. One system was based on the unimolecular tunnel notion of ion transport and was mainly synthesized by T. James.[59,60] As illustrated in Figure 1.11 all transporters use 18-crown-6 derivatives based on tartaric acid as a rigid core. Macrocycles were attached as wall units to both faces of the crown ether, and were terminated by hydrophilic head groups. Twenty-one different compounds were synthesized,

varying in head group, and number, position, length and polarity of the wall units. In all cases a mixture of stereo- and regio-isomers was obtained. These transporters are fairly rigid due to the specific conformation of the crown ether core. A systematic study was performed on the cation transport in unilamellar vesicles using the pH-stat technique and the results were compared with gramicidin and valinomycin.[58,61] The structure of the channel had a pronounced influence on the transport rate and ion selectivity, and on the mechanism of ion transport. In the absence of bilayer clamp experiments, a crude distinction between carrier, ion channel and inactive compounds was possible.

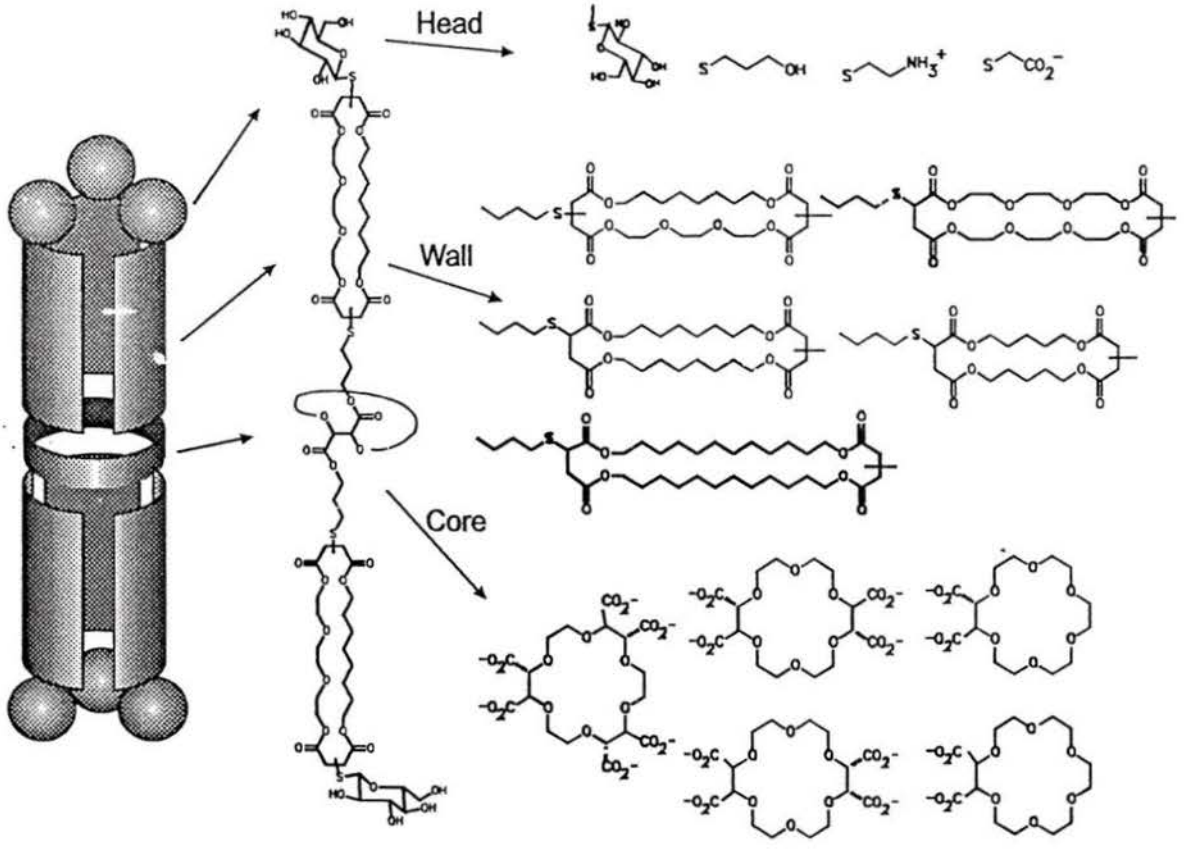

Figure 1.11: Crown ether channels from a combination of subunits

The other system was designed to form channels *via* the aggregation of compounds with a polar and an nonpolar side, similar to the aggregates formed by amphotericin B. The transporters were bola-amphiphiles consisting of two macrocyclic tetraester units linked by a spacer, and having two hydrophilic head groups as illustrated in Figure 1.12. These bola-amphiphiles were mainly synthesized by Zojaji[62] and their transport behaviour was evaluated using the pH-stat technique. As predicted, the kinetic measurements indicated that the rate-limiting process involved small aggregates of bola-amphiphiles. Low selectivity between alkali metal cations was observed and some transporters mediated proton transport in the absence of a cation gradient. The observed range of activities indicated that most likely a population of pores was formed with reproducible mean properties.[62]

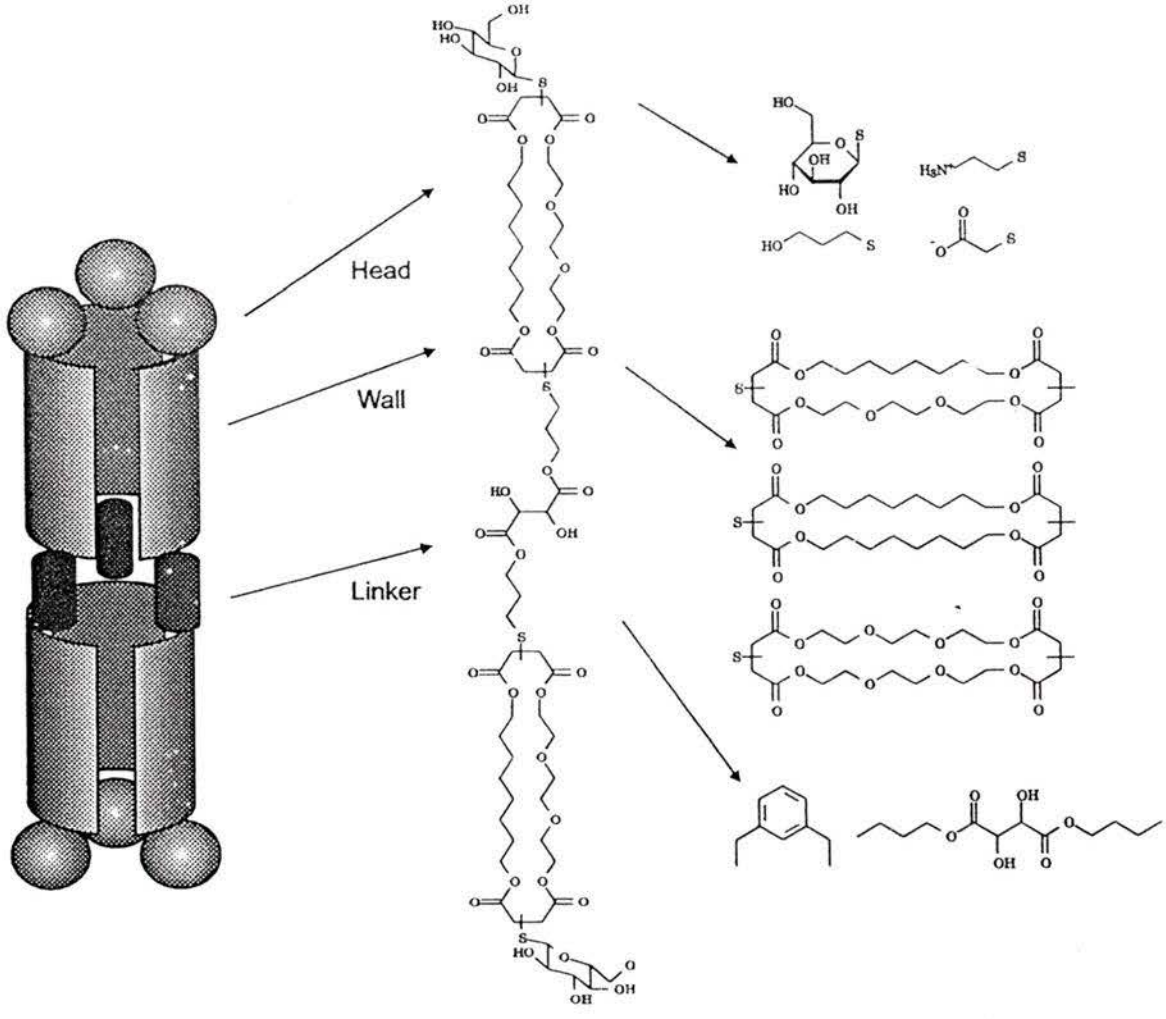

Figure 1.12: Channels formed *via* aggregation of bola-amphiphiles

1.5 New generation of bola-amphiphiles

Based on the results of the transport studies of the two types of transporters previously synthesized in our group,[59,62,63] a new series of bola-amphiphiles was developed. The wall units of the most active transporters were joined *via* a new, less bulky linker with fewer functional groups. The length and flexibility of the linker was varied and the effect on the ion transport behaviour was studied using the pH-stat technique. In addition, the head groups were modified to achieve a voltage-gated ion channel. As determined by the pH-stat technique all bola-amphiphiles were substantially more active[64] than the previous suite of pore forming compounds.[62] The transporters synthesized by Xin Zhou[64] are summarized in Figure 1.13.

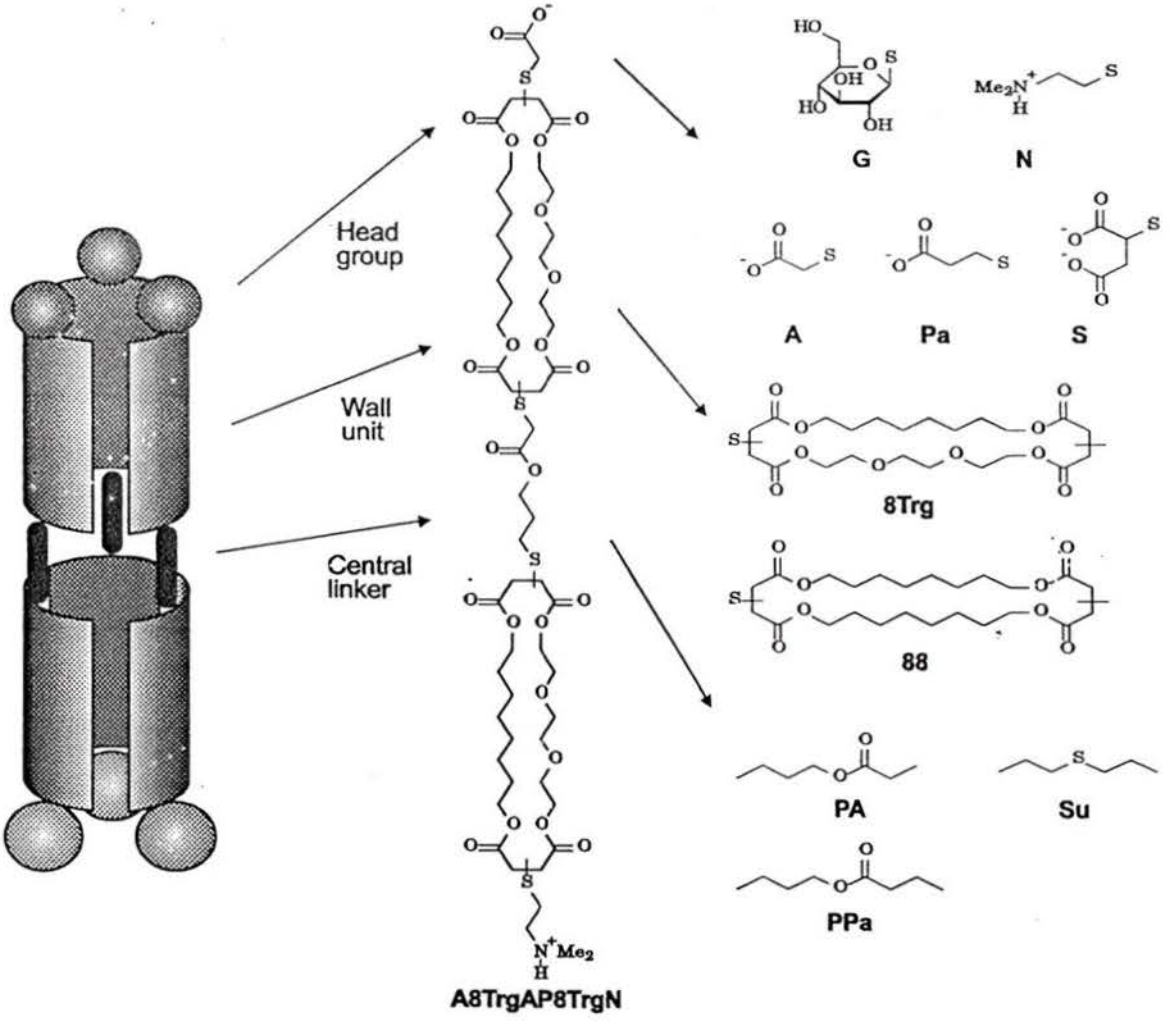

Figure 1.13: Modular set for bola-amphiphiles synthesized by X. Zhou.[64]

A semi-systematic naming system was used to describe the similar products in a simple way. Names and substructures are equated in Figure 1.13. Each synthon was assigned a letter or number name: **A** = 2-mercaptoacetic acid, **G** = 1-mercapto-β-D-glucose, **N** = N,N-dimethylamino ethanethiol, **Pa** = 3-mercaptopropionic acid, **S** = 2-mercaptosuccinic acid, **8** = from 1,8-octanediol, **Trg** = from triethylene glycol, **P** = 3-mercaptopropyl, and **Su** = 2-mercaptoethyl sulfide. The wall units were named as a combination of the synthon abbreviations with the exception that the maleate esters are implied. Thus, **88** = the macrocyclic tetraester from 2 mol of 1,8-octanediol and 2 mol of maleic anhydride, and **8Trg** = the macrocyclic tetraester derived from 1 mol of 1,8-octanediol, 1 mol of triethylene glycol and 2 mol of maleic anhydride. The final structures were named in the order: head group 1-wall unit-linker-wall unit-head group 2. As shown in Figure 1.12, **A8TrgAP8TrgN** represents: a mercapto acetic acid head group - the wall unit derived from 1,8-octanediol and triethylene glycol - a central linker derived from 2-mercaptoacetic acid and 3-mercaptopropanol - the same wall unit - a N,N-dimethylamino ethanethiol head group. This naming system does not keep track of the regio- and stereoisomers.[59]

1.6 Objective of this dissertation

The transport mechanism of the naturally occurring peptides gramicidin and alamethicin have been studied extensively over the past 30 years.[9,11,13,14] More than three hundred scientific publications on the details of gramicidin have appeared in the past ten years alone. On the other hand, very few mechanistic studies have been performed on non-peptidic artificial ion channels. The ion transport mechanism of these relatively small molecules is expected to be different from the mechanism of the ion channel proteins. A bilayer association and penetration step is generally involved for the artificial transporters while the protein channels remain in the membrane at all times. Furthermore, the small transporters move freely in the bilayer and the onset of the transport event is generally due to the association of several of these molecules. In proteins the switching between open and closed states is presumably caused by small conformational changes due to an external stimulus.[10] Nevertheless, the investigation of the ion transport mechanism of artificial ion transporters can reveal valuable

information on the different factors that control the formation of these transport systems. Understanding how aqueous pores can be assembled and stabilized in bilayer membranes will ultimately lead to the *control* of the permeability of membranes. This knowledge will be useful for the development of new antibiotics or artificial devices such as sensors. The bilayer clamp technique is an ideal tool for the investigation of the transport properties of ion transporters since it allows observation on the single molecule level and offers easy access to both faces of the bilayer membrane. Therefore, mechanistic details can be gained on the switching behaviour of these channels. Previous structure-activity studies performed in our group using the pH-stat technique, revealed that the ion transport behaviour of bola-amphiphiles was very sensitive to structural alterations.[61-63] The goal of the research presented in this dissertation is to use the bilayer clamp technique to investigate the pore-forming ability of a new and more active series of bola-amphiphiles synthesized by X. Zhou.[64] These molecules are designed to form aggregates and we expect that small structural alterations will influence the association and dissociation behaviour of these transporters. We pose the question whether ion transport by bola-amphiphiles can occur by one of the mechanisms illustrated in Figure 1.3. If indeed all transporters can be classified by these mechanisms, are the differences in ion selectivity and kinetic order that are observed in the vesicle experiment simply due to different pore sizes? Therefore we wanted to explore the activity and study the mechanism of a large number of transporters in planar bilayers rather than simply choose the most active molecule in vesicle membranes and examine its behaviour in detail. Inevitably, the broad knowledge and information gained with this approach will be achieved at the expense of a less detailed description of individual molecules.

The influence of the size and charge of the head groups, the hydrophobic/hydrophilic balance of the wall units, and the length and flexibility of the linker on the transport mechanism of these bola-amphiphiles has been studied in planar bilayer membranes. The results will be compared to the vesicle experiments performed by X. Zhou.[64] In addition, the activity of one of the unimolecular ion channels previously studied by James[58] and the activity of a membrane disrupting agent synthesized by B. Zeng[65] will be presented. Thus, a wide range of transport mechanisms has been uncovered.

2. Experimental

2.1 Chemicals

Egg phosphatidylcholine (PC), diphytanoyl phosphatidylcholine (diPhyPC) and egg phosphatidic acid (egg PA) were purchased from Avanti Polar Lipids. They were shipped in Dry Ice and stored at -12 °C. Cholesterol was purchased from Sigma/Aldrich. Decane (99%), Triton X-100, methanol and chloroform (HPLC grade) were purchased from Aldrich. Gramicidin D, alamethicin, and valinomycin were obtained from Sigma/Aldrich. Chloride salts of alkali and alkaline cations were purchased from Aldrich, purity was 99.8 % or better and the salts were used without further purification. Only D^3 (deionized, double distilled) water was used.

2.2 Instrumentation

A model BC-525A bilayer clamp (Warner Instrument Corporation) has been used for planar bilayer experiments. The analog output signal was monitored with a 100 MHz oscilloscope (Tektronix) and recorded with a x-y chart recorder (Kipp&Zonen). The signal was analog filtered with a 8-pole Bessel filter (Frequency Devices, model 902) and digitized with a 333 kHz digitizer (Axon Instruments, Digidata 1200A). Data acquisition and analysis was performed using the pClamp6 software package (Axon Instruments). In some cases the data was additionally filtered digitally with a Gaussian filter. The headstage and the bilayer chamber were placed on a floating table (TMC) and electrically shielded by a home built Faraday cage fabricated from solid aluminium.

2.3 Planar Bilayer Experiments

Stock solutions of 17 mg/ml lipid in chloroform were prepared and stored at -12 °C under argon. Stock solutions contained either diPhyPC or a mixture of PC, egg PA, and cholesterol in 8:1:1 molar ratio. Egg-PA and PC were handled under argon. To prepare the spreading solution for planar bilayer experiments the chloroform was removed

on a rotary evaporator. Alternatively a constant stream of argon was used to evaporate the solvent. The lipids formed a colorless film on the walls of a round bottom flask and were further purged with argon. Decane was added to obtain 17 mg/ml lipid dispersions. The spreading solution could be stored for up to 48 hours under argon at room temperature provided the relative humidity was between about 10 and 60 percent. At higher humidities the lipid dispersions turned quickly into gels and were unusable for bilayer formation.

Figure 2.1 illustrates a block diagram of the experimental set-up and a typical bilayer clamp experiment. The bilayer chamber consists of a PVC cuvette holder with two chambers and a polystyrene cuvette which fits one chamber. A hole of 0.25 mm diameter was drilled through the cuvette. A fine camel-hair paintbrush was used to spread the lipid dispersion over both sides of the aperture in the dry cuvette. The decane was evaporated under a gentle stream of nitrogen. This lipid film served as a primer to facilitate subsequent bilayer formation. The bilayer chamber was then assembled and filled with electrolyte. The cuvette holder held 5 ml of electrolyte while the cuvette was filled with 2.6 ml. Care was taken to ensure equal electrolyte levels to prevent the formation of a pressure gradient. Electrical contact was made via Ag/AgCl electrodes placed directly into the solutions. One end of a silver wire of 0.5 mm diameter was coated with silver chloride by repeatedly dipping the wire into a silver chloride melt. A copper pin was attached to the opposite end of the wire to allow integration into the circuit. Electrode pairs were normally stable for several months. The bilayer clamp provides a voltage of up to ±120 mV dc to buck off input offset errors and solution junction potentials. Corrections to the junction potentials were made prior to bilayer formation and were checked at the end of an experiment. Junction potentials were typically between ±10 mV and stable throughout an experiment. Junction potentials greater than 10 mV were taken as evidence of degradation of the electrodes in which case a new pair of electrodes was used. In order to form bilayers, the spreading solution was painted across the aperture which led to an immediate drop in conductance. The originally thick film was thinned to a bilayer by removing excess decane by brushing across the hole. The formation of the bilayer could be followed by using the capacitance test function of the bilayer clamp. A 100 Hz triangle wave is fed to

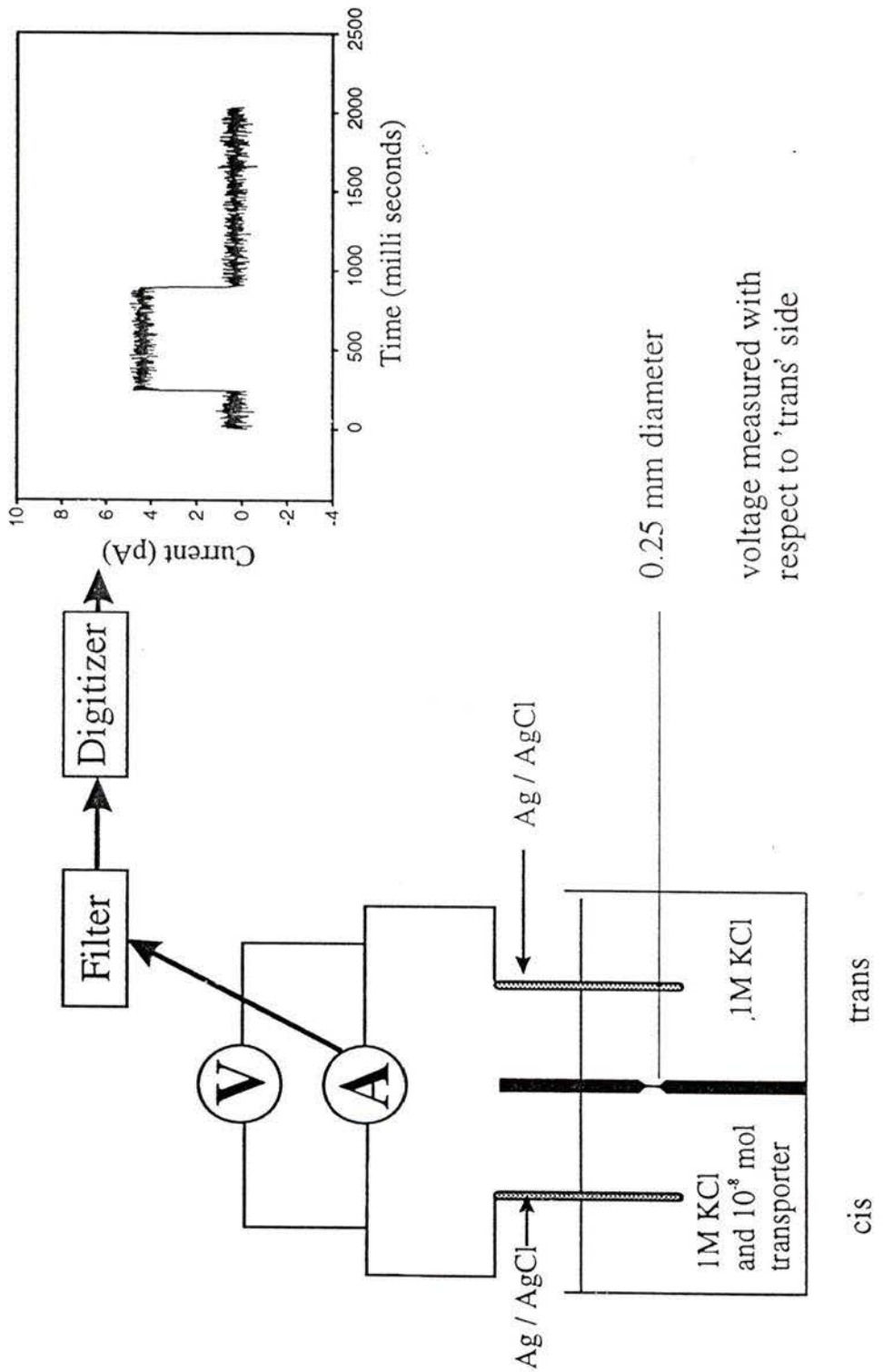

Figure 2.1: Schematic representation of a typical bilayer clamp experiment.

the headstage and integrated over the input capacitance. This signal is differentiated and results in a 100 Hz square wave at the output. The peak to peak value of this signal is proportional to the input capacitance with a sensitivity of 0.1 mV/pF. The thinning to a bilayer can then be directly monitored since the thickness of the membrane is inversely proportional to the capacitance[66] according to equation 1.

$$C = \varepsilon_0 \varepsilon A \ d^{-1} \qquad (1)$$

where C is the capacitance, ε_0 the permittivity in vacuum, ε the dielectric constant of the lipid core, A the membrane area and d the thickness.

The final capacitance should be in the range of 160 to 200 pF. Membranes were checked for leakage by applying transmembrane potentials of ±120 mV. Leakage manifested itself in two ways. A high conductance of the bilayer, i.e. greater than 20 pS implies a generally poorly sealed membrane. Brief events of bilayer breakdown were also occasionally observed upon application of the transmembrane potential. Bilayers with conductances of greater than 10 pS or that displayed brief breakdown events were not used for transport studies.

In a typical single-channel experiment such as depicted in Figure 2.1, aliquots of 10^{-3} to 10^{-4} M methanolic solution of transporter were added to the cuvette holder (*cis*-side) using a microliter syringe. A transmembrane voltage of typically ±120 mV was then applied to aid insertion into the bilayer. Voltages are measured with respect to the *trans*-side of the bilayer. The current as a function of time was measured using the Fetchex data acquisition program. The records were usually analog filtered with one tenth of the sampling frequency. Channel activity was unambiguously detected by the presence of step changes in the current as the channel switches from a "closed" to an "open" state. The bilayer chamber was dissembled at the end of an experiment and rinsed with 2 % (vol./vol.) Triton-X 100 solution followed by distilled water and ethanol. After

experiments with alkaline metal cations the chambers were soaked in 0.1 M EDTA over night following the normal cleaning procedure and then rinsed again with distilled water and ethanol.

To determine the charge selectivity of ion transporters the reversal potentials were measured. Bilayers were formed between two different electrolytes. The junction potentials in these experiments were sometimes higher than in symmetric salt solutions depending on the combination of electrolytes. In experiments with two cations in competition 1 M chloride salts of the ions in questions were employed. The dilution potentials were determined from 0.1 M and 0.5 M salts. No attempts to control the ionic strength have been made. Enough transporter had to be added to ensure macroscopic (nA) currents across the bilayer to avoid artifacts from periods of low channel activity. Usually a potential of ±100 mV was applied initially until channel activity was established. The reversal potential was then manually approached from both directions. Following this estimation, a voltage ramp crossing the region of interest, typically with a rate of 2 - 13 mV s^{-1}, was applied using the Clampex data acquisition program. A current-voltage diagram was constructed as an average of 10 - 20 cycles and the reversal potential was determined from the voltage intercept. The manual and averaged values generally agreed within ±2 mV.

2.4 Analysis of single-channel recordings

Typical single-channel current events for natural ion channels appear as rectangular pulses of fixed amplitude as shown in Figure 2.1.[67] A single-channel record yields two direct observables, time and current amplitude. Numerous examples can be found in the literature where models to describe the opening and closing mechanism of channels have been proposed and statistical analysis of single-channel recordings has been used to probe the validity of these models, see references 13, 26, 27, and 68-70 for examples. A brief description of the principles of the analysis of single-channel recordings is given in the

following paragraphs. Details on the analyses performed on my experimental data will be found in the appropriate results section of this thesis.

The single-channel current amplitudes reported for most natural examples are very consistent and the amplitude distribution can be fitted to a Gaussian curve.[67] The variability of the amplitude from one opening to another is due to the variable duration of events with long events giving the most precise estimates. In some experiments step-like conductance changes of more than one amplitude are observed. This may happen because two or more different types of channel are active. Alternatively a single type of channel may exhibit more than one conductance state.[19,67] The amplitude distribution can therefore be used to distinguish between multiple channel populations or multiple conductance levels.

The distribution of the open times and the distribution of the closed times can provide information on the kinetics of the system.[71] The opening and closing of channels (gating) are assumed to be Markov processes. That means the probability for a channel to open is not dependent on the history.[71] When only one channel is present in the preparation and there is only one open state, i.e. no multiple conductance states, the time a channel spends in the open state is expected to be exponentially distributed with a mean that is inversely proportional to the sum of the transition rates that lead away from the state.[71] Thus, rate constants can be obtained for the opening and closing and a mechanism can be inferred. An excellent discussion on the principles of the stochastic interpretation of single-channel data is given by Colquhoun and Hawkes.[71] When the preparation contains more than one channel molecule problems arise. In this case one can not be sure whether a particular opening arises from the same channel as the preceeding opening. This means that the distribution of the shut periods can not easily be interpreted. In cases where multiple openings are observed at the same time, information on the open time for a particular channel is lost. Only a distribution for the mean open duration for a population of channels can be obtained.[71]

2.5 Charge selectivity

The charge selectivity of a transporter can be measured by determining the reversal potential for two ions in competition.[10,12] The reversal potential is the potential at which there is no net ion flux with different electrolyte solutions on the two sides of the bilayer. If a channel is permeable to multiple species there is generally not a thermodynamic equilibrium but a steady state. The Goldmann-Hodgkin-Katz equation (2) describes this situation.[10] Illustrated is the form for mixed Cs^+ and Na^+ chlorides, other cations can be substituted.

$$V_{rev} = \frac{RT}{F} \ln \left(\frac{P_{Na}\gamma_{Na}[Na^+]_{trans} + P_{Cs}\gamma_{Cs}[Cs^+]_{trans} + P_{Cl}\gamma_{Cl}[Cl^-]_{cis}}{P_{Na}\gamma_{Na}[Na^+]_{cis} + P_{Cs}\gamma_{Cs}[Cs^+]_{cis} + P_{Cl}\gamma_{Cl}[Cl^-]_{trans}} \right) \quad (2)$$

where V_{rev} is the reversal potential, P_x and γ_x the permeability and activity coefficient for species x, respectively, F is the Faraday constant, R the gas constant and T the absolute temperature. Under the assumption that the potential drops linearly across the membrane, the permeabilities can be considered as the product of the diffusional mobility of an ion within the channel and the ion's partition coefficient from aqueous solution to the channel. It should be noted that only the permeability ratios can be determined but not the permeability coefficient for each ion. Cation:anion selectivity is measured from the single-salt dilution potential with different concentrations of the ion on the two sides of the membrane. The equilibrium potential for the cation, derived from thermodynamics, will be found for a perfectly cation selective channel. On the other hand the reversal potential will always be zero if the channel is nonselective or for symmetric salt solutions.

2.6 Development of an analog signal processing device

Many of the artificial ion transporters studied in this thesis display erratic transport behaviour in planar bilayer membranes. This behaviour is evident as brief openings on the order of 100's of microseconds and varying amplitudes. To fully describe each signal the

sampling interval should be shorter than one third of the signal duration. Typical raw data acquisition requires a large disk space. Experience with the Digidata 1200A digitizer shows that at a sampling rate of 100 kHz 6 Mbytes per minute of experimental data are acquired. Typical experiments last for about 30 minutes requiring 180 Mbytes of disk space at this sampling frequency. Not only does this create a problem with memory management it also makes data analysis very time consuming. In a lot of cases the observed erratic activity does not seem to be due to simple membrane disruption but due to more defined species. Therefore we considered it desirable to develop a system that would allow us to quantify properties such as the total current carried in each of the short openings and the time scales of events. Presumably information such as overall increase of transport activity over time and the relative frequency of openings can be extracted from such data. For example, for the voltage-gated compound S8TrgPA8TrgA presented in chapter 4, it would have been desirable to be able to count the number of openings at each applied transmembrane potential directly. We therefore decided to design a device that would integrate the incoming signal directly and keep tags on the occurrence of events. The data thus obtained would be written directly to a file that would then only contain 5 columns: the integrated signal, its duration, the time between events, the total time elapsed at the onset of the signal and the total number of events. This file will therefore report a summary of events rather than raw data. Presumably much longer experiment times become possible by limiting the amount of disk space needed to store the data.

2.6.1 Design principle

The Analog Signal Processor (ASP) is an analog voltage integrator that allows the determination of the total current carried within a single transport event and the determination of the duration of each event. It offers the advantage of converting the result of a signal manipulation directly to a value that can be written to a file. The output signal of the bilayer clamp is a continuous voltage that is proportional to the current flow across the lipid bilayer membrane. This comprised the input signal of the ASP. When a

transport event occurs a trigger will change its state from low to high and the ASP starts the integration of the input signal. The trigger also starts an external counter to obtain information on the signal duration. At the same time a continuously running clock is tagged to keep track of when the signal started in real time. The output signal of the ASP is a continuous voltage corresponding to the integrated input voltage. This output signal is sent to the A/D board. When the trigger ends (high to low transition) the last output signal value is held by the ASP for long enough to allow digitization and the counter is stopped. The negative edge of the trigger also initiates the analog to digital conversion of this data point. The A/D conversion can alternatively be triggered by a second trigger pulse that is initiated by the negative edge of the first trigger. The integrated signal value is written to a file together with the duration of the transport event. The total time elapsed and the time between events is also reported. Figure 2.2 illustrates the design principle of the ASP.

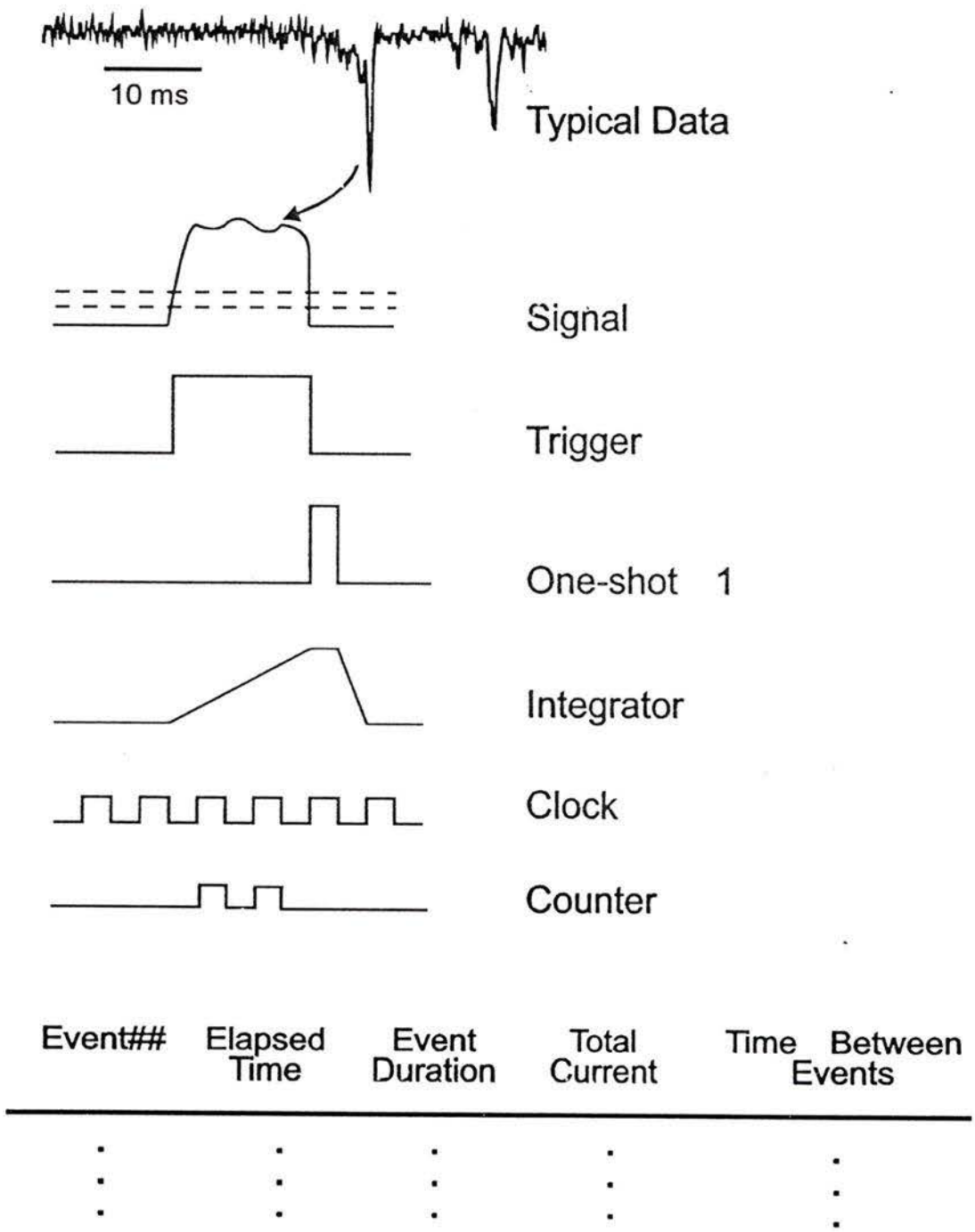

Figure 2.2: Design principle of the Analog Signal Processor.

2.6.2 Hardware description

Diagram 1 summarizes the signal flow. The analog input signal is a voltage corresponding to the current flux across the membrane and can be either positive or negative, depending on the potential applied across the bilayer membrane. This signal is fed to an integrator and a threshold detector (voltage comparator). To ensure that only positive voltages reach the inputs of integrator and comparator, the analog input signal can be inverted. The comparator goes into its positive saturation limit when the input exceeds a preselected threshold voltage. The output of the comparator is a digital signal with a low-high transition at the onset of a transport event. The negative edge of the threshold detector output indicates that the event is over and triggers a one-shot monostable multivibrator which produces a logic signal of 10 µs length. The onset of this pulse disconnects the input signal from the integrator input and triggers the analog to digital conversion of the integrator output voltage. Note that the Digidata 1200A imposes an upper limit of 10.24 V on the output voltage. The negative edge of the one-shot multivibrator triggers a second one-shot monostable multivibrator to produce a logic pulse of 50 µs duration which is fed into an AND gate. The output of a second voltage comparator that monitors the voltage on the capacitor of the integrator is also fed into the AND gate. Since under the chosen conditions the integrator output will always be a negative voltage it has to be inverted before it reaches the comparator's input. As long as the capacitor carries more than a preset amount of charge and the 50 µs pulse is active the output of the AND gate will be high and the capacitor will be discharged by closing a FET switch. As soon as the capacitor charge falls below the preset threshold value or the 50 µs are over the FET switch will be opened and the capacitor can be recharged. Figures 2.3.1 to 2.3.4 show the circuit diagram for the device.

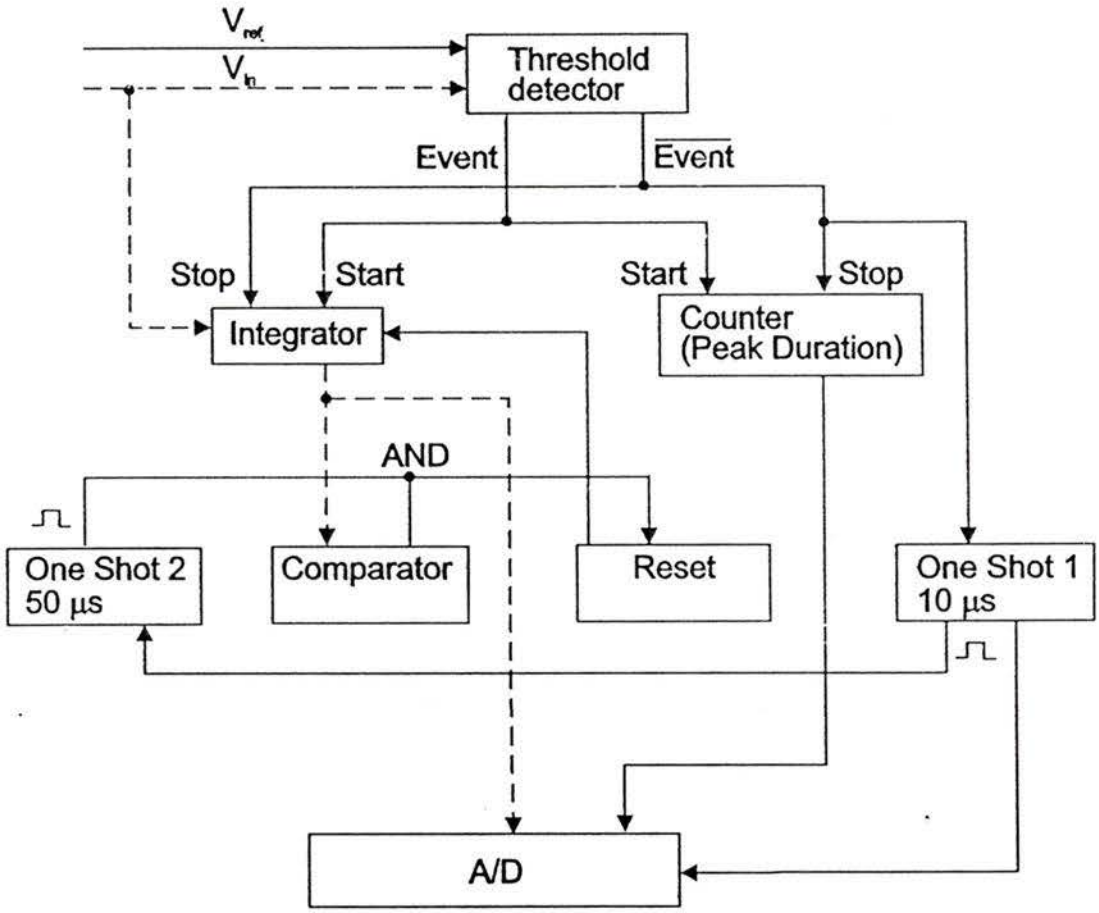

Diagram 1: Summary of the signal flow where the input signal is indicated by the dashed line.

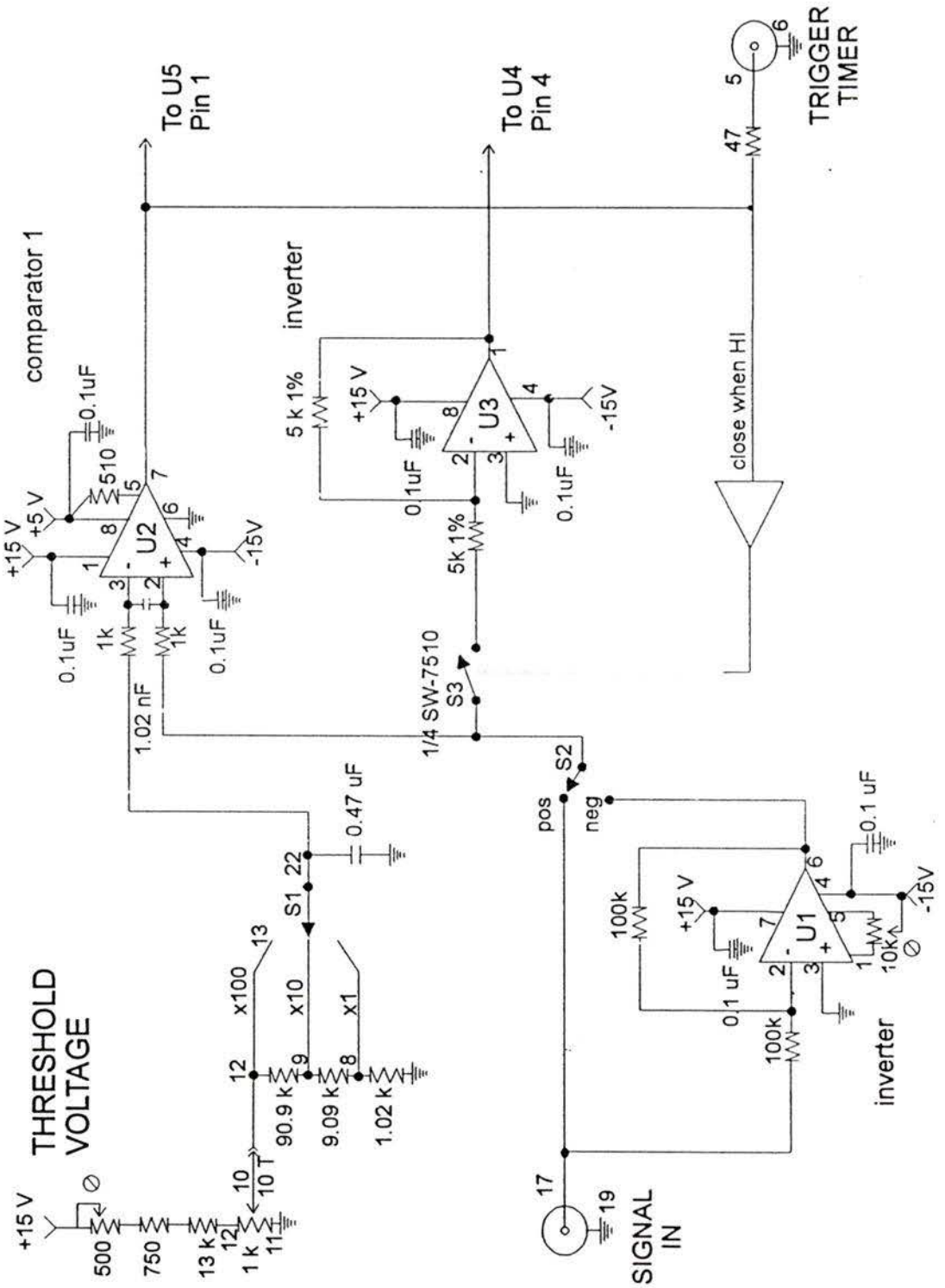

Figure 2.3.1: Circuit diagram for the Analog Signal Processor analog section I.

U1 = AD711, U2 = AD790, U3 = 1/2 AD712

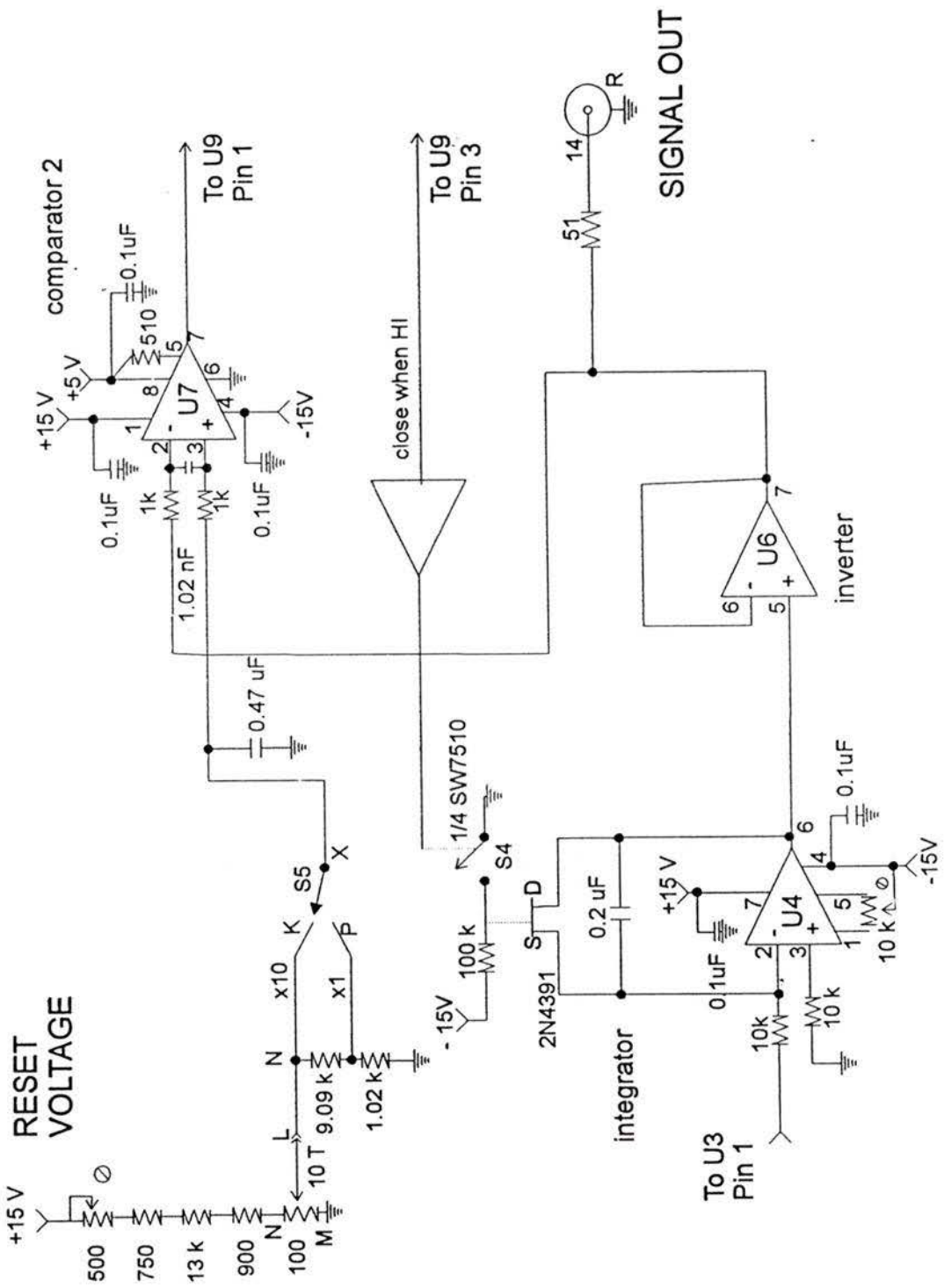

Figure 2.3.2: Circuit diagram for the Analog Signal Processor analog section II. U4 = AD711, U6 = 1/2 AD712, U7 = AD790.

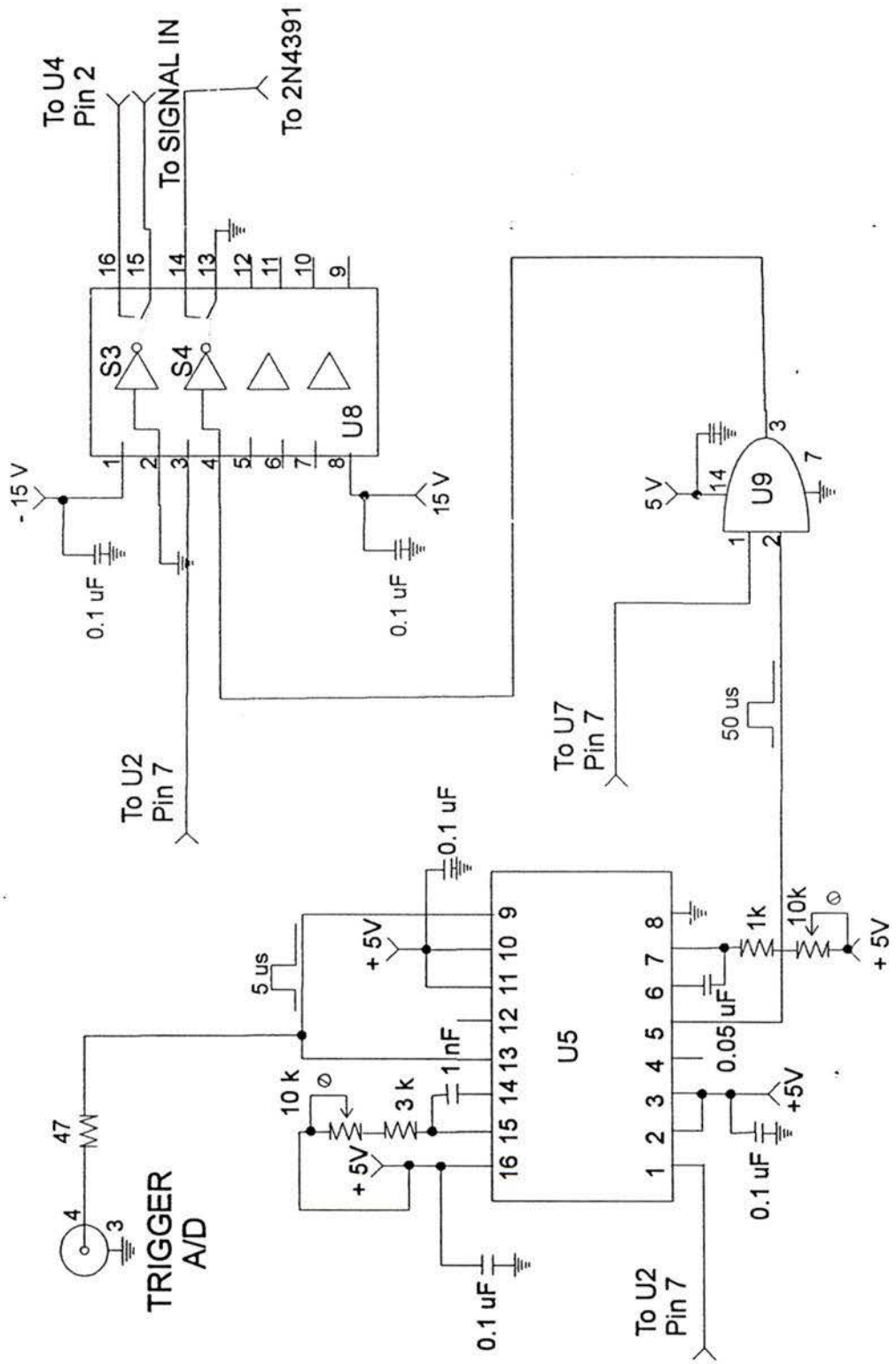

Figure 2.3.3: Circuit diagram for the Analog Signal Processor section III.

U5 = 74LS123, U8 = SW-7510 FQ, U9 = 1/4 74LS08

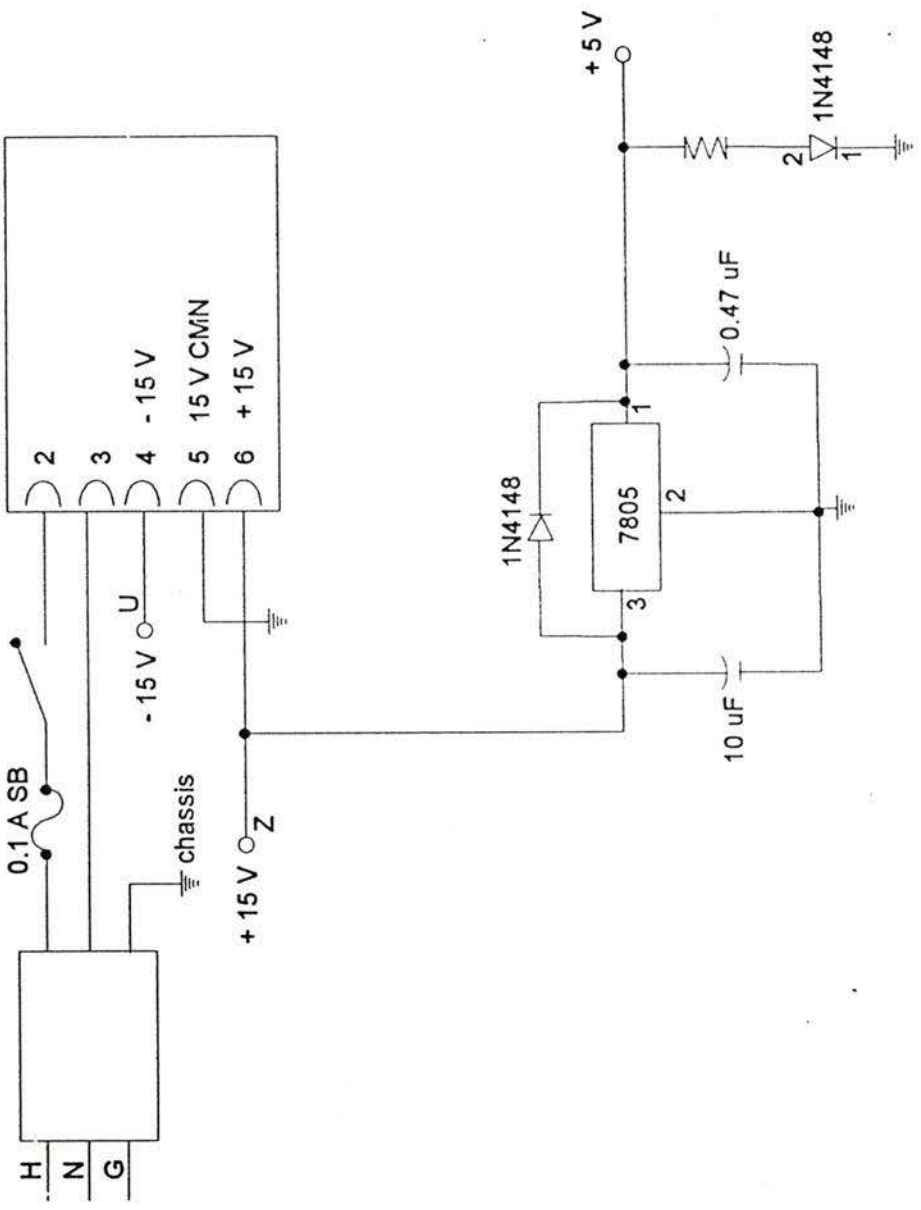

Figure 2.3.4: Power supply circuit for the Analog Signal Processor

An image of the front panel is shown in Figure 2.4. The THRESHOLD VOLTAGE block contains controls to select the voltage above which a signal will be integrated. FINE is a ten turn control with a maximum sensitivity of 1 mV/turn. The COARSE control can decrease the sensitivity up to 100 mV/turn. The polarity of the signal can be selected by a toggle switch. The threshold voltage ranges from 0 - 1 V.

The RESET function determines to which voltage the integrating capacitor will be discharged. The instrument will be ready to integrate the next signal after the capacitor is discharged to the reset voltage or after 50 µs, whichever occurs first.

FINE is a ten turn control with a sensitivity of 1 mV/turn that selects the reset voltage.

The sensitivity can be decreased ten times with the COARSE switch. The reset voltage ranges from 0 -100 mV.

SIGNAL IN: connects the ASP (Analog Signal Processor) to the incoming signal.

SIGNAL OUT: is a voltage that is proportional to the integrated signal.

TRIGGER A/D: provides a 10 µs long pulse that triggers the A/D converter to read the value at signal out.

TRIGGER TIMER:triggers the counter of the A/D converter to give the starting time of a signal and its duration.

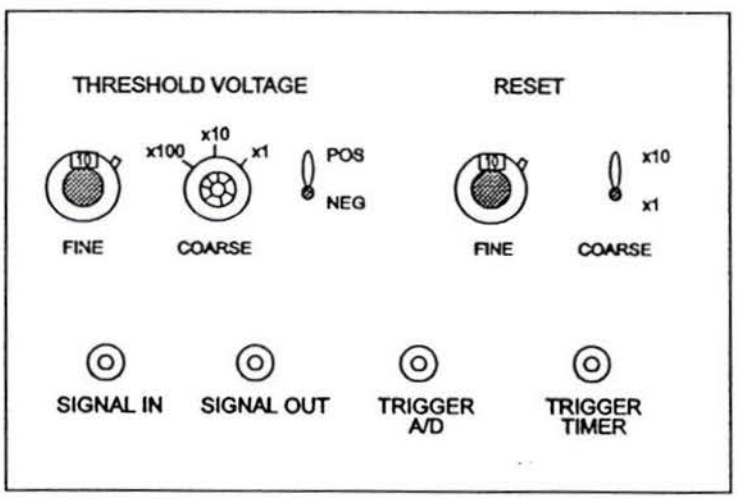

Figure 2.4: Image of the front panel.

2.6.3 Interfacing and description of the data acquisition program

The output voltage from the Analog Signal Processor (ASP) is connected to the Digidata 1200A board in order for A/D conversion to take place. The programming part of this project was done by David Robertson. Data acquisition uses the LINX technology. The software is written in Visual Basic (VB) for a 16 bit Microsoft Windows platform on a personal computer (PC). The VB modules compile to an executable file 'ai.exe' that can be attached to a MSWindows icon. The user can access the Digidata 1200A card and the software *via* the icon. The software starts up, initializes the Digidata 1200A, and presents a dashboard view of the experimental functions which is shown in Figure 2.5. The sampling frequency, the analog input channel of the Digidata 1200A switchbox and the filename can be selected. The 'Trigger' is set to 'external' and 'Mode' to 'auto'. The graphing function was disabled.

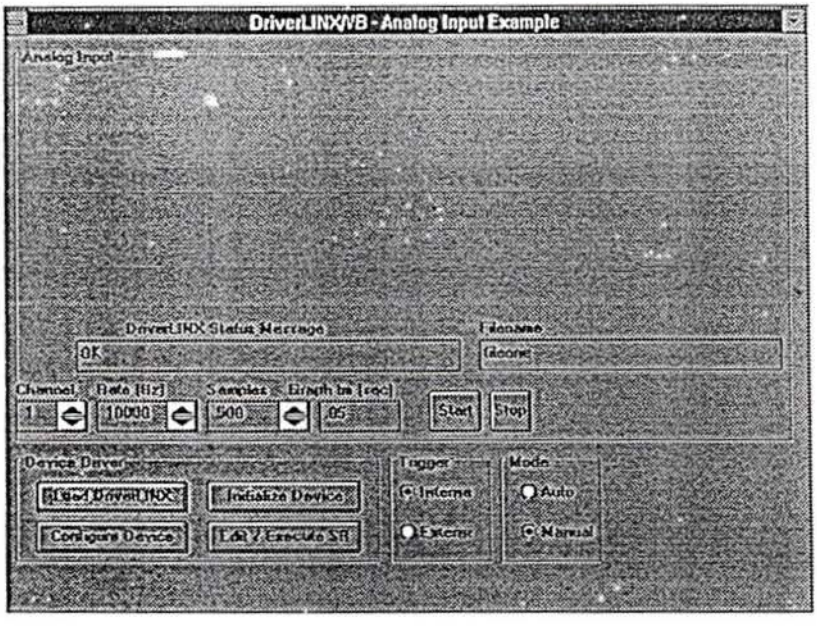

Figure 2.5: Illustration of dashboard view.

Diagram 2 describes the logic of the data acquisition program. Upon starting, the data is sampled at the selected frequency under the control of the Digidata 1200A and continuously written to a buffer. After the arrival of an external trigger the buffer content is transferred by DMA to the personal computer while a second buffer is being loaded. The software is event driven and the external trigger causes a series of calculations on the PC. The results of this calculations, i.e. ASP output signal, duration of the signal (acalc), time between signals (precalc), and total time elapsed (ccalc), are then sent to the text file. Data acquisition occurs continuously until terminated by the user. A flow diagram of the data acquisition part of the program is shown in diagram 2 while the code is listed in Appendix 1.

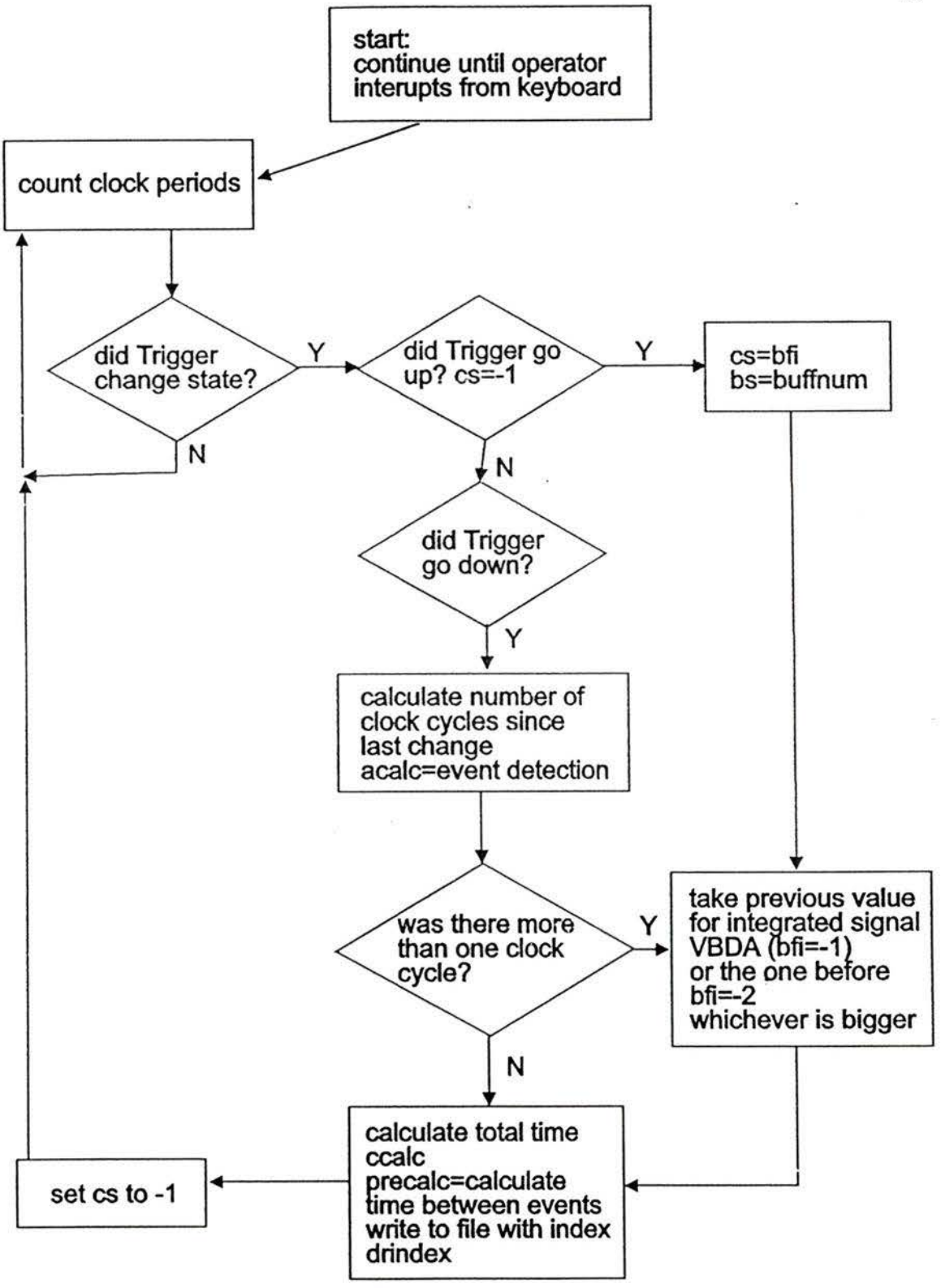

Diagram 2: Flow diagram of the data acquisition part of the program ai.VB. Buffer-fill-index=bfi; VBDATAArray=VBDA; changestate=cs; bufferstart=bs.

2.6.4 Testing of the Analog Signal Processor

To test the ASP a 100 Hz sine wave with 2 V peak-to-peak amplitude was generated with a function generator (Wavetek) and fed to the signal input of the device. Only the positive going part of the sine wave should be registered by the ASP. The output signal is expected to be a rising signal with a plateau of 10 μs duration during which the signal will be digitized. This was indeed observed and is shown in Figure 2.6.

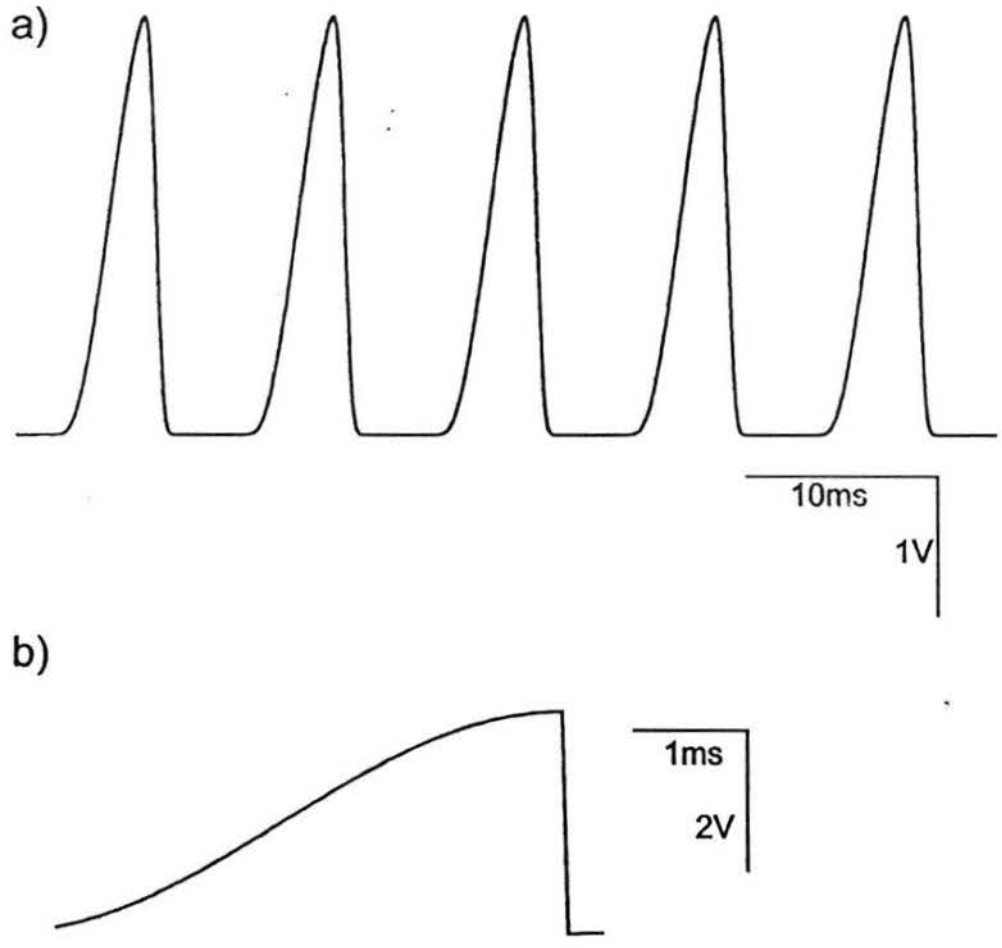

Figure 2.6: A) Signal output of the ASP with a 100 Hz sine wave, 2 V p-p as analog input signal. B) shows an expansion of part a) to illustrate the plateau.

The corresponding file that was generated with the ai.VB program is shown in Table 1. The signal is truthfully represented by the acquired file. The error in voltage is ± 0.005 V. The initial value for "time since last event" is without physical meaning.

Table 1: Sample file generated with the "ai" program for a 100 Hz, 2 V p-p sine wave, 10 kHz sampling frequency.

event no.	elapsed time (ms)	duration (ms)	potential (volt)	time since last event (ms)
0	4.9	4.8	3.1653	-10594.8
1	14.9	4.9	3.1703	10
2	24.8	4.9	3.1753	9.9
3	34.7	4.8	3.1603	9.9
4	44.7	4.9	3.1703	10
5	54.6	4.9	3.1753	9.9
6	64.5	4.8	3.1653	9.9
7	74.5	4.9	3.1703	10
8	84.4	4.9	3.1703	9.9
9	94.3	4.8	3.1603	9.9
10	104.3	4.9	3.1703	10
11	114.2	4.8	3.1753	9.9
12	124.1	4.8	3.1603	9.9
13	134.1	4.9	3.1703	10
14	144	4.8	3.1703	9.9
15	153.9	4.8	3.1603	9.9
16	163.9	4.9	3.1653	10
17	173.8	4.8	3.1703	9.9
18	183.8	4.9	3.1753	10
19	193.7	4.9	3.1703	9.9
20	203.6	4.8	3.1703	9.9
21	213.6	4.9	3.1753	10
22	223.5	4.9	3.1653	9.9
23	233.4	4.8	3.1703	9.9
24	243.4	4.9	3.1753	10
25	253.3	4.9	3.1653	9.9
26	263.2	4.8	3.1703	9.9
27	273.2	4.9	3.1753	10
28	283.1	4.8	3.1653	9.9
29	293	4.8	3.1703	9.9
30	303	4.9	3.1753	10

Table 2 shows a file that was acquired for the voltage-gated compound S8TrgPA8TrgA at +60 mV in 1 M KCl. The threshold potential was set to 1 mV with a sampling frequency of 10 kHz. The incoming signal was analog filtered with 1 kHz. The device is clearly able to detect events of several 100's of microseconds as can be seen in the "duration" column. Varying potentials corresponding to different amounts of total current carried are also evident.

Table 2: Test file generated with the ai.VB program. 10 kHz sampling frequency, 1 kHz analog filtered. S8TrgPA8TrgA at +60 mV in a diPhyPC bilayer, 1 M KCl electrolyte.

event no.	elapsed time (ms)	duration (ms)	potential (V)	time since last event (ms)
0.00	0.30	0.30	0.01	-30482.30
1.00	1.50	1.10	0.02	1.20
2.00	5.80	4.10	0.07	4.30
3.00	7.60	1.70	0.02	1.80
4.00	12.30	4.50	0.06	4.70
5.00	14.50	2.00	0.03	2.20
6.00	15.10	0.40	0.01	0.60
7.00	18.00	2.70	0.01	2.90
8.00	18.30	0.10	0.01	0.30
9.00	19.10	0.40	0.01	0.80
10.00	19.80	0.20	0.01	0.70
11.00	20.60	0.50	0.01	0.80
12.00	22.20	1.10	0.01	1.60
13.00	22.90	0.30	0.01	0.70
14.00	23.60	0.50	0.01	0.70
15.00	24.30	0.10	0.01	0.70
16.00	25.10	0.50	0.01	0.80
17.00	27.20	1.60	0.02	2.10
18.00	27.80	0.20	0.01	0.60
19.00	28.30	0.30	0.01	0.50
20.00	29.40	0.20	0.01	1.10
21.00	30.40	0.90	0.01	1.00
22.00	30.80	0.20	0.01	0.40
23.00	31.20	0.20	0.01	0.40
24.00	31.80	0.30	0.01	0.60

The potential for the Analog Signal Processor as a useful tool in the analysis of erratic transport events in planar bilayers has been demonstrated. It is expected to prove helpful for the quantification of the number of openings per time period as was required for the voltage-gated compound, S8TrgPA8TrgA, in chapter 4 of this thesis. Due to time constraints, however, further experiments have not been carried out.

3. Pore-forming bis-macrocyclic bola-amphiphiles

The channel-forming activity of a suite of compounds with the macrocyclic 8Trg wall units was studied initially. Based on observations of a related suite of compounds prepared earlier in our group[62] we envisaged that the hydrophilic polyether part of the wall units would provide the driving force for the formation of aggregates in bilayer membranes. The hydrophilic segments will be oriented towards the inside of the aggregate thereby creating an aqueous pore whereas the hydrophobic segments interact with the lipids in the membrane. Selectivity between different cations may be achieved by introducing differently charged head groups. Another goal of this study was to investigate the possibility of controlling the switching between the on and off state of the channel. The introduction of a large molecular dipole is expected to provide a sensor for the applied transmembrane voltage. The four compounds studied are depicted in Figure 3.1.

Between pH 5 - 10 the head groups **A** (2-mercaptoacetic acid) and **N** (N,N-dimethylamino ethanethiol) will be charged as -1 and +1, respectively while **G** (1-mercapto-β-D glucose) will be neutral. In this pH range the compound with a positively and a negatively charged head group, N8TrgPA8TrgA, will have the largest molecular dipole moment and is a potential candidate for voltage-gating. An overall dipole of 144 Debye has been calculated by assuming an overall transporter length of 30 Å, a charge difference between the two ends of 2 point charges and neglecting any other contributions to the dipole moment.[14] A symmetric transporter, A8TrgPA8TrgA, with no dipole has been synthesized as control. Compounds with only one charged head group have molecular dipoles of about 72 Debye.

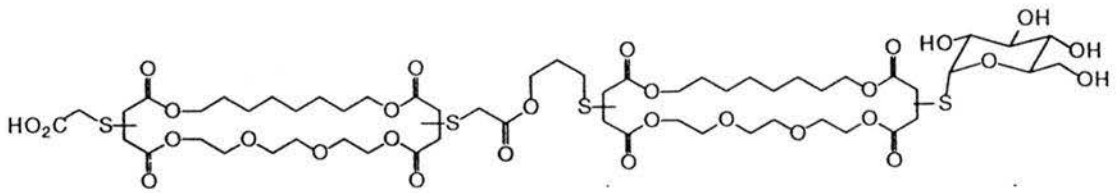

A8TrgAP8TrgG

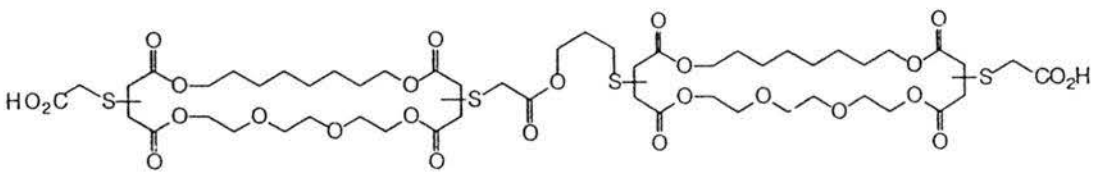

A8TrgAP8TrgA

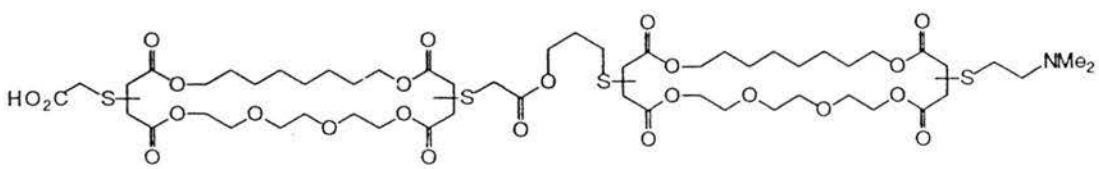

A8TrgAP8TrgN

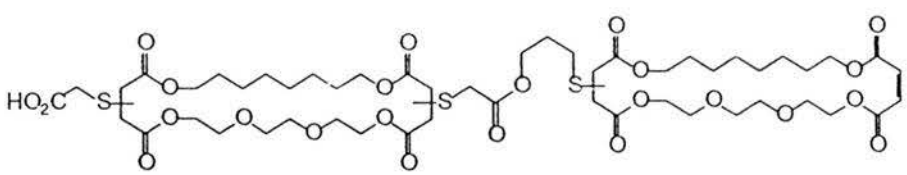

A8TrgAP8Trg

Figure 3.1: Structures of the bola-amphiphiles A8TrgAP8TrgX.

Table 3 summarizes transport studies of these four compounds conducted with the pH-stat vesicle assay.[64,72] Only one compound, A8TrgPA8TrgA, a dianion at the pH of the experiment, displayed a significant selectivity for potassium. For the other compounds the effect of the head groups on the transport rates of alkali metal cations remained

modest. The apparent kinetic order has been determined to be about 2 indicating the formation of small aggregates in all cases.

Table 3: Transport of alkali metal ions across vesicle membranes by bola-amphiphiles. The results were taken from Fyles *et al.*[72]

Transporter	rate x 10^{10}, mole $H^+ s^{-1}$					Apparent
	Li^+	Na^+	K^+	Rb^+	Cs^+	Kinetic order
G8TrgPA8TrgA	20	24	22	a	19	2.0
N8TrgPA8TrgA	12	13	11	13	13	2.3
A8TrgPA8TrgA	4.4	5.1	10	7.2	5.3	1.8
8TrgPA8TrgA	4.6	a	6.2	5.7	5.4	2.1

a: not determined

As we expected these results imply aggregates as the active structures and show that the head groups indeed influence the selectivity between alkali metal cations. While vesicle experiments generally yield information on an ensemble of transporters, planar bilayer experiments can in principle probe the activity of single molecules. Furthermore, the transmembrane potential can not easily be varied in the vesicle assay and therefore the possibility of a voltage-sensitive active structure can not be investigated.

3.1 Typical activity in planar bilayer membranes

Figure 3.2 shows a typical single-channel recording for A8TrgPA8TrgA in 1 M CsCl. A total of 40 nmol of compound were added to the cis compartment and a transmembrane potential of 100 mV was applied.

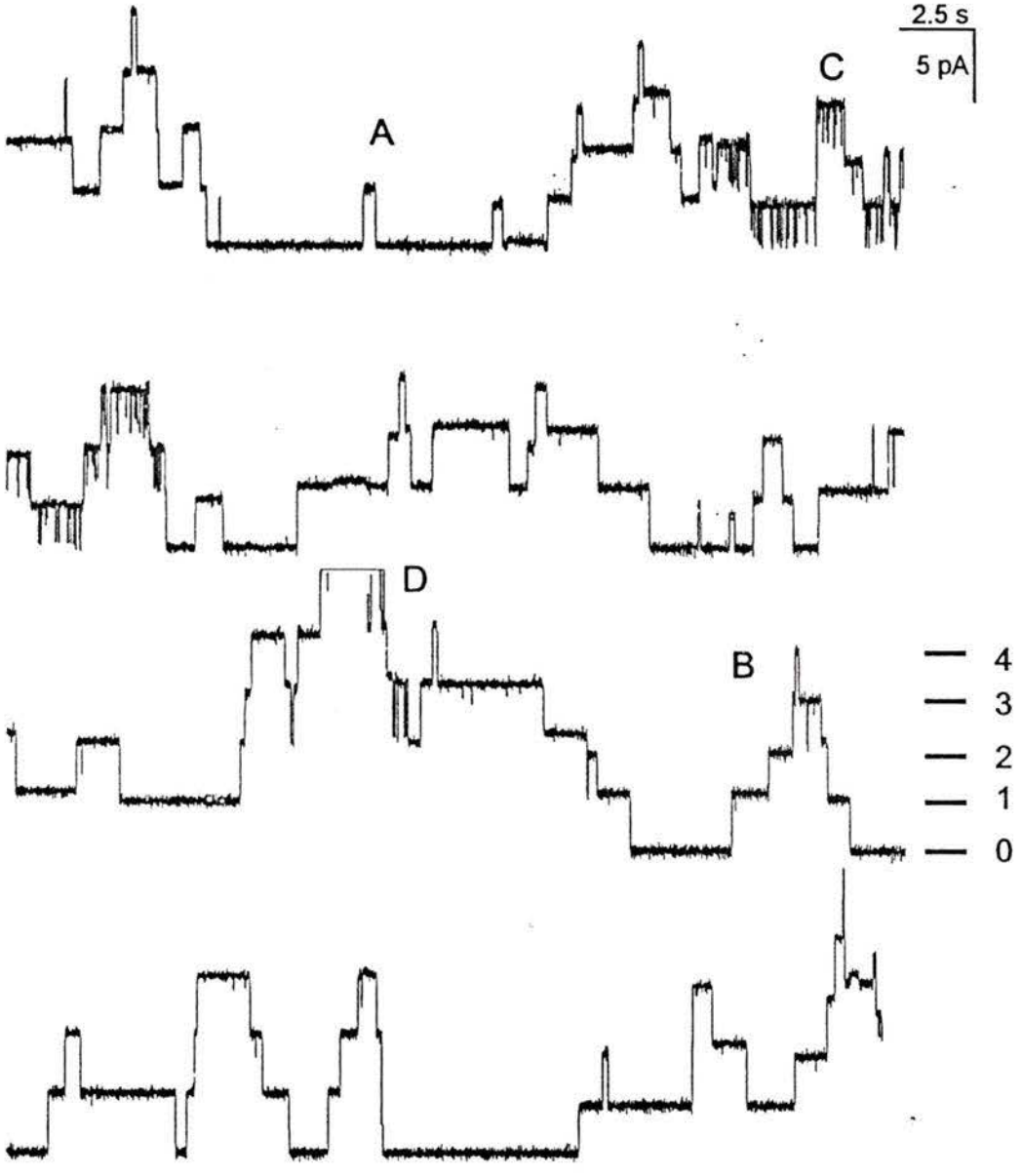

Figure 3.2: Typical example of transmembrane currents produced by 40 nmol of A8TrgPA8TrgA in a diPhyPC bilayer separating 1 M CsCl symmetrical electrolyte at 100 mV applied transmembrane potential. This 2 minutes long trace was recorded 30 min. after addition of the transporter to the cis compartment. The data was acquired at 1 kHz and was analog filtered with 100 Hz.

The displayed section of the experiment was recorded about 30 minutes after addition of the transporter and is representative of a behaviour sustained over periods of up to one hour. Step conductance changes consistent with the switching on and off of a channel-type transporter can be observed. This type of activity is also characteristic for protein channels that conduct cations and of small peptides that are known to operate with a channel-type mechanism such as gramicidin. Rarely, however, were single square topped events such as the ones marked with "A" observed. The more frequently observed behaviour was a series of steps of apparently the same height such as in section "B" of the record. The total number of levels is not immediately clear. Near "B" at least 4 discrete levels can be observed and close to "D" more than 5 levels are apparent. The straight line indicates where data has been cut off the display. Many of the openings have durations of several seconds, but some much shorter "flickering" events, indicated by "C", are evident as well. Figure 3.3 illustrates this type of behaviour further. Part a) shows a 15 second long piece of the record presented in Figure 3.2. An expansion of the time scale is shown in part b) of the Figure. These "flickering" events seem to be fast open-close transitions of one particular channel where the active structure does not close completely.

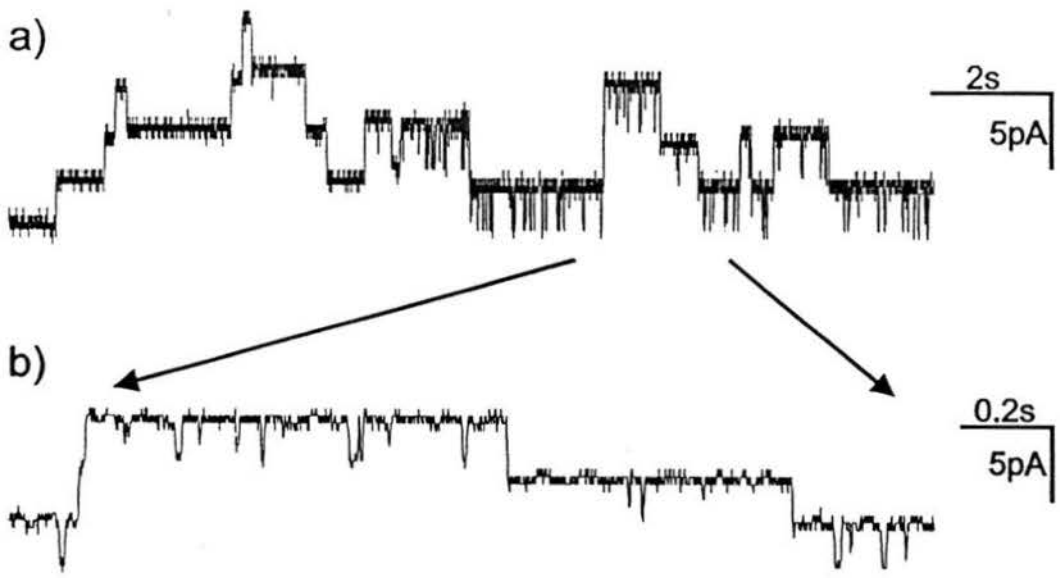

Figure 3.3: a) 15 seconds of the first data trace shown in Figure 3.2. b) Expansion of the section indicated by the arrows in part a).

This behaviour is typical for all bola-amphiphiles in this series. The formation of multiple channels could be observed in all cases within 15 minutes or less after addition of methanolic solutions of the transporter to the aqueous phase. Controls establish that the observed currents were not due to disruption of the membrane with methanol. No detectable effect of up to 4 % methanol (vol./vol.) has been observed whereas typical experiments involve less than 2% methanol.

In a typical experiment discrete single channel openings such as in "A" in Figure 3.2 can be observed initially. As the experiment progresses, however, individual levels can not be discerned within the multiple openings. The multiple-step behaviour persists until the membrane ruptures. The bilayer capacitance is usually stable during the course of the experiment at no applied transmembrane potential. In a few cases the capacitance decreased. This decrease was accompanied by a loss of transport activity. Assuming a constant membrane area a decrease in capacitance indicates an increase in bilayer thickness. The loss of observed activity suggests that at this point the bilayer thickness exceeds the maximum span of the transporter. Multiple step behaviour such as depicted in Figure 3.2 precludes the determination of the kinetics of the onset of pore formation. In general, kinetic information can be obtained from the distribution of dwell times and the probability of a channel being open under conditions where a single molecule is present in the membrane. When multiple channels are present it is possible to determine the number of conducting structures in each burst such as indicated by "B" in Figure 3.2 and therefore the average dwell time of an ensemble of channels. The value of information thus gained, however, is limited. We chose to limit the analysis of such a record to information on the distribution of step heights. This can be obtained by constructing a current amplitude histogram such as depicted in Figure 3.4. The solid curves are Gaussian fits to the clusters of peaks in the histogram calculated with a Simplex least square fit routine provided by the pClamp6 suite. The maximum of each Gaussian gives the average current carried at each level, and the width represents its distribution.

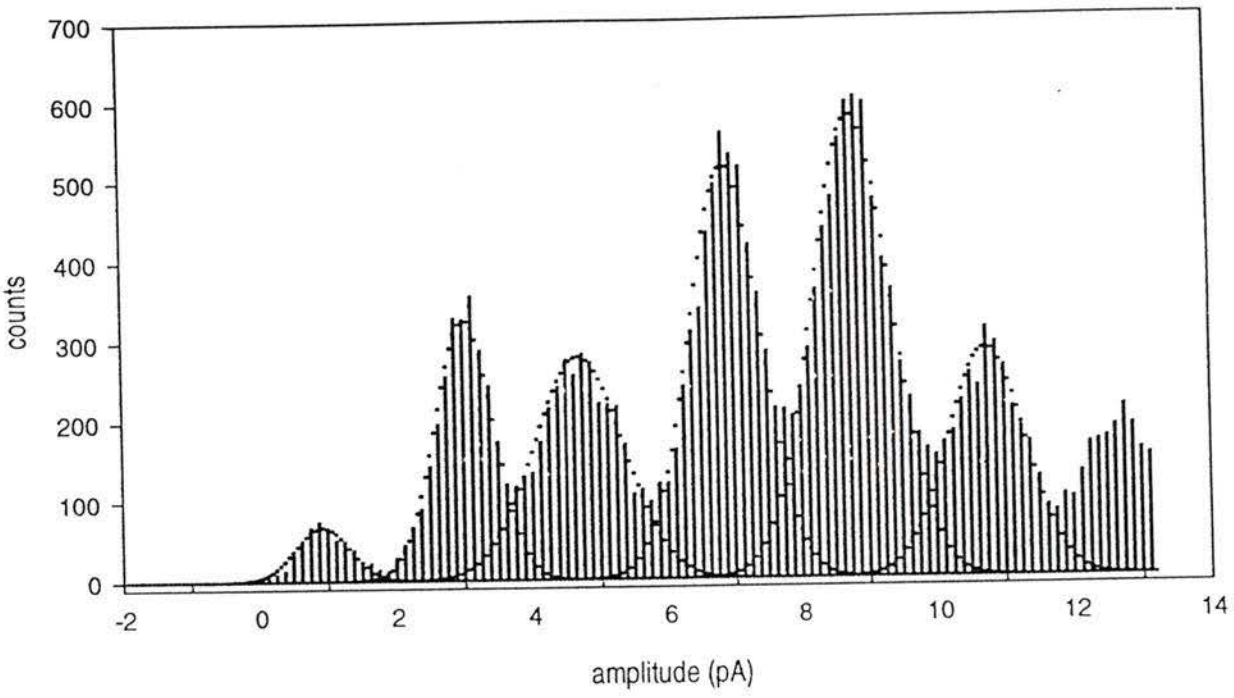

Figure 3.4: Amplitude histogram for the experiment of Figure 3.2. The curves are Gaussian fits to the histogram data.

3.2 Are the active structures aggregates?

The question now arises whether the multiple levels in Figure 3.2 are multiple copies of the same species or multiple conductance states of different sized aggregates. The former possibility can be observed for high concentrations of gramicidin whereas the latter one is exemplified by alamethicin. Planar bilayer experiments for both peptides have been performed to illustrate these possibilities. Figure 3.5 compares a record for A8TrgPA8TrgA (b), with multiple channels from gramicidin (a), and the burst openings of alamethicin (c). Both the regular openings and the long dwell times observed for the bola-amphiphile are similar to the openings observed for gramicidin.

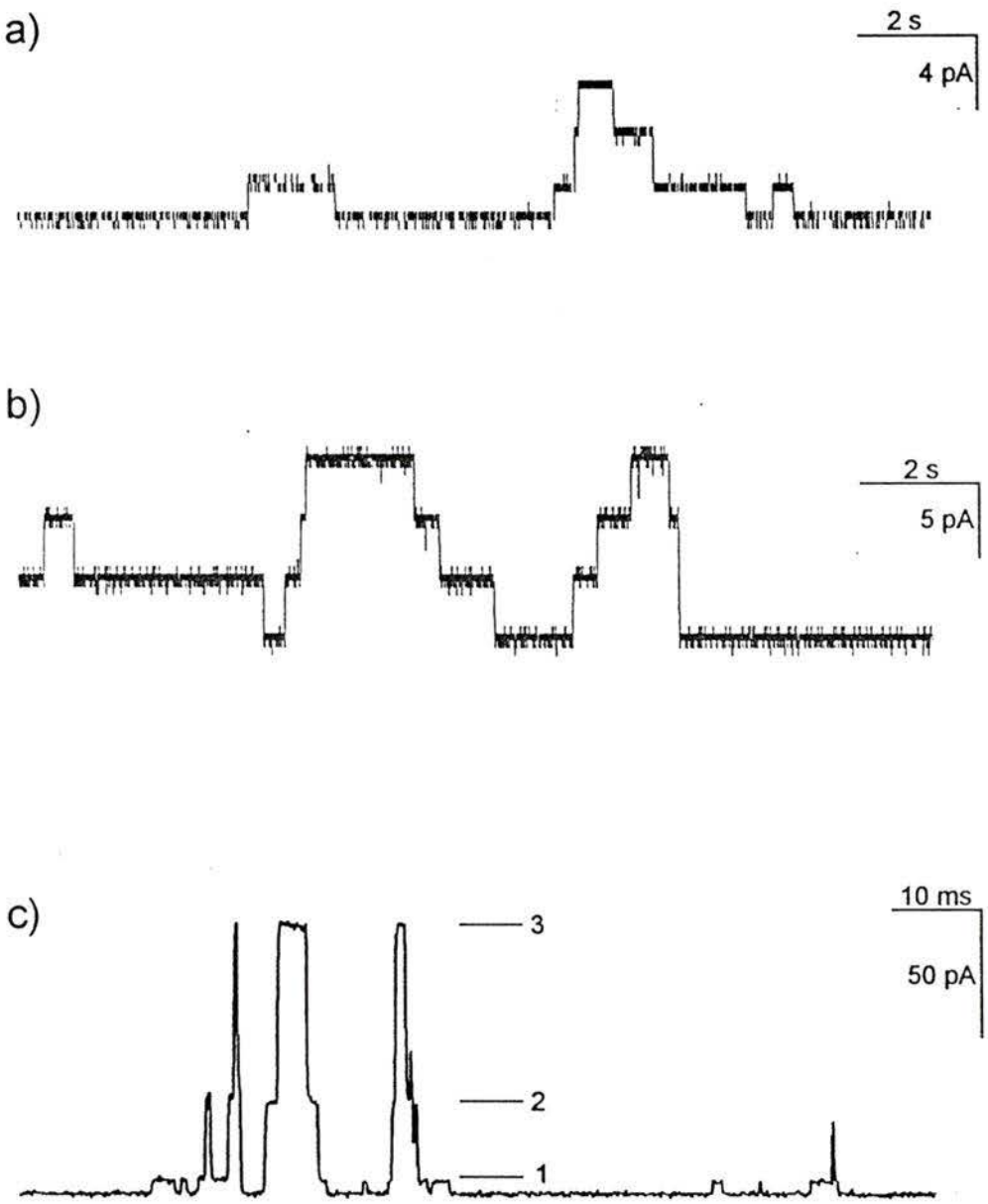

Figure 3.5: Comparison for transmembrane currents induced by a) gramicidin, b) A8TrgPA8TrgA, and c) alamethicin. a) 25 fmol gramicidin, PC:PA:Chol bilayer, 1 M KCl, 120 mV, sampled at 1 kHz, analog filtered at 100 Hz. b) conditions as for Figure 3.1. c) 0.15 nmol alamethicin, diPhyPC bilayer, 1 M KCl, + 60 mV, sampled at 25 kHz, analog filtered at 2 kHz. Levels 1 - 3 added as a visual aid.

Gramicidin forms channels by dimerization of two molecules in opposing bilayer leaflets. Each channel has the same stoichiometry and roughly the same dimensions. The conductance is therefore a linear function of the level number where the slope yields the specific conductance for a single active structure. This is illustrated in Figure 3.6 a). Alamethicin on the other hand is believed to form aggregates of different size by addition or deletion of monomers to an already existing pore (barrel stave model).[19] The conductance should initially increase much more steeply upon enlargement of the central water-filled pore. The change in conductance from the pentamer to the hexamer is expected to be larger than the change from heptamer to octamer.[19] Thus a plot of conductance as a function of level number eventually levels off, as depicted in Figure 3.6 b).

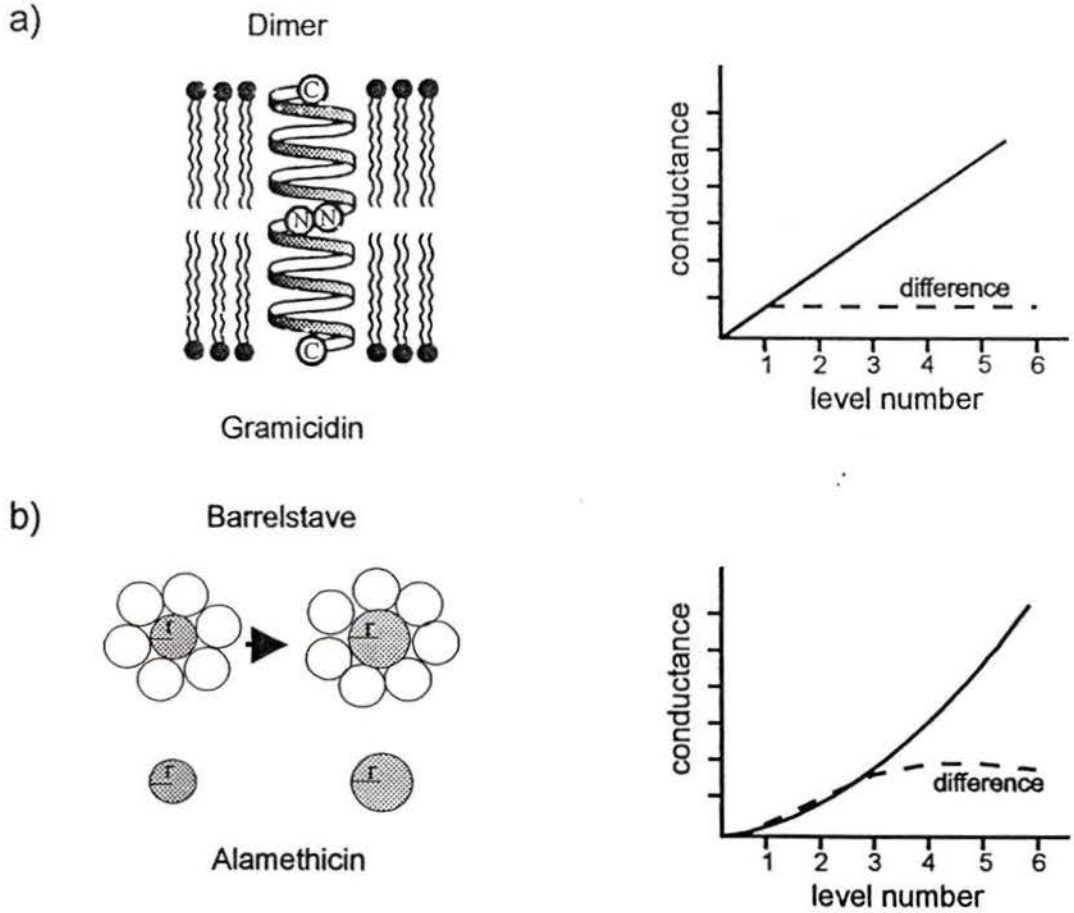

Figure 3.6: Schematic depiction of the proposed model of pore formation by gramicidin, a), and alamethicin, b), and the expected plots of conductance as a function of level number.

The plot of the current as a function of level created from the amplitude histogram shown in Figure 3.4 is presented in Figure 3.7. We notice that the characteristic increase in level spacing observed for alamethicin does not apply to A8TrgPA8TrgA. A straight line with slope 37.6 pS/level can be fit to the data. A plot of the difference between steps, which is also linear, shows that indeed a regular progression of steps is observed, implying multiple copies as found for gramicidin.

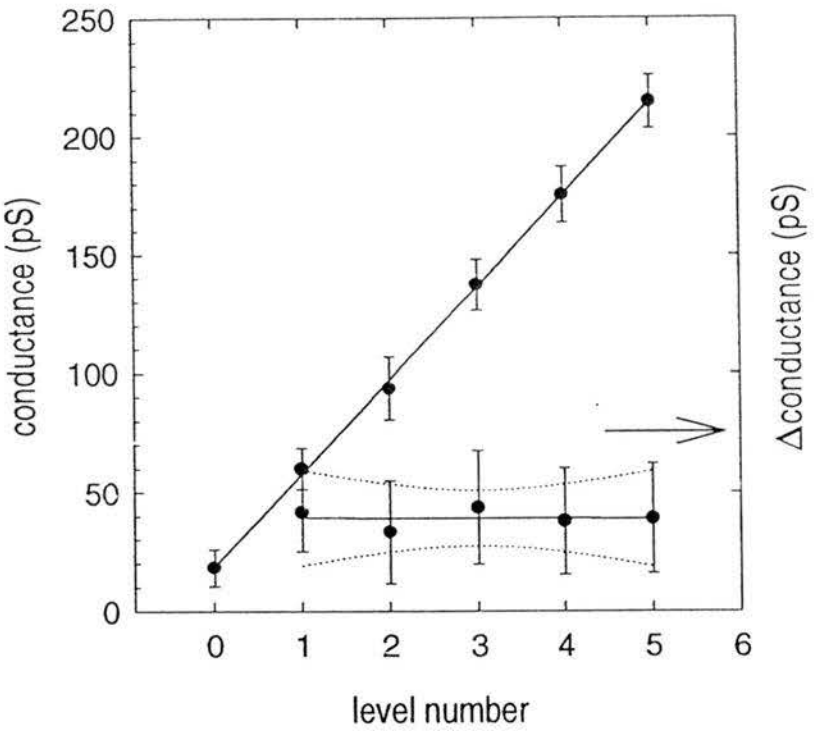

Figure 3.7: Plot of conductance as a function of the step number.

This holds against a barrel-stave model for pore formation as is proposed for alamethicin. Rather, the active species must be a monomer or an aggregate of defined stoichiometry. In view of the kinetic order of about 2 in the vesicle experiment[64] it is most likely that dimers are the active species. Higher oligomers can not be excluded but a larger spread in the observed amplitudes would be expected for that case.

If the active structures are indeed dimers, differences in conductivity between the head-to-head and head-to-tail dimers may be anticipated for the bola-amphiphiles with different head groups. Figure 3.8 shows 20 seconds of typical single-channel recordings for the compounds with the A, N, and G head group. These traces occurred early in an experiment where mostly single step changes in conductance were observed.

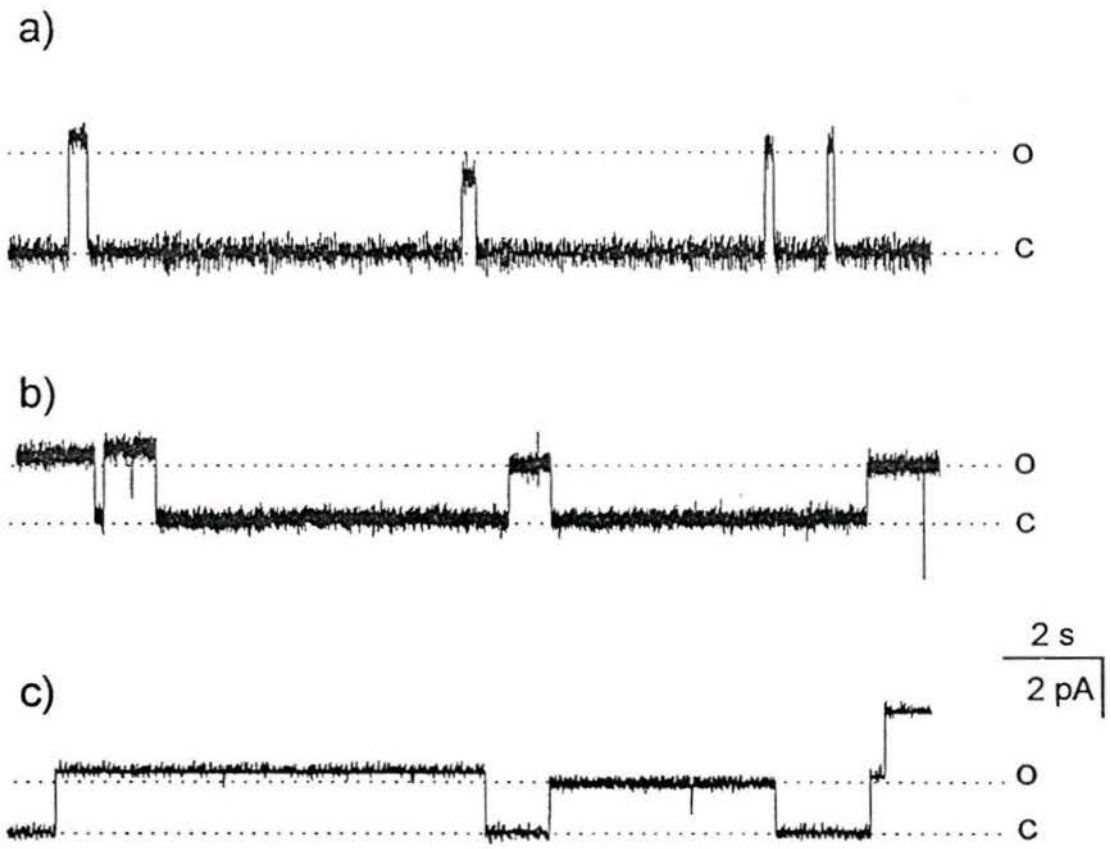

Figure 3.8: Transmembrane currents induced by 40 nmol of bola-amphiphile in 1 M KCl and diPhyPC bilayers. a) A8TrgPA8TrgA, + 100 mV b) N8TrgPA8TrgA, + 120 mV c) G8TrgPA8TrgA, + 120 mV. Data for a) and c) was acquired at 1 kHz and analog filtered at 100 Hz while in b) the sampling frequency was 10 kHz and 1 kHz filtering.

Visual inspection of these traces indeed reveals small differences in step height between successive openings. These differences, however, are also observed in a) for the symmetric compound and can therefore not be attributed to different dimers. Statistical analysis of amplitude histograms of these records does not substantiate the observation of distinctly different step heights, as no sub conductance states can be detected. Conformational differences of the aqueous pore formed by the bola-amphiphiles are believed to be the cause for these small differences.

3.3 Ion selectivity

Figure 3.9 shows a current-voltage diagram for A8TrgPA8TrgA with three electrolytes.[73] Each point was determined from the mean step-height for multiple channel openings in the current-time record at the indicated voltage by the procedure illustrated in Figure 3.4. The slope of each line is the specific conductance for each electrolyte. An ohmic current response is observed for applied transmembrane voltages for all electrolytes and all compounds in this series, indicating that the ion translocation through the pores is not rectified.

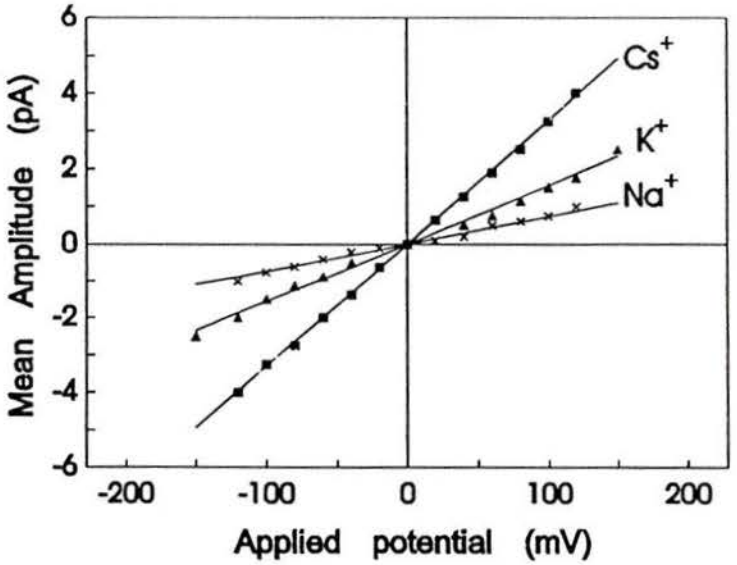

Figure 3.9: Current-voltage diagram for A8TrgPA8TrgA in diPhyPC bilayers for the electrolytes indicated in the Figure.

A modest selectivity between alkali metal cations is observed, with cesium being the most easily transported ion. Table 4 summarizes the specific conductances with different electrolytes.

Table 4: Specific conductances of multiple channel records in diPhyPC bilayers determined by W. Van-Straaten Nijenhuis

Compound	specific conductance 1 M CsCl (pS)	specific conductance 1 M KCl (pS)	specific conductance 1 M NaCl (pS)
8TrgPA8TrgA	32.9 ± 0.3	15.5 ± 0.4	7.7 ± 0.3
A8TrgPA8TrgA	29.3 ± 0.9	15.0 ± 0.5	9.9 ± 0.3
N8TrgPA8TrgA	32.5 ± 0.5	15.8 ± 1.1	9.0 ± 0.2
G8TrgPA8TrgA	33.1 ± 0.6	16.3 ± 0.4	9.4 ± 0.4

The principal finding of Table 4 is that the structure of the compounds play only a minor role in determining the selectivity. All compounds show cation selectivity in the order $Cs^+ > K^+ > Na^+ > Li^+$, following Eisenmann selectivity sequence I or II. This selectivity sequence follows the mobility of the cations in water and indicates an aqueous pore that is large enough for the ions to flow through without undergoing specific interactions with the oxygen atoms in the wall units and the linker. The energy barrier for cation transport therefore does not appear to lie at the channel entrance in the head group region but deeper in the bilayer. The observed selectivity sequence varies from the ones observed with the vesicle assay.[64,72] A single opening of an ion channel can equilibrate the content of a typical vesicle used in this assay within about 100 ms. Therefore, in contrast to the planar bilayer experiment, the vesicle assay does not monitor the ion translocation step. Rather the onset of ion transport is the rate process observed.

The cation:anion selectivity can be determined from the reversal potential, V_{rev}, the potential at which there is no net ionic current in the presence of a concentration gradient across the bilayer. The Goldmann-Hodgkin-Katz equation[10,12,22] (equation 2) relates the reversal potential to the ion concentrations on the two sides of the bilayer (subscript *cis* and *trans*)

$$V_{rev} = \frac{RT}{F} \ln \left(\frac{P_{Na}\gamma_{Na}[Na^+]_{trans} + P_{Cs}\gamma_{Cs}[Cs^+]_{trans} + P_{Cl}\gamma_{Cl}[Cl^-]_{cis}}{P_{Na}\gamma_{Na}[Na^+]_{cis} + P_{Cs}\gamma_{Cs}[Cs^+]_{cis} + P_{Cl}\gamma_{Cl}[Cl^-]_{trans}} \right) \quad (2)$$

where the symbols have the same meaning as in chapter 2. To obtain the cation:anion permeability ratio, P_K/P_{Cl}, the same electrolyte at two different concentrations can be used. Direct substitution of the concentrations in equation 2 gives the permeability ratios listed in Table 5. Figure 3.10. a) shows the current-voltage diagram of a multi channel experiment under symmetric electrolyte conditions. Ohmic current response passing through the origin can be observed. In part b) of Figure 3.10 a typical experiment for the determination of cation:anion permeability is shown. The voltage at which there is no net current flow is + 36.8 ± 0.6 mV, indicating a cation selective pore. It is evident that the current-voltage diagram does not follow Ohm's law anymore. The currents carried at negative potentials are much higher than the currents carried at positive potential. This is expected for a cation selective pore.[33] Negative current flux corresponds to the movement of ions from the *trans* to the *cis* side, in this case from the compartment with the more concentrated electrolyte to the compartment of lesser concentration.

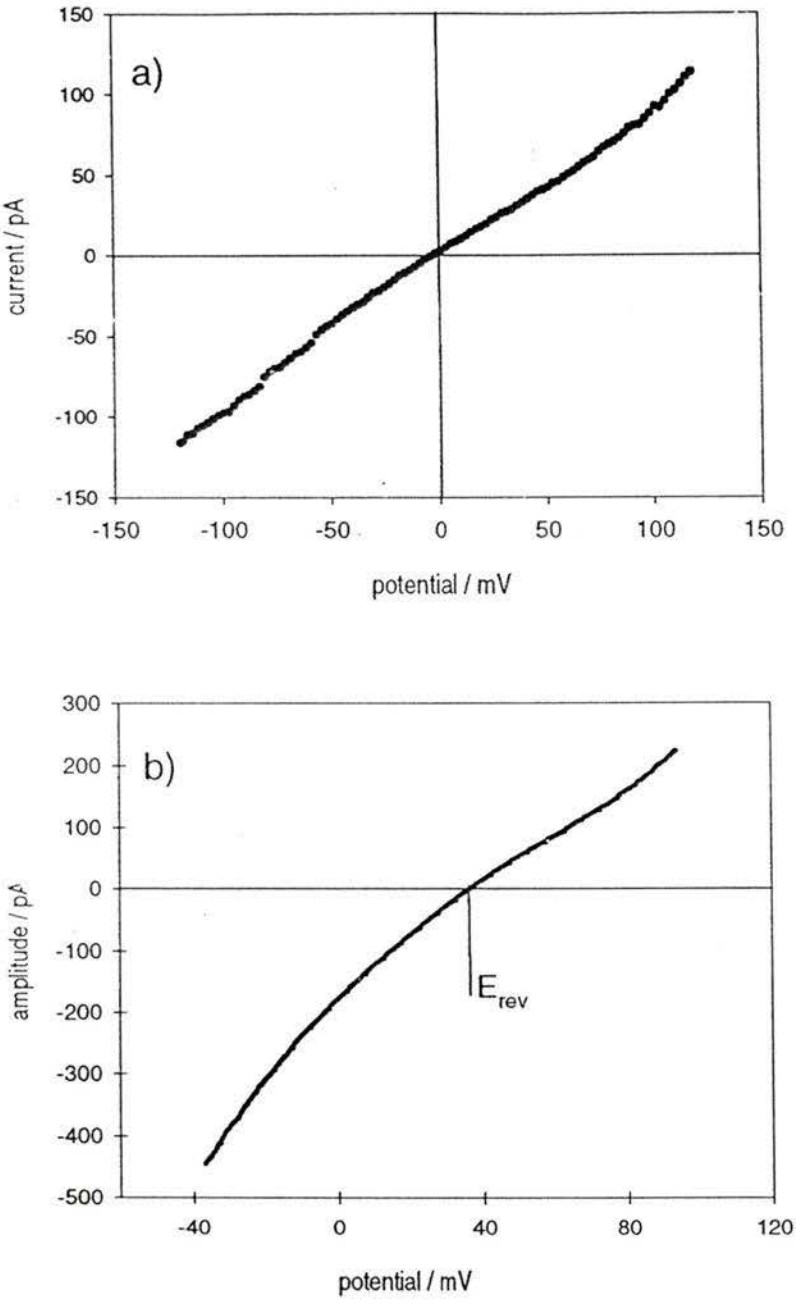

Figure 3.10: a) Current-voltage diagram for multiple step conductance changes induced by 70 nmol G8TrgPA8TrgA in a diPhyPC bilayer, 1 M KCl electrolyte. 20 cycles of a voltage ramp from -120 to + 120 mV were averaged. b) Average of 10 cycles of a voltage ramp from -40 to 100 mV. Currents were induced by 60 nmol of A8TrgPA8TrgA in a diPhyPC membrane, 0.5 M KCl(trans) and 0.1 M KCl(cis).

The selectivity between different cations can be expressed in two ways. It can be described as the ratios of the specific conductances for different salts in independent experiments.[22] Alternatively, it can be determined from the reversal potentials for two cations in competition. With NaCl on the *trans* side of the bilayer and CsCl in the *cis* compartment, equation 2 can be rearranged so that the permeability ratio is given by equation 3:

$$\frac{P_{Na}}{P_{Cs}} = \exp\left(\frac{V_{rev} F}{R T}\right) \qquad (3)$$

Table 5 gives the permeability ratios calculated from V_{rev} for the transporters, in comparison with conductance ratios calculated from the data of Table 4.

Table 5: Ion selectivity of transporters[a]

Compound	Cs:Na Conductance Ratio	K:Na Conductance Ratio	Cs:Na Permeability Ratio (V_{rev} (mV))[b]	K:Na Permeability Ratio (V_{rev} (mV))[b]	K:Cl Permeability ratio (V_{rev} (mV))[b]
8TrgPA8TrgA	4.3 ± 0.3	2.0 ± 0.2	32 ± 1 (89 ± 0.7)	24 ± 0.2 (81.2 ± 0.2)	9.0 ± 5 (31.1 ± 3.4)
A8TrgPA8TrgA	3.1 ± 0.3	1.5 ± 0.2	8.3 ± 0.4 (54.4 ±1.1)	[c]	25 ± 4 (36.8 ± 0.6)
N8TrgPA8TrgA	3.6 ± 0.3	1.7 ± 0.3	6.5 ± 0.5 (-44 ± 2)	3.9 ± 0.3 (-21 ± 2)	9.5 ± 0.5 (31.1 ± 0.6)
G8TrgPA8TrgA	3.5 ± 0.4	1.7 ± 0.4	5.5 ± 1.0 (48 ± 2)	1.1 ± 0.3 (35 ± 2)	8.0 ± 5 (29.8 ± 6)

[a] The conductance ratios are determined from the data of Table 4.

[b] Permeability ratios are determined from reversal potentials. DiPhyPC bilayers, 300 K. Electrolyte concentrations for cation:cation permeability ratios are 1 M. Reversal potentials are reported in mV for: $NaCl_{cis}$:electrolyte$_{trans}$. Negative values indicate NaCl in the *trans* compartment. Cation:anion permeability ratios have been determined using 0.5 M KCl_{trans} and 0.1 M KCl_{cis}.

[c] Not determined.

Several structurally related trends are apparent. The marked K^+:Cl^- selectivity of A8TrgPA8TrgA must be related to its net dianionic charge relative to the mono-anionic and zwitterionic members of the series. Due to this negative charge anions are repelled from the channel entrance. Moreover 8TrgPA8TrgA shows very significant discrimination against Na^+ relative to the other compounds, probably due to the single head group. Monomers of this compound can approach each other more closely due to reduced steric and electrostatic repulsion. The resulting aqueous pore possesses a smaller diameter and the ions that can most easily be stripped of their hydration shell can migrate through the pore faster. The same selectivity sequence is observed for the experiments with different ions in competition as for the single salt experiments. Note that the permeability ratios are greater than the conductance ratios. This is a significant excursion from systems such as gramicidin where the converse is normally observed.[10,18,19] It implies that the conducting pores in this series are flexible and form an aqueous environment according to the passing ions needs. When all ions are of the same type as in the single electrolyte cases, no reorganization during an open state is required and the observed conductivities follow the mobility of the ion in water. Between competing cations, energy barriers for reorganization would favor ions of a similar type following one another. The observed selectivities would then imply that expansion of the pore is less unfavorable than contraction. These results therefore suggest that a cation-dependent channel structure is formed.

3.4 Effect of electrolyte concentration on the specific conductance

The question arises whether the pores are occupied by single ions at a time or whether multiple ions can enter the channel structure. At low electrolyte concentrations ions will move through the pore independently and the ionic flux will be exactly proportional to the ionic concentration. If a pore can bind only one ion at a time the ionic flux will saturate under the assumption that the ions bind to specific sites in the pore. A

plot of the specific conductance as a function of electrolyte concentration should exhibit a maximum when multiple ions can occupy the channel.[20,22] This possibility has been investigated for G8TrgPA8TrgA and potassium chloride as electrolyte. Figure 3.11 demonstrates that while the specific conductance is a linear function of the electrolyte at low concentrations, the plot indeed exhibits a maximum at a concentration of 1 M KCl.

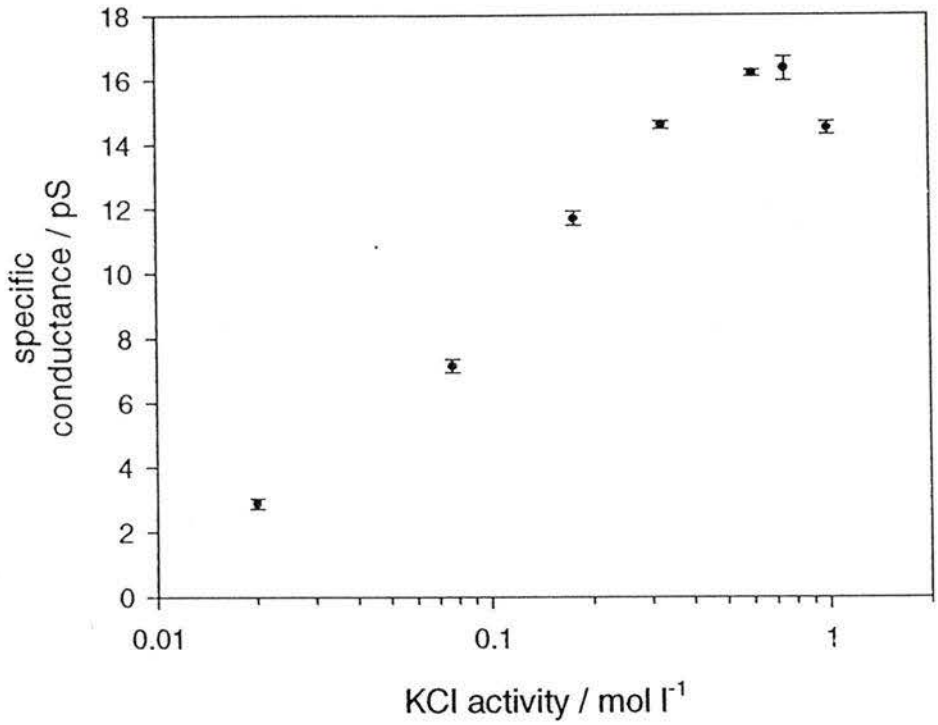

Figure 3.11: Specific conductance of G8TrgPA8TrgA as a function of electrolyte activity. DiPhyPC bilayers, KCl activities as indicated on the graph.

The influence of the electrolyte on the ion transport is also manifested in other ways. About twice as much transporter had to be added to the aqueous phase for electrolyte concentrations below 0.5 M as for higher salt concentrations, i.e. 80 nmol as opposed to 40 nmol of compound. The time required until transport events could first be observed was about four times as long as for higher salt concentrations, up to 45 minutes in contrast to 5 to 10 minutes. These observations can be ascribed to the effect of the ionic strength on the partition coefficient from the aqueous phase to the bilayer. At higher

electrolyte concentrations more transporter will be partitioned into the membrane. Qualitatively, the dwell times of the observed step conductance changes were longer at higher salt concentrations and "flickering" events such as depicted in figure 3.2 were less frequent. At higher ionic concentrations more ions will be available to pass through the pore and the open structure will be kinetically stabilized by a constant stream of ions interacting with the pore walls.

3.5 Mechanism

Although the ion selectivity sequences for the investigated bola-amphiphiles are different in planar and curved (vesicle) membranes, the general features of the mechanism for ion transport are assumed to be the same. The difference in selectivity is attributed to the different nature of the kinetic processes being observed. While single-channel experiments examine the ion translocation step directly, vesicle experiments probe the onset of ion transport. In a multiple channel case such as this very little information on the initiation (gating) of the openings can be obtained. Vesicle experiments, on the other hand, assume that channel activity is high[58,62,74] and the kinetics report only the initiation events. In the pH-stat experiments performed by X. Zhou[64] a pH gradient of one unit is maintained across the vesicle membrane, corresponding to a transmembrane voltage of +60 mV. Typical vesicles are of about 350 nm diameter and hold 5×10^5 protons at pH 5.5. The content of such a vesicle could be equilibrated by a 15 pS channel in 100 ms with a single channel opening. The openings in Figure 3.2 are much longer than this. Therefore the initiation of channel openings must be differently dependent on the cations than the actual ion translocation step.

The uniformity of the step conductance changes in planar bilayers implies that the active structures are remarkably similar. The apparent kinetic order of 2 in vesicles invoke aggregates of bola-amphiphiles as the conducting structures. The simplest model consistent with results from both planar bilayer and vesicle experiments would be active

dimers. While the formation of higher aggregates can not be excluded, a model of oligomers in equilibrium with monomers analogous to alamethicin is not supported by the single channel data. Rather multiple copies of a discrete species are assumed to be the active structure. The observed cation selectivity, although modest, further substantiates the postulation of small aggregates. Large pores composed of several monomers are not expected to discriminate between ions. Unfortunately no spectroscopic probes are present in this suite of compounds to study the features of the proposed aggregates. Figure 3.12 illustrates some possible intermediate stages for A8TrgPA8TrgA.

Initially the compound must diffuse to the membrane. State A represents the result of the diffusion step. No specific interaction between the bola-amphiphile and the bilayer is implied. U-shaped insertion of the compound into one leaflet of the bilayer, state B, can be envisaged, followed by the penetration of one of the head groups, state C. Alternatively, this transmembrane state can be achieved by direct insertion. A second head group penetration can then generate another U-shaped conformation in the opposite bilayer leaflet, state D. This transfer of a molecule from one bilayer leaflet to the other is generally called flip-flop, implying no specific mechanism. All head groups in this suite of compounds are small and polarizable and can presumably penetrate the bilayer easily. States A to D must all be inactive for ion translocation assuming that the insertion proceeds one molecule at a time. No direct evidence on the rates of these steps exists but we assume that they are slower than the channel initiation steps that follow. Generally transmembrane motions of lipids or related bola-amphiphiles[75-77] are several orders of magnitudes slower than lateral diffusion rates.

Several possibilities exist for the ion conducting states. Two U-shaped states could dimerize to generate state E. Alternatively, side-to-side dimerization of B or D could lead to active structures (not illustrated). This possibility is regarded as unlikely as studies of bola-amphiphilic bis-crownethers support the role of state B as a precursor to membrane disruption.[65] U-shaped insertion is also implicated in the membrane disrupting systems

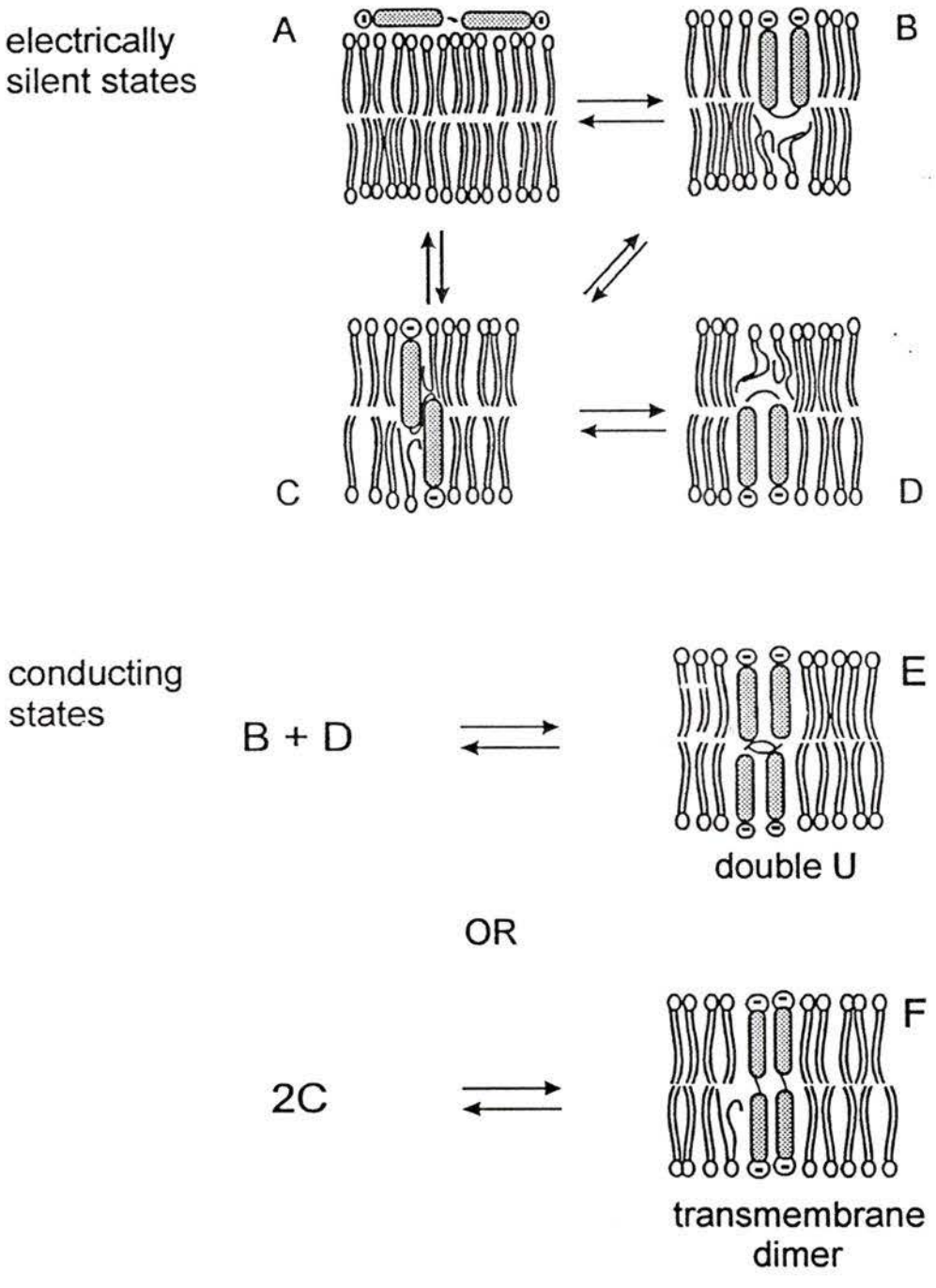

Figure 3.12: Schematic of states leading to pore formation by bola-amphiphiles

reported by Regen.[44,78] The transmembrane dimer represented by F is the most likely responsible for the observed ion transport. The long dwell times of the conducting states point towards a relatively stable structure that can resist the lipid movement in the bilayer leaflets. Phosphatidylcholines possess lateral diffusion constants on the order of 10^{-8} cm^2 s^{-1}.[79] Thus the pore encounters a multitude of collisions with lipid molecules without dissociating. It is unlikely that a structure as depicted in E would persist in such circumstances over several seconds, unless specific stabilizing interactions such as hydrogen bonds are present. Note that there are no groups capable of forming hydrogen-bonds in the linker or wall units of the transporter molecules. Dimerization or aggregation allows for both hydrophobic and hydrophilic interactions to be satisfied. In an aggregate the hydrophilic parts of the wall units point towards each other and thereby stabilize an aqueous fjord deep within the hydrophobic part of the bilayer. This keeps the hydrophilic part in contact with a polar environment. The presence of water in the pore will stabilize the aggregate and an open state should be energetically preferred over the closed state. The hydrophobic parts of the wall units will interact with the lipid environment. Changes in the order of the lipids in the bilayer membrane can also occur upon aggregation.[14] This mainly entropic effect is similar to the hydrophobic effect in aqueous solutions. Aggregation will lead to an overall decrease in order of the lipid molecules as the number of lipids directly interacting with the monomers is decreased. Further a large mismatch between the lipid bilayer and the hydrophobic thickness of the transporter molecule has been shown to result in aggregation and domain formation of peptides.[80,81] This effect, however, should be largely dependent on the type of lipid used. Electrostatic effects due to the head groups of the transporters will also be important. Head groups of opposite charge such as **A**(-1) and **N**(+1) should favor dimerization in the head-to-tail orientation while head groups of like charge will destabilize the aggregate due to repulsive forces.

The pores formed are flexible and can accommodate the passing ions. Two factors seem to determine the ion selectivity. The head groups can control cation:anion selectivity by repelling anions from the channel mouth. They can also control the actual size of the aqueous pore via head group repulsion. From a steric point of view monomers of

8TrgPA8TrgA with a single head group can clearly approach each other much more closely than the compounds with two head groups. A difference in conductivity for dimers with different head groups may be expected. This is not supported by the data and the above presented illustration is assumed to be valid for all compounds in this series.

Although the interaction of the electric field with the dipole of N8TrgPA8TrgA is quite large and can potentially lead to orientation of the molecule in the membrane, the expected voltage dependent behaviour was not observed. The energy for a dipole aligned parallel to the electric field[82] is described by equation 4:

$$\Delta G = 2 N_A \mu E \qquad (4)$$

where N_A is Avogadro's constant, μ the dipole moment and E the electric field across the membrane. Assuming a bilayer thickness of 4 nm and a dipole moment of 144 D, a transmembrane potential of 120 mV would lead to an energy difference between the two transmembrane states of 18 kJ/mol. Neglecting all other contributions to the energetics of pore formation this energy difference can clearly be large enough to lead to rectification if the energy barrier for flip-flop is indeed high. Three possible explanations can be envisaged for the absence of voltage-dependent current flow.

A) The transporter molecules may indeed all be aligned in the preferred orientation at the time of insertion into the membrane, and remain in this conformation throughout the experiment. An absence of rectification implies that there is no major difference at the channel mouth on both sides of the membrane and no difference in energy for ion flux in either directions is encountered.

B) Alternatively it can be envisaged that the transporter molecules insert into the bilayer not according to the dipole energetics but according to kinetic effects. Both transmembrane conformations are presumably in energy wells with respect to an unaligned conformation. However, the permeability coefficient for the two head groups may be

different and therefore one head group may preferentially insert into the membrane. Assuming that there still exists a high energy barrier for the flip-flop from one conformation to the other several possibilities exist. Only the head-to-head dimers may be conducting at the energetically preferred potential. Upon reversal of the transmembrane potential these close and the tail-to-tail dimers open. Of course the possibility of head-to-tail dimers can not be dismissed. These should be energetically favored over the symmetric dimers by a few kJ/mol[14] due to decreased dipolar repulsion. The formation of these dimers would be not voltage dependent.

C) The energy barrier for flip-flop might not be as high as imagined and rapid reorientation of the transporter molecules can take place in response to the transmembrane potential. This possibility may be tested by changing the transmembrane potential during the open time of a single channel. However, the rapid onset of multi step changes in the conductance precluded these experiments.

In conclusion this suite of compounds has proven that it is possible to achieve pore formation by small aggregates that are cation selective and display step conductance changes similar to natural ion channels. The goal of realizing a voltage sensitive ion transporter, however, has not been achieved and modifications to the design proposal are necessary.

4. A voltage-gated artificial ion channel

The previous chapter investigated the ion transport properties of a suite of bis-macrocyclic bola-amphiphiles in planar bilayers. All compounds displayed step conductance changes and modest ion selectivity. However, our goal of *regulating* the ionic flux has not been realized with these transporters.

To date only a few synthetic voltage-gated ion channel systems are known and most of them are based on peptides.[19,34,35,83,84] Alamethicin is a classic example of a voltage-gated peptide that occurs in nature.[19] Lear *et al.* have synthesized a series of model peptides that differed only in the charge at the N-terminus.[35] Diminishing the electrostatic asymmetry of the peptide led to a less rectified current-voltage response. A non-peptidic tetraalkyl ammonium-butylene glycol phosphomonoester ion pair shows a range of voltage-gating behaviours which vary with each experiment.[48] The observed voltage response of these systems is attributed to the re-orientation of dipoles in response to the applied transmembrane potential.

The results presented in the previous chapter show that a large molecular dipole may be a necessary, but not a sufficient condition for voltage-gating, as ohmic current-voltage responses were observed for the investigated bis-macrocyclic bola-amphiphiles. We concluded from the data that the bola-amphiphile head groups, carboxylate, monosaccharide, and ammonium, are able to penetrate the bilayer and either transmembrane orientation depicted in Figure 3.12 can be achieved. Otherwise we would expect to observe differences in the single-channel conductance between head-head and head-tail orientations of monomers in the channel. Control over the head group penetration step while still maintaining a large molecular dipole might be expected to lead to voltage-gating. Suppose that some asymmetry could be imposed on the bola-amphiphile by making one of the head groups very hydrophilic. This would inhibit its transfer through the bilayer and impose a transmembrane conformation on the transporter where the more

hydrophilic head group resides on the side of the membrane to which the compound was added. This is illustrated in Figure 4.1. Thus only head-to-head aggregates would form and an applied transmembrane potential could then influence all dipoles in the same fashion. This would appear as rectified voltage dependence in the conductance. Limits to the size and charge of the head group had to be considered in the design as steric and electrostatic repulsion will disfavor the formation of aggregates.[64]

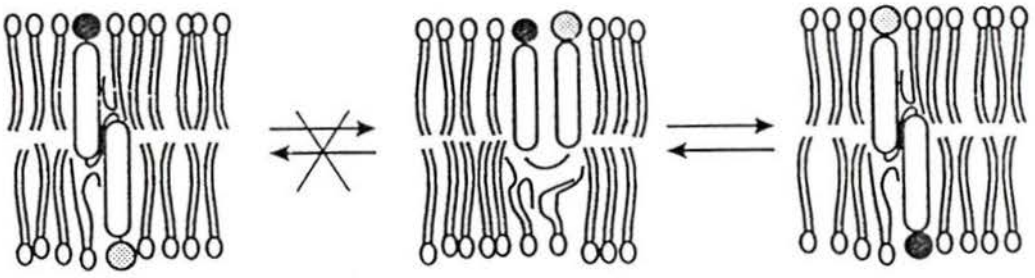

Figure 4.1: Proposed mechanism that will lead to rectified current-voltage response. The shaded circle represents the very hydrophilic head group while the dark circle stands for the less hydrophilic one.

Xin Zhou synthesized a suitable compound, S8TrgPA8TrgA, and investigated its transport behaviour in vesicles.[64] It is expected that the (2-mercapto succinic acid) head group **S** will not be able to traverse the bilayer since it carries two negative charges at a pH of greater than 6.

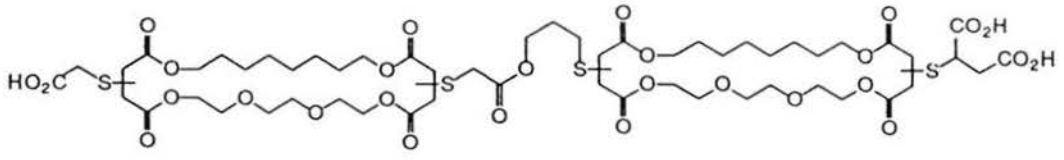

A8TrgAP8TrgS

The transport activity in vesicles was examined using the pH-stat technique.[64,72] A potential gradient of + 60 mV relative to the external phase was established *via* a pH gradient of one unit (pH 6.6 internal solution, pH 7.6 externally set pH).[64] A marked dependence of transport activity on the concentration of the bola-amphiphile was observed that deviated from the previously reported behaviour.[72] At a concentration of 5.3 μM a small initial disruption is followed by a slow transport rate near the detection limit for the experiment. Doubling the concentration results in a greater than 16-fold increase in rate. Further increases in concentration do not further accelerate the transport.[64] This very narrow window of concentration through which S8TrgPA8TrgA shifts from being virtually inactive to maximally active precluded the determination of the kinetic order for this compound. However, it is certainly larger than 2-3 as found for the bola-amphiphiles described in chapter 3,[64,72] and indicates that the active structures are aggregates.

Vesicle studies on the cation selectivity of S8TrgPA8TrgA revealed a significant difference in rates between the alkali metal cations. Addition of 21 μM of transporter induced the following rates (x 10^{10}, mol H^+ s^{-1}): Rb^+ (14), Cs^+ (3.4), K^+ (2.0), Na^+ (1.4), and Li^+ (0.5). These differences are 2-5 times greater than previously observed for the related compounds.[64,72] This effect is consistent with an increase in cation selectivity upon introduction of high anionic charge in the head group region. The selectivity follows Eisenmann II sequence,[22] indicating a predominantly electrostatic interaction between the hydrated ion and S8TrgPA8TrgA.

4.1 Typical single-channel activity

Relatively high concentrations of bola-amphiphile (100-140 nmol) are required to induce transport. Figure 4.2 shows typical currents induced by 140 nmol of S8TrgPA8TrgA in a diphytanoyl phosphatidylcholine bilayer. This record occurred about 35 minutes after the addition of the compound to the *cis* compartment of the bilayer chamber. In contrast to the previously investigated bola-amphiphiles[72] no step conductance changes can be observed. The current amplitudes of each event are at least

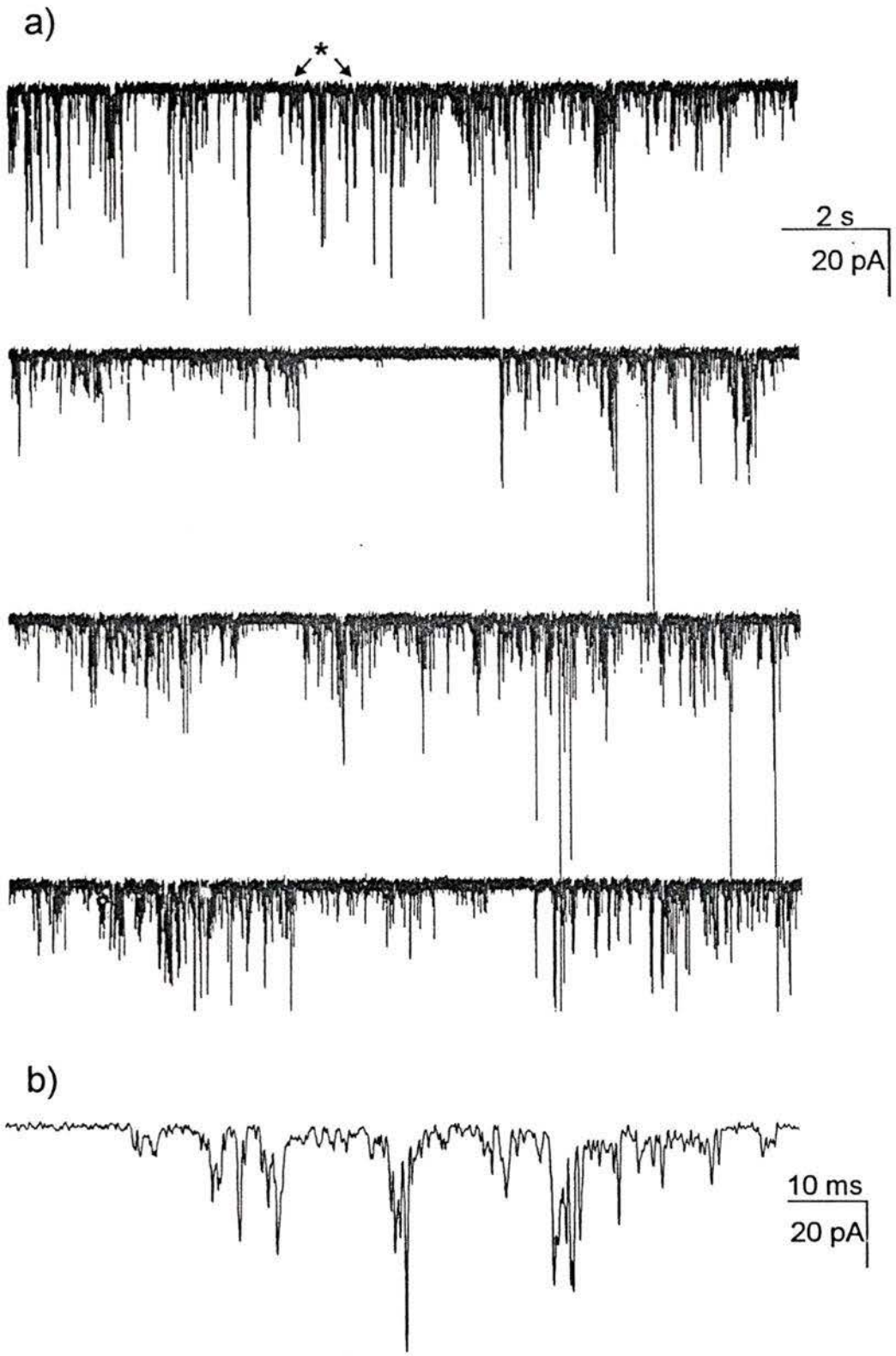

Figure 4.2: a) Typical single-channel activity of S8TrgPA8TrgA in diPhyPC bilayers. The applied transmembrane potential was -120 mV, 1 M KCl as electrolyte. B) Expansion of the labeled fragment in a). The data was sampled at 20 kHz and analog filtered at 2 kHz.

one order of magnitude larger than for the compounds with singly charged head groups and vary over a wide range of values. On the other hand the duration of the transport events is much shorter, between 0.5-10 ms, contrasting with the long duration of the openings induced by the other bola-amphiphiles in this series.[72] Transport events occur in clusters of bursts of high activity followed by periods of quiescence. This irregular behaviour may be related to the succinate, as dianionic head groups will strongly repel each other within an oriented cluster.

4.2 Macroscopic current-voltage response

The erratic current-time behaviour of S8TrgPA8TrgA precludes analysis to the same level of detail as presented for the previous set of compounds.[72] However, the macroscopic current-voltage response can be inspected for voltage-dependent behaviour. Sufficient bola-amphiphile was added to the *cis* compartment to ensure multiple channels and a voltage ramp from -100 to +100 mV was applied at a rate of 6.3 mV s^{-1}. Figure 4.3 b) shows that significant current is carried only at negative applied potentials. The few cycles displayed in figure 4.3 b) occurred near the beginning of the experiment. The current asymmetry collapsed over a period of 10-15 minutes and current was carried at both positive and negative applied potentials as shown in Figure 4.3 c). This is more clearly illustrated in the current-voltage diagrams given in Figure 4.3 d). A strongly rectified response is shown from the average of the first seven voltage ramps. This rectification is not evident in the average of later traces.

Alamethicin, a typical peptide example for voltage-gated pore formation, shows similar time-dependence in its current-voltage response.[19] Initially alamethicin induces current only at *cis*-positive potential, while current carried at later stages of an experiment is no longer rectified. This has been attributed to a leakage of alamethicin through the bilayer.[19] We assume that the time-dependence of S8TrgPA8TrgA can be attributed to a similar phenomenon. Presumably the succinate head group is initially located at the *cis* side of the bilayer and remains there in the early stages of the experiments. This

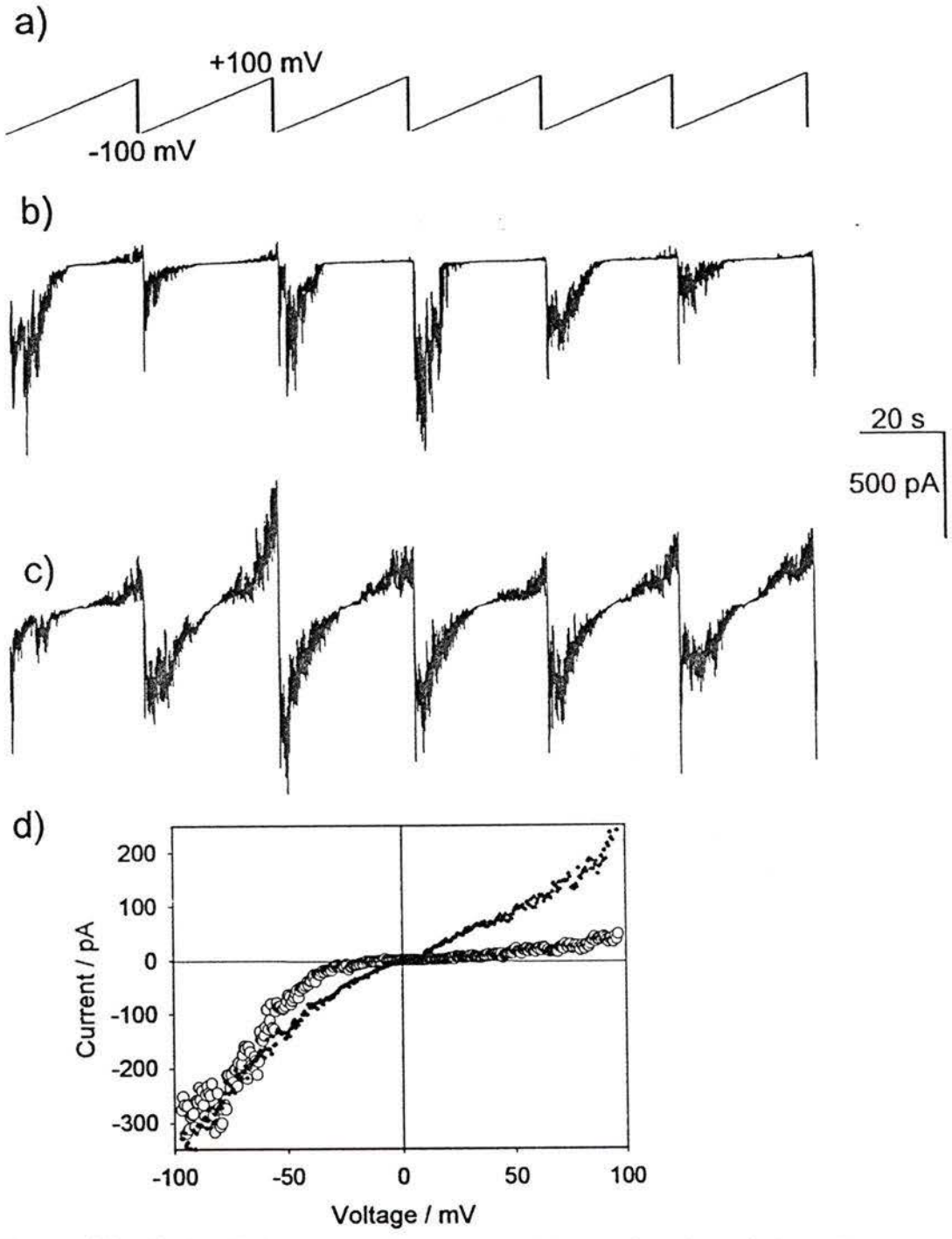

Figure 4.3: A) Applied transmembrane potential as a function of time; b) current as a function of time in response to varying applied potential (4.3.a) early in the experiment; c) current as function of time later in the same experiment; d) current averaged over cycles 1-7 (O) and 8-20 (●) as a function of applied potential for the experiment above, data set reduced 1:50. (118 nmol of S8TrgPA8TrgA, 1 M LiCl, diPhyPC, 500 Hz sampling frequency, 100 Hz filtered).

asymmetric orientation in the bilayer at early times leads to the observed voltage-gating. As the experiment progresses the succinate head group eventually crosses the bilayer, possibly assisted by the defects created in the membrane due to the activity of the bola-amphiphile. The sense of voltage-gating should then be dependent on the side of the membrane to which S8TrgPA8TrgA is added. Consistent with this prediction, addition of the transporter to the opposite compartment results indeed in current rectification opposite to that illustrated in Figure 4.3, i.e. currents are carried at *cis* positive potentials. When the compound is mixed with lipid prior to bilayer formation only ohmic current-voltage response was observed.

Two possibilities present themselves as the cause for the observed voltage-gated behaviour. The channels may increase in size in response to the applied potential. Alternatively, the number of active channels in the preparation may increase for a given potential. The irregular behaviour of the single-channels as exemplified by Figure 4.2 limits our ability to address this question directly, but qualitative information is available from square-wave conductance change experiments. As seen In Figure 4.4 a) the potential was switched from -120 mV to + 120 mV. The change in transmembrane potential produced a large capacitive current. The second segment shows high activity prior to the reversal of the potential that subsided immediately upon switching the voltage. However, the third segment shows a delay of about 100 milliseconds in which positive current was carried. This suggests a structured channel environment that can persist at the "wrong" potential. Figure 4.4 b) shows a smaller change in applied potential, from -120 mV to -80 mV. Less current is carried at the less negative potential due to the smaller driving gradient. It is also evident that there are fewer openings at –80 mV. A manual analysis of 12 traces of 20 seconds duration suggests that at –80 mV there are about 20 % of the number of events at -120 mV. Although this number by itself has no statistical significance, taken together, this qualitative analysis suggests that S8TrgPA8TrgA is voltage-gated by virtue of larger numbers of open channels occurring at more negative potentials.

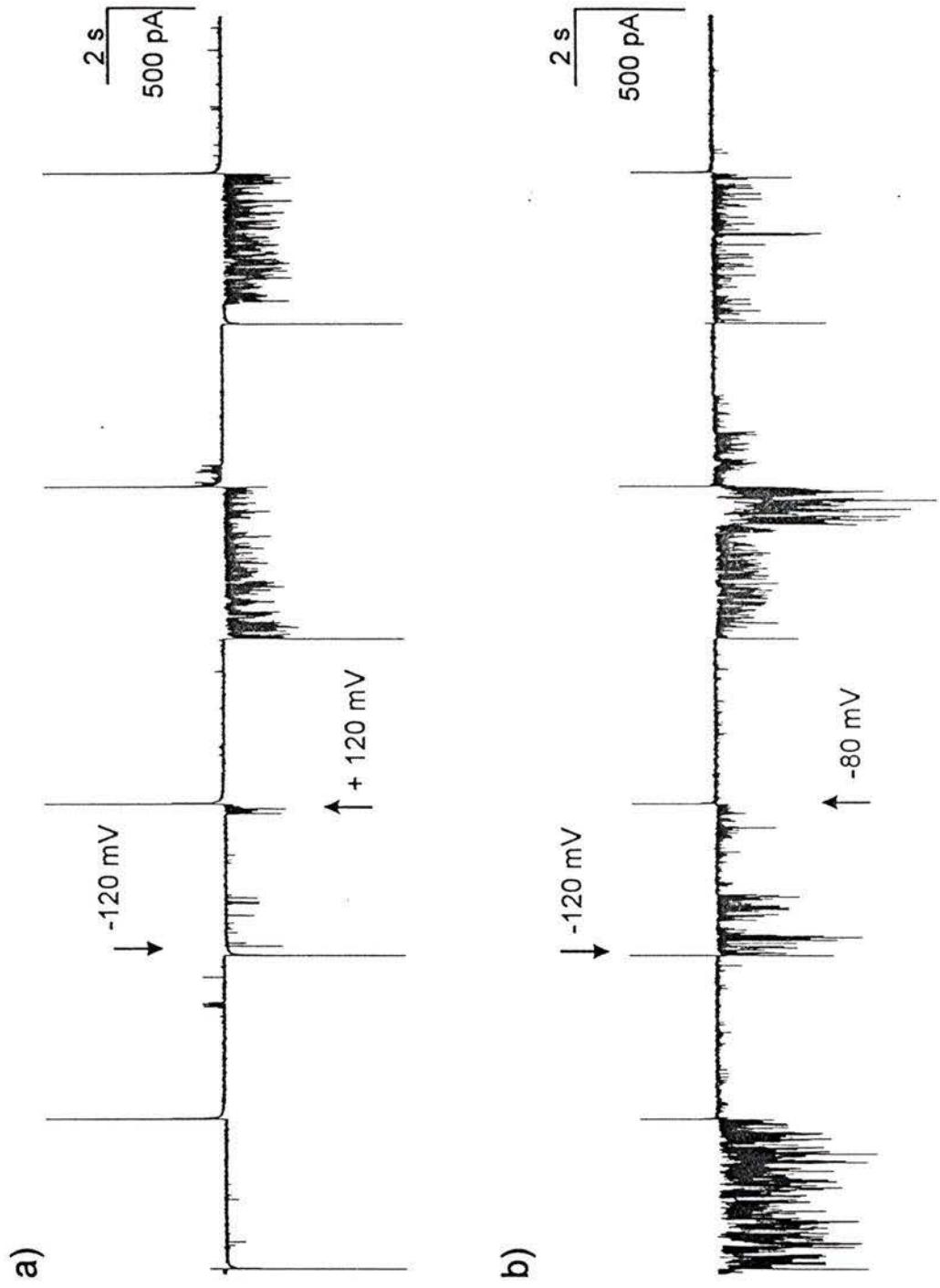

Figure 4.4: Current-time relationships for 200 nmol of S8TrgPA8TrgA in response to a square-wave change in applied potential; 1 M KCl as electrolyte, diPhyPC; a) -120/+120 mV b) -120/-80 mV, sampling frequency was 2 kHz.

4.3 Ion selectivity

Several electrolytes have been investigated to determine ion selectivity. Under similar conditions as in Figure 4.2 when LiCl, NaCl, KCl, CsCl, and RbCl were used as electrolytes no differences were apparent in the conductance behavior. In all electrolytes 100-140 nmol of S8TrgPA8TrgA were required to induce transport in diPhyPC bilayers and the current-time relationships were similar to Figure 4.2. First activity was generally observed about 20 minutes after addition to the *cis* compartment of the bilayer chamber. The current amplitudes varied over a wide range of values, from 10 to 1000 pA, while the duration of the transport events was between 0.5-10 ms. The transport events occurred in clusters of bursts of high activity followed by periods of quiescence in all experiments. S8TrgPA8TrgA displayed a rectifying current-voltage relationship in all electrolytes. The total amount of current carried during voltage-ramps varied between experiments. However, this variation was also observed for duplicate experiments using the same electrolyte and can therefore not be attributed to differences between the cations. The observed similarity in conductance behaviour is not surprising given the large pores implied by the high and erratic current amplitudes observed. On the other hand the pores should discriminate between anions and cations since the head groups render the channel entrance highly anionic. A dilution potential of -31.4 mV was determined from the currents induced by 230 nmol S8TrgPA8TrgA in 0.5 M KCl_{cis} : 0.1 M KCl_{trans}. According to equation 2 the pores formed are 14 times more permeable to potassium ions than to chloride ions. This compares well with the related bola-amphiphiles[72] but is significantly less than the extent of charge selectivity achieved by A8TrgPA8TrgA, the transporter with two monoanionic head groups. The repulsive forces between the head groups of S8TrgPA8TrgA will be greater than for A8TrgPA8TrgA since the succinate group is larger, more hydrophilic and higher charged than the acetate group. Thus monomers of A8TrgPA8TrgA can approach each other more closely leading to tighter pores whereas S8TrgPA8TrgA will form wider pores. The extent of charge selectivity is expected to be inversely related to the diameter of the pore. Therefore limitations are imposed by

repulsive forces between head groups which lead to larger pores and loss of ion selectivity.

4.4 Mechanism

The initial hypothesis is that the channels formed by S8TrgPA8TrgA are similar to those formed by the other bola-amphiphiles in this series.[72] Several additional features are present. The high apparent kinetic order and cation selectivity from the vesicle experiment[64] and the voltage-gating and orientation dependent openings need to be incorporated into the mechanism. Figure 4.5 shows a proposed mechanism. State A describes a non-specific association of S8TrgPA8TrgA with the bilayer. Insertion to a U-shaped conformation can be envisaged (state B). Due to the dianionic head group the processes involving the penetration of the succinate head group (B to D, C to D) are assumed to be slower than the corresponding processes involving the penetration of the monoanionic acetate head group (B to C). Therefore the first transmembrane conformation achieved by monomeric S8TrgPA8TrgA will be with the succinate head group on the *cis* side of the bilayer, state C. Application of a *cis*-negative potential will lead to an ion conducting pore as illustrated by state E, while the application of a *cis*-positive potential will not. The applied transmembrane potential may aid the conformational change from the U-shaped state B to a transmembrane orientation (state C or D). At *cis*-positive potentials the preferred anti-parallel alignment of the transporters molecular dipole vector with the electric field vector can be achieved and the transmembrane state C will be stabilized. Conversely, *cis*-negative transmembrane potentials will lead to the energetically disfavoured parallel alignment of the dipole vector of state C with the electric field. State D would be the more favoured transmembrane orientation of S8TrgPA8TrgA at this potential. However, this orientation of the transporter can not be achieved due to the high charge of the head group. The conformational change from state B to C may be followed by aggregation of several monomers of type C leading to an ion-conducting pore. The pores formed at *cis*-negative potentials must be larger and more loosely structured than the dimers proposed for the other bola-amphiphiles in this suite.[72] This is supported by the high apparent kinetic order

in the vesicle experiment[64], the lack of ion selectivity in the ion translocation step and the rather erratic activity in the single-channel record. The observed erratic activity may be related to the repulsive forces between the head groups of the monomers in an aggregate. The succinate head groups repell each other both electrostatically and sterically leading to channel openings of short duration. Reducing these head group repulsions by masking the charges of the succinate group is expected to facilitate aggregate formation and lead to more stable and longer lived channels. The marked preference for Rb^+ in the vesicle experiment[64] suggests that the channel initiation step is dependent on the interaction of the head groups with mobile counterions in solution. The observed voltage-dependence is proposed to be due to the asymmetric insertion of the transporter into the membrane and the alignment of the molecular dipole with the electric field.

Related to the proposed mechanism is the origin of a small voltage dependent process observed for gramicidin.[85] Under conditions of low electrolyte concentration (0.01 M) and high applied potential (up to 500 mV) the current approaches a saturation limit as the potential increases. This has been attributed to the creation of a double-layer at the mouth of the gramicidin channel (interfacial polarization). Since gramicidin is neutral, no equilibrium double-layer would be created in the absence of current flow. Conversely, S8TrgPA8TrgA and the related derivatives are charged under the experimental conditions, and double-layer effects would be expected to be more significant. A similar type of saturation at high applied potentials should be observed. Unfortunately, our experimental set-up will not support the high potentials required.

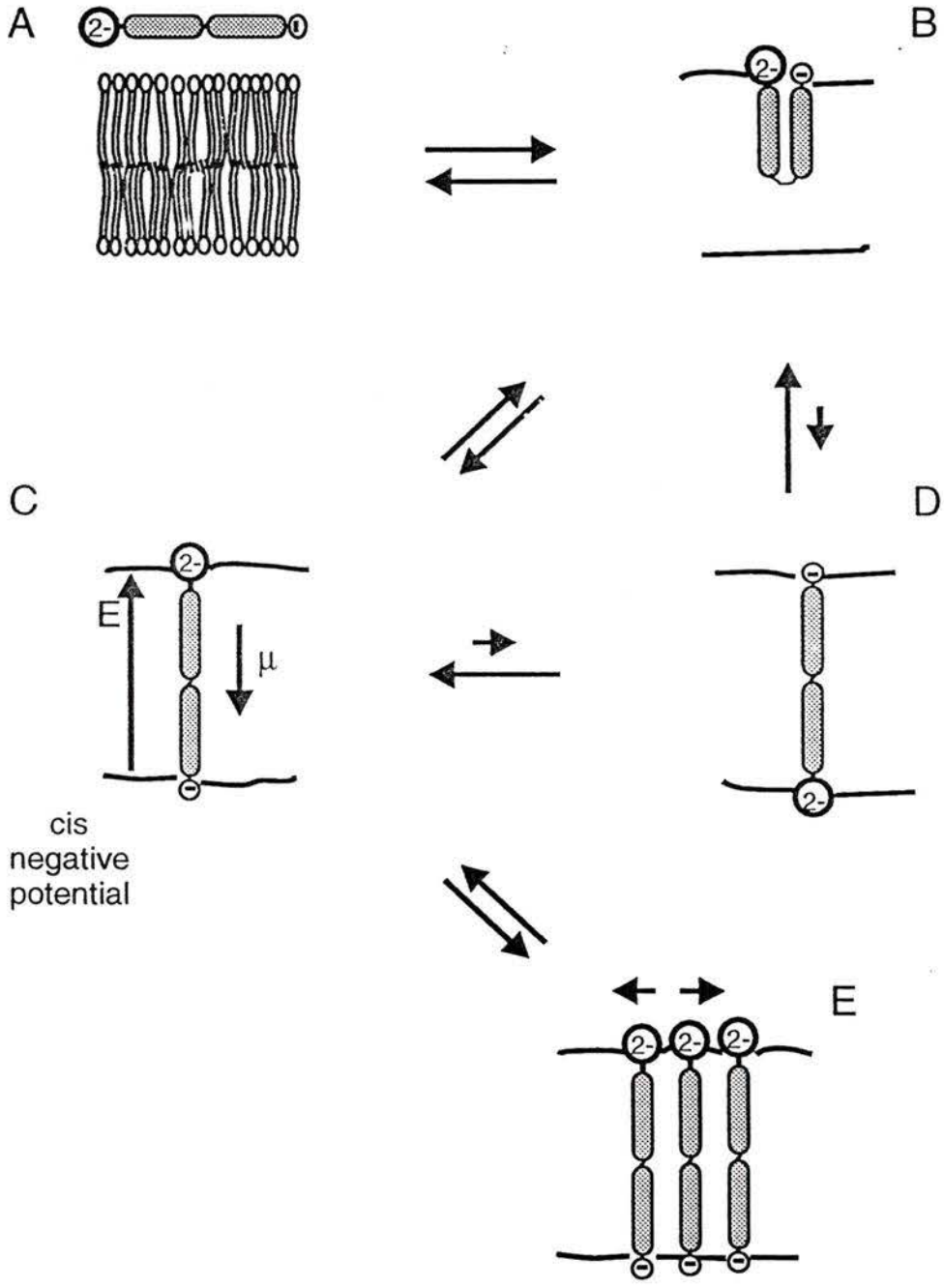

Figure 4.5: Proposed mechanism for the pore formation of S8TrgPA8TrgA.

4.5 Test of mechanism

We propose that the observed current rectification of S8TrgPA8TrgA can be attributed to the asymmetric insertion of the transporter and the preferred anti-parallel alignment of its molecular dipole with the electric field. The short open duration of the ion channels are supposedly related to the electrostatic and steric repulsions of the succinate head groups inside an aggregate. If these assumptions are correct, ohmic current response and channel openings of longer duration may be expected upon minimizing the repulsive interactions. Several aspects of this have been probed and are described in the following paragraphs.

4.5.1 Asymmetry of orientation

The asymmetric insertion of S8TrgPA8TrgA into the bilayer was investigated first. We assume that the short duration of the channel openings is due to destabilizing head group repulsion of the dianionic succinates. It may be expected that more regular single-channel events will be observed upon random insertion of the transporter into the bilayer. To achieve this, 110 nmol compound were mixed with 2 µmol lipid (5% mol/mol) prior to bilayer formation. No step conductance changes similar to Figure 3.1 were observed. However, as illustrated in Figure 4.6 the channels formed displayed prolonged open times of up to 400 ms. The current amplitudes were widely distributed but lower relative to the ones exemplified by Figure 4.2, generally of less than 10 pA. Single-channel events were observed upon application of cis-positive and -negative potentials, hence the current rectification was lost. This result implies that the asymmetric orientation of the transporter in the membrane and the dianionic charge of the head group lead to the observed erratic single-channel behaviour and voltage-gating.

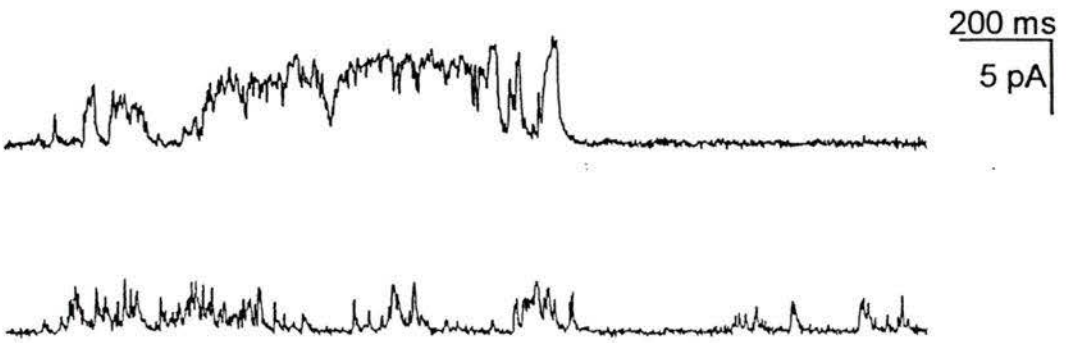

Figure 4.6: Current-time relationship for 5 mol% S8TrgPA8TrgA in diPhyPC, 1 M KCl, +120 mV. The data was acquired with 10 kHz and filtered with 1 kHz.

4.5.2 Effect of pH

At pH 6.4 the succinate head groups will be approximately 15% mono protonated and 85% fully deprotonated, assuming $pK_{a1} = 4.1$ and $pK_{a2} = 5.6$.[86] At lower pH, further protonation of the succinate head group will occur thereby reducing the head group repulsions. The effect of a shift of pH to 5.9 is illustrated in Figure 4.7. Under these conditions the succinate head groups are approximately 40% mono protonated and 60% fully deprotonated. The main open state was an extremely long-lived pore with an open time of several minutes. The current amplitude was -8.65 ± 0.5 pA which corresponds to a specific conductance of 72.2 pS, approximately 5 times larger than the specific conductance of the related compounds discussed in chapter 3. This long-lived state was interrupted by shorter-lived open states (50-100 ms) carrying currents between -11 to -18 pA. Since the short-lived states are not integer multiples of the long-lived state we interpret these as either different open states of the long-lived channel or as the activity of a second channel. The long open duration of the channel may be explained by the formation of hydrogen bonds between the head groups of monomers in the pore which can lead to considerable stabilization of the aggregate. The long-lived state displayed an ohmic current-voltage response indicating that the structure is not inherently rectifying. Recall

that at pH 6.4 the duration of the openings was too short to investigate the current-voltage response of a single active structure (Figure 4.2). Under the more acidic conditions of pH 5.9, we can not be assured of the orientation of S8TrgPA8TrgA with respect to the *cis*-face of the bilayer. We assume that protonation of the succinate head group will facilitate transfer through the bilayer to result in a random transmembrane distribution. Nevertheless, it has been demonstrated that the reduction of repulsive forces in the head group region of the bola-amphiphiles promotes aggregation and leads to better-defined structures.

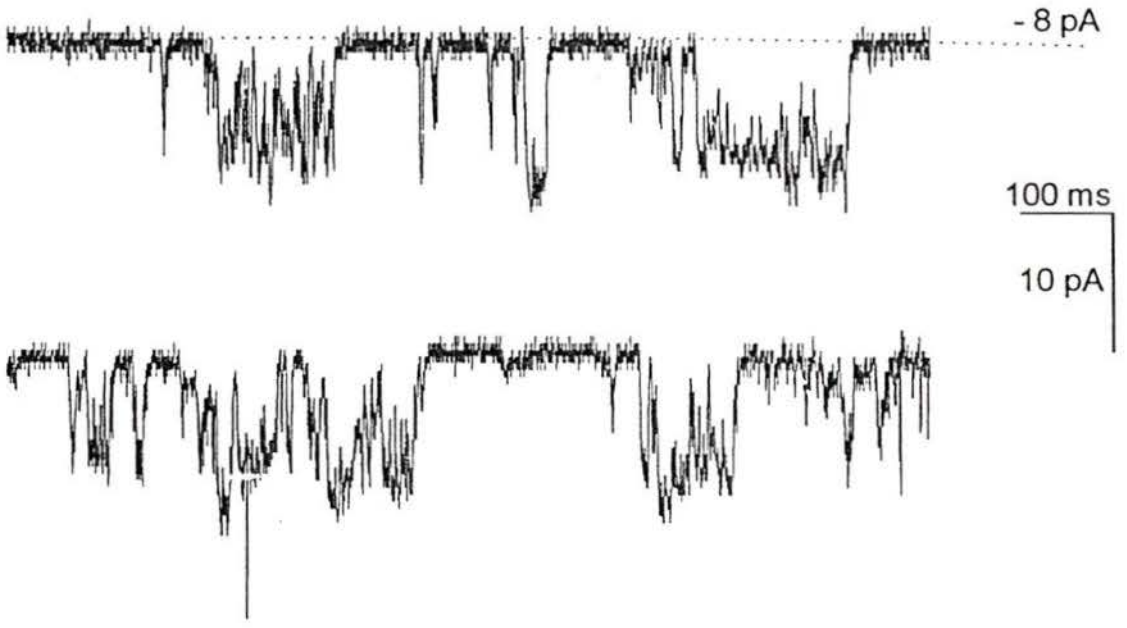

Figure 4.7: Currents induced by 200 nmol of S8TrgPA8TrgA added to the *cis* compartment; 1 M KCl, 5 mM MES, pH 5.9, -120 mV, diPhyPC. Sampling frequency was 10 kHz and the data was filtered at 1 kHz.

4.5.3 Effect of divalent cations

If the mechanism proposed in chapter 4.4 is correct, then the highly-charged aggregates should be stabilized by cations which mask head-group charge repulsions. Divalent cations would be expected to be much more effective in this type of masking than

monovalent cations. Thus low concentrations of alkaline metal ions are expected to lead to stabilization of the aggregates. Figure 4.8 shows that this is indeed the case. A quantity of 200 nmol of S8TrgPA8TrgA was added to the *cis* compartment of the bilayer chamber, which was filled with 1 M KCl and 1.6 mM $BaCl_2$. In addition to the short-lived erratic transport events that are generally observed at pH 6.4 (refer to Figure 4.2) well-defined step conductance changes were observed. These have open times of 10 to 100 milliseconds with clearly defined square topped current amplitudes. These well-defined channels usually opened one at a time while multiple openings, typical for the related bola-amphiphiles,[72] were only occasionally observed. The distribution of the current amplitudes of these step conductance changes was not uniform but ranged from 3 - 12 pA per opening. We take this as evidence for the formation of aggregates with irregular numbers of monomers or different arrangements of the same numbers of monomers. The aggregates do not increase in size by addition of monomers during the open state as is typical for alamethicin[19] but must be formed prior to the opening process. The occasional occurrence of longer-lived (about 500 ms) open states with slowly increasing amplitude supports the notion of flexible pores. Formation of channels displaying step conductance changes is not dependent on the transmembrane potential as shown in Figure 4.8 a) +120 mV and Figure 4.8 b) -120 mV. Macroscopic currents induced by S8TrgPA8TrgA under these conditions were still somewhat rectified as illustrated by Figure 4.8 c). The current response to the first voltage ramp was rectified while the next voltage ramp induced non-rectified behaviour. After going through an intermediate stage in the third segment the current response was rectified again in the last trace shown. This must be due to the electrostatic and non-covalent nature of the interaction of Ba^{2+} ions with the dianionic head group. The barium ions will respond to the applied transmembrane potential and therefore stabilize the aggregate preferentially on the *cis*-face of the bilayer. However, it can be envisaged that aggregates once formed and stabilized by Ba^{2+} might be stabilized and persist even at the "wrong" potential.

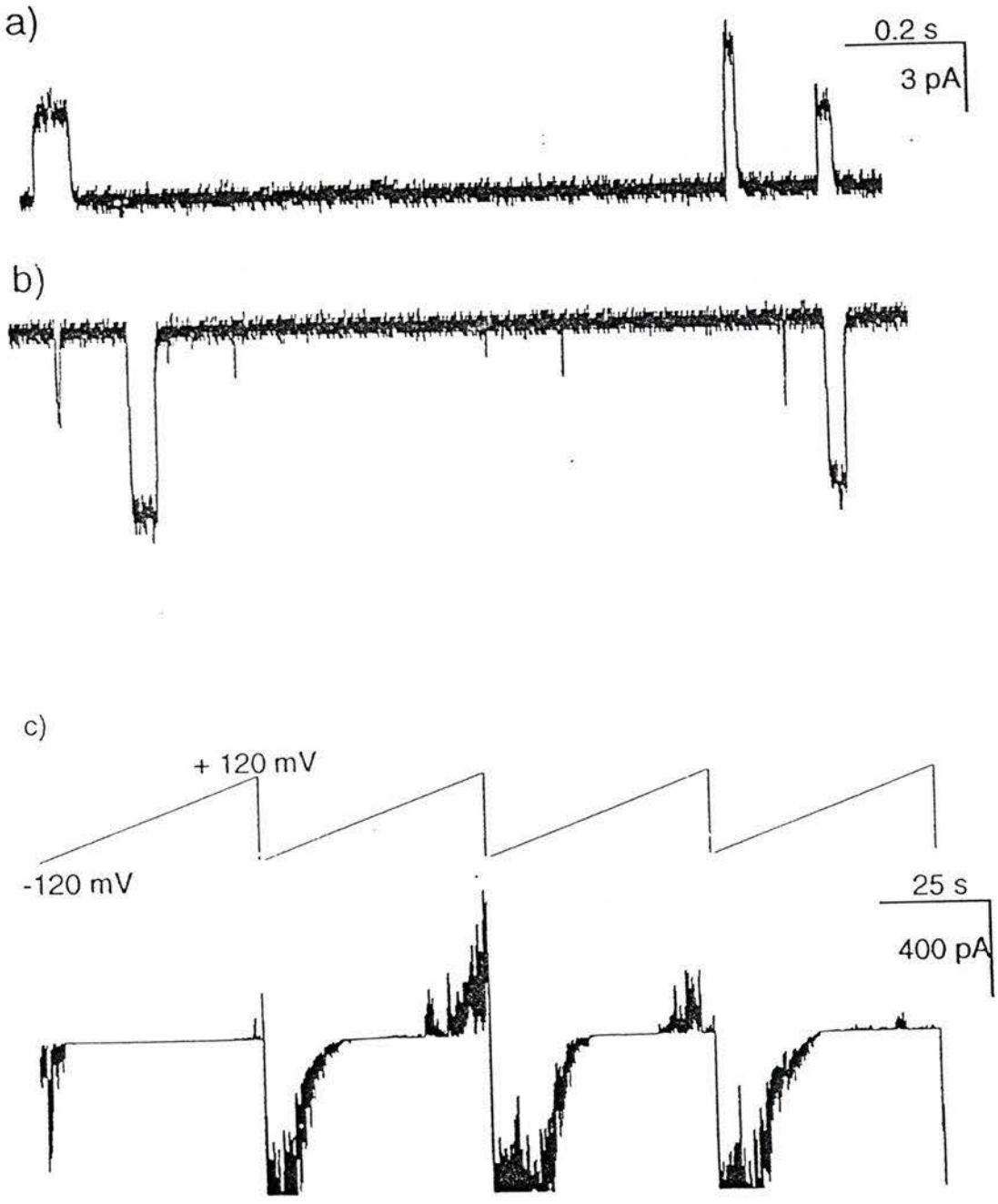

Figure 4.8: Current-time relationships of 200 nmol S8TrgPA8TrgA; 1 M KCl, 1.6 mM $BaCl_2$, pH 6.4, diPhyPC. a) +120 mV; b) -120 mV; c) upper trace shows the applied transmembrane potential as a function of time; lower trace shows the current-time response to this transmembrane potential. The data for a) and b) was acquired at 20 kHz and filtered at 2 kHz, c) was sampled with 200 Hz and filtered with 100Hz.

4.6 Conclusion

It has been shown that electrostatic interaction of the head groups can influence the aggregation and voltage-gated behaviour of bola-amphiphiles. The influence of pH and divalent cations is illustrated in Figure 4.9. Divalent cations are apparently more effective in masking the dianionic head groups than monovalent ions (a). Thus, the formed active structures display step-like conductance changes of varying amplitude, indicating pores of different diameter. The current-voltage response remains predominantly rectifying implying the voltage-dependence of counterion concentration in the electric double layer. Protonation reduces the charge on the dianionic succinate and allows for hydrogen bonding between head groups. Hydrogen bonding increases the stability of the aggregates which is manifested in the observed open times of minutes. Reducing the 2- charge potentially facilitates the transfer of the monoanionic succinate head group across the bilayer leading to a random orientation of transporter in the membrane.

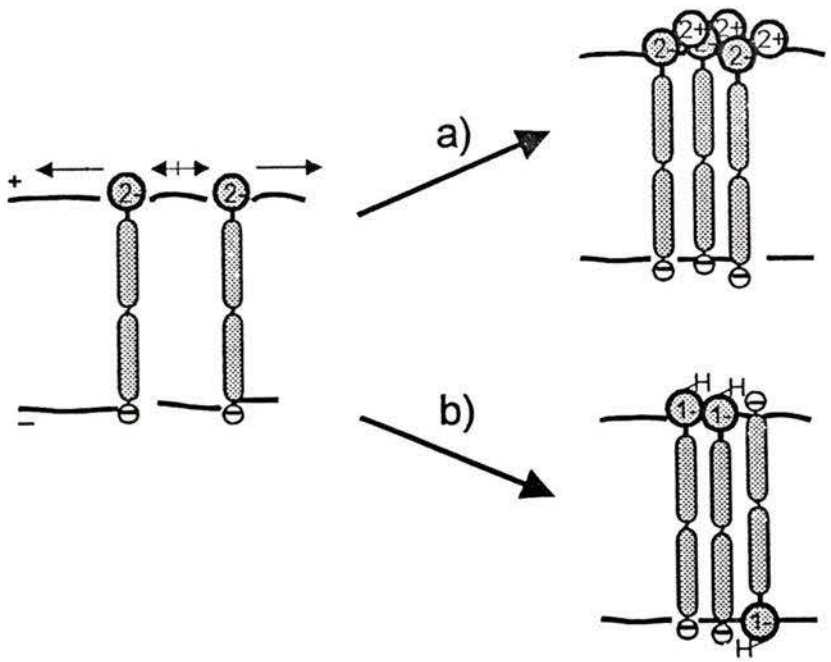

Figure 4.9: Illustration of the effect of Ba^{2+} ions and pH on the aggregation of S8TrgPA8TrgA. The observed activity does not depend on the sense of the transmembrane potential.

Comparing the behaviour of S8TrgPA8TrgA in planar bilayer membranes to that of the related compounds[72] suggests that *regulation* of ion transport can be achieved by controlling the forces leading to stabilization and destabilization of aggregates. For the previous suite of transporters the wall units seemed to dominate the transport behaviour with only small differences due to the head group.[72] On the other hand the dianionic head group seems to dominate the activity of S8TrgPA8TrgA. Under conditions where the succinate is dianionic, large and loosely-structured aggregates are formed that are not very stable under *cis*-positive potentials due to an unfavorable interaction with mobile ions in solution. Thus the control of external conditions, in this case the counterion concentration, can be used to switch the ion transport on or off. Reduction of the head group repulsion by protonation can lead to randomly oriented stable aggregates that display ohmic current-voltage responses. Stabilizing interactions due to hydrogen bonds can lead to long-lived extremely stable channels.

5. Unusual transport behaviour of bis-macrocyclic bola-amphiphiles that contain a hydrophobic wall unit

The presence of ionophilic sites in artificial ion transporter molecules is regarded as essential for transport activity.[62,64] The transporter must accommodate the solvation requirements of the ions in transit. This can be achieved either by partial replacement of the ion solvation sphere by transporter-ion interactions or by introduction of water in the lipid core of the bilayer. In the suite of bola-amphiphiles described in chapters 3 and 4, the ionophilic sites were provided by ether oxygen atoms in the wall units and ester oxygen atoms in the linker and the walls.[64,72] By replacing some of these donor atoms we wanted to explore the importance of the hydrophilic/hydrophobic balance in the wall units for the ion transport ability of the compounds. Less hydrophilic wall units based on the macrocyclization of two 1,8-octanediol molecules were synthesized by Xin Zhou and a bola-amphiphile with two monoanionic head groups, A88PA88A, was realized.[64] Thus a direct comparison to A8TrgPA8TrgA with its more hydrophilic wall units becomes possible. We expected that this replacement of four oxygen atoms in the structure would not be drastic enough to quench the activity of the compounds completely but would lead to well behaved step-like conductance changes of smaller current amplitude than observed with A8TrgPA8TrgA. A second bola-amphiphile, Pa88PPa88Pa has been synthesized with 3-mercapto propionic acid as head groups.[64] This compound is 3 carbon atoms longer than A88PA88A, one in each head group and one in the linker, amounting to a difference in length of about 2.5 Å. This allows for comparison of the importance of transporter length and flexibility. The structures of the two bola-amphiphiles are shown below.

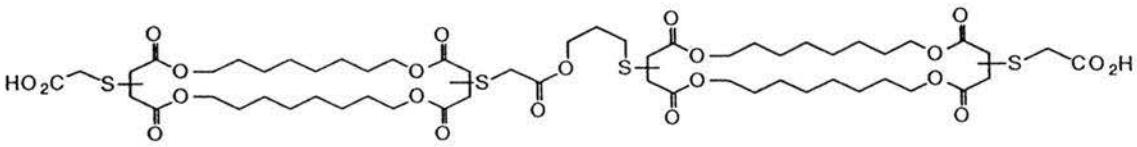

A88PA88A

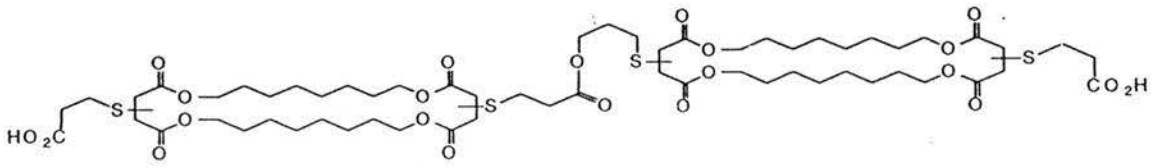

Pa88PaP88Pa

As previously the activity of these transporters was first studied using the pH-stat assay.[64] The apparent kinetic order of both compounds was about one (A88PA88A: 0.94, Pa88PPa88Pa: 1.0), indicating an unimolecular initiation step for transport. The bola-amphiphiles displayed cation selectivity as summarized in Table 6.[64]

Table 6: Transport of alkali metal ions across vesicle membranes by bola-amphiphiles.[64]

Transporter	[Tr] (μM)	Rate x 10^{10}, mol H^+ s^{-1}				
		Li^+	Na^+	K^+	Rb^+	Cs^+
A88PA88A	21	2.8	1.6	11	19	5.1
Pa88PPa88Pa	21	2.4	1.5	5.1	6.5	3.6

The compounds are cation selective in the order $Rb^+ > K^+ > Cs^+ > Li^+ > Na^+$. This Eisenmann III sequence suggests a stronger interaction between the cations and the transporter molecule than was observed for the 8Trg suite (Table 3). As apparent in Table 6, A88PA88A is more active than its slightly longer relative. Both the apparent kinetic order and the cation selectivity differ from the behaviour observed for the compounds with the more hydrophilic 8Trg wall units.[64,72]

5.1 Typical activity in planar bilayers

Figure 5.1 shows the typical activity of A88PA88A and Pa88PPA88Pa in diphytanoyl phosphatidylcholine bilayers with 1 M KCl as electrolyte. The illustrated behaviour was observed in at least 6 independent experiments. To ensure that the unusual signal shape was not due to artifacts caused by decomposition products, a second batch of A88PA88A was synthesized by X. Zhou which displayed the same qualitative behaviour. A total of 80 nmol compound had to be added before transport activity could be observed while 40 nmol of A8TrgPA8TrgA induced current flow under similar conditions. More A88PA88A is expected to be located in the bilayer since its partition coefficient from aqueous phase to a hydrophobic environment would be higher than for A8TrgPA8TrgA,[87] yet more bola-amphiphile had to be added to observe activity. This may imply that the more hydrophobic 88 wall unit is less efficient in the stabilization of aqueous fjords in the bilayer environment. The possibility that A88PA88A self-associates in the aqueous phase and forms aggregates such as micellescan not be ruled out with certainty.

Clearly the transport behaviour is different compared to that of the compounds with 8Trg wall units.[72] The transport events are neither step changes in conductance such as observed for A8TrgPA8TrgA and illustrated in Figure 3.2, nor erratic events such as observed for S8TrgPA8TrgA (Figure 4.2). Instead a rapid increase in current flow was observed that reached a maximum and then decays. In these experiments the rise times were always faster than the decay times. In the following discussion, signals of this characteristic shape will be referred to as 'sharkfins' due to their appearance. The current amplitudes for the transport events were not integer multiples of each other but were widely distributed. However, as opposed to the erratic events observed for S8TrgPA8TrgA, the variations were within the same order of magnitude and between 1 and 6 pA. The initial rate of the conductance increase for these compounds is three orders of magnitude slower than the change in conductance for A8TrgPA8TrgA. While the latter changes from a closed to an open state within several microseconds the former is on the order of tens of milliseconds. The open states of A88PA88A (Figure 5.1, part a)) persisted for several seconds during which the current decayed in an almost linear fashion.

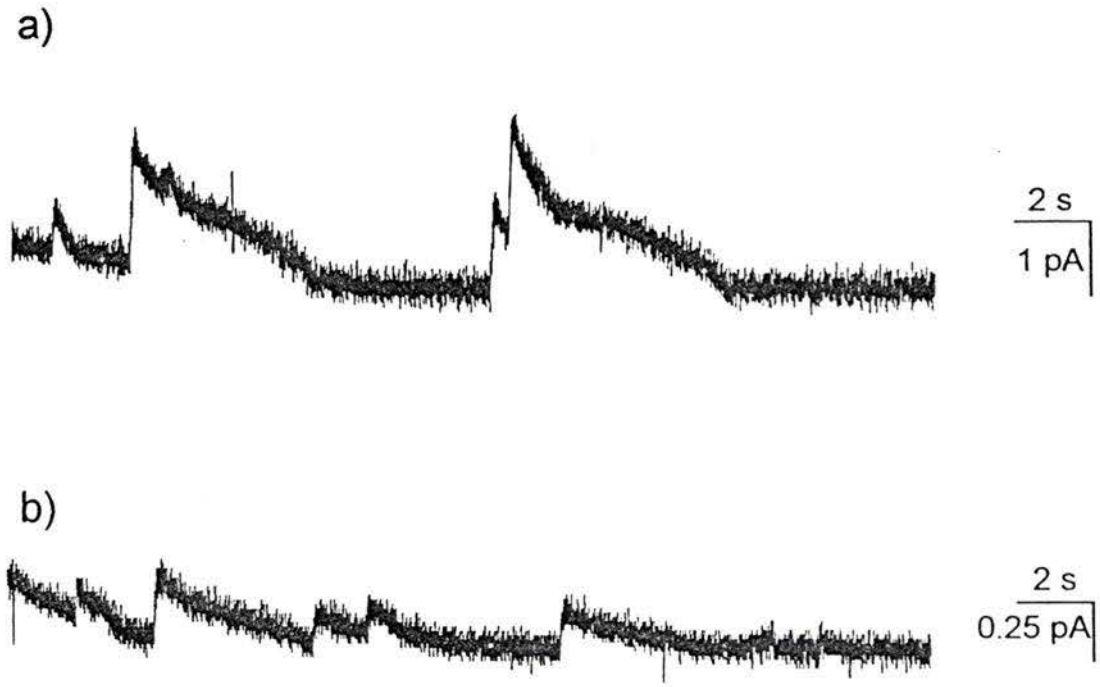

Figure 5.1: Typical currents induced by 40 nmol of two bis macrocyclic bola-amphiphiles in diPhyPC bilayers with 1 M KCl as electrolyte and +120 mV applied transmembrane potential, a) A88PA88A b) Pa88PPa88Pa. Data was acquired at: a) 2 kHz, 500 Hz analog filtered; b) 10 kHz, 100 Hz analog filtered.

Occasionally another rapid rise occurred on top of a decay. The two traces presented in Figure 5.1 were recorded 5 minutes after addition of the compound to the *cis* compartment. Evidently A88PA88A carried more current in each open state than Pa88PPa88Pa; note the different scale bars in the Figure. The characteristic signal shape, however, was similar. Upon reversing the applied transmembrane potential current flux in the opposite direction was observed. These openings had the same range of current amplitudes and duration than the ones at positive potentials. As the experiments progressed in time the current amplitudes and the duration of the observed events increased. We take this as evidence that aggregates are the active structures. As time progresses presumably more transporter molecules become incorporated into the bilayer leading to the formation of larger aggregates. In addition to the activity described here,

erratic openings of 0.5-5 ms duration and variable amplitude (10-1000 pA) were observed occasionally (data not shown). While these openings were of comparable duration and current amplitude as the ones observed for S8TrgPA8TrgA (refer to Figure 4.2), they do not appear as frequently and the predominant signal type for the 88 bola-amphiphiles was the 'sharkfin' signal described above.

5.2 Cation dependence

Since both bola-amphiphiles displayed a marked cation selectivity in the vesicle assay[64] we wanted to investigate the cation dependence of the ion translocation step. Figure 5.2 shows typical examples for the currents induced by 80 nmol of A88PA88A with different electrolytes. The nature of the cation does indeed have an effect on the transport behaviour. The characteristic signal shape was observed for all electrolytes. While the opening process was not affected by the nature of the cation chosen, the closing process was dependent on the cation. The decay of the current amplitude was slowest when 1 M CsCl was employed as electrolyte and fastest when 1 M LiCl was used. Typical event durations were 4-10 seconds for CsCl, 2-6 seconds, for KCl, and 1-2 seconds for LiCl. This implies that the cations can stabilize the aqueous pore that is formed.

For Pa88PPa88Pa the nature of the cation had no apparent influence on the closing time as illustrated in Figure 5.3 for LiCl and KCl. This is consistent with the less pronounced ion selectivity found in the vesicle assay.[64]

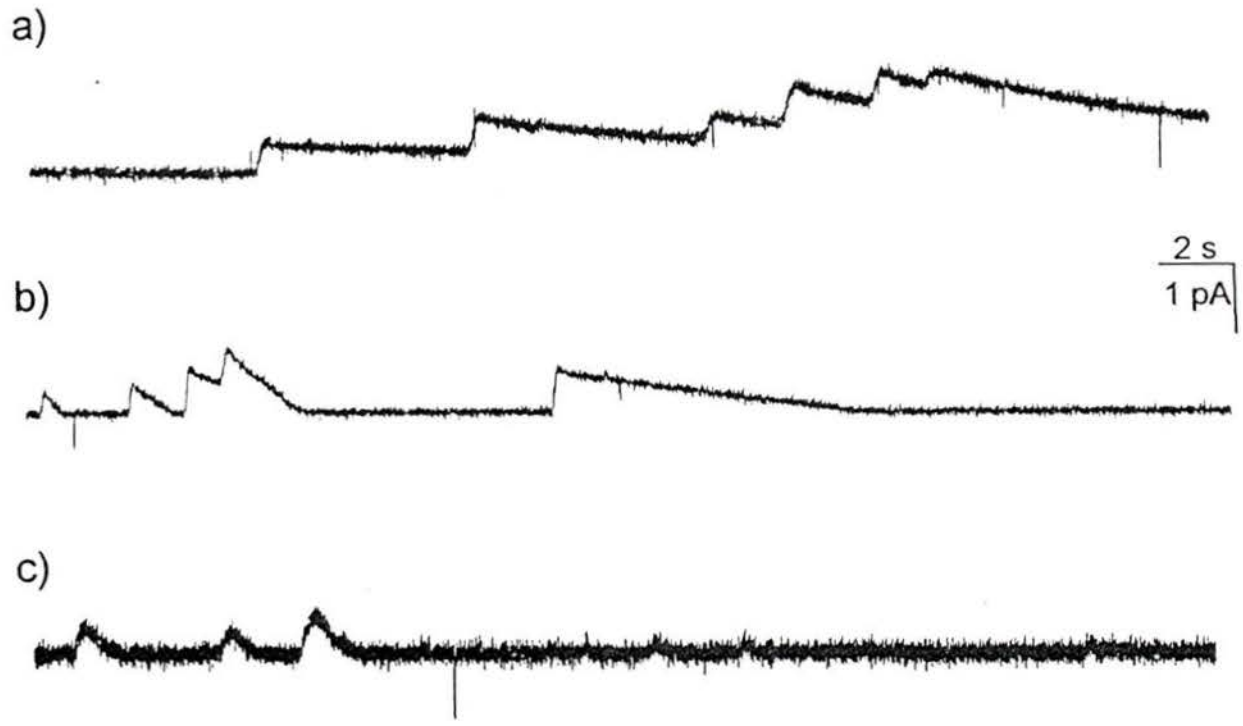

Figure 5.2: Current induced by 80 nmol of A88PA88A. A transmembrane voltage of +120 mV was applied for each trace shown. Bilayers were formed from diPhyPC and the electrolytes were 1 M; a) CsCl (5 kHz sampled, 500 Hz filtered), b) KCl (2 kHz sampled, 500 Hz filtered), c) LiCl (10 kHz, 1 kHz).

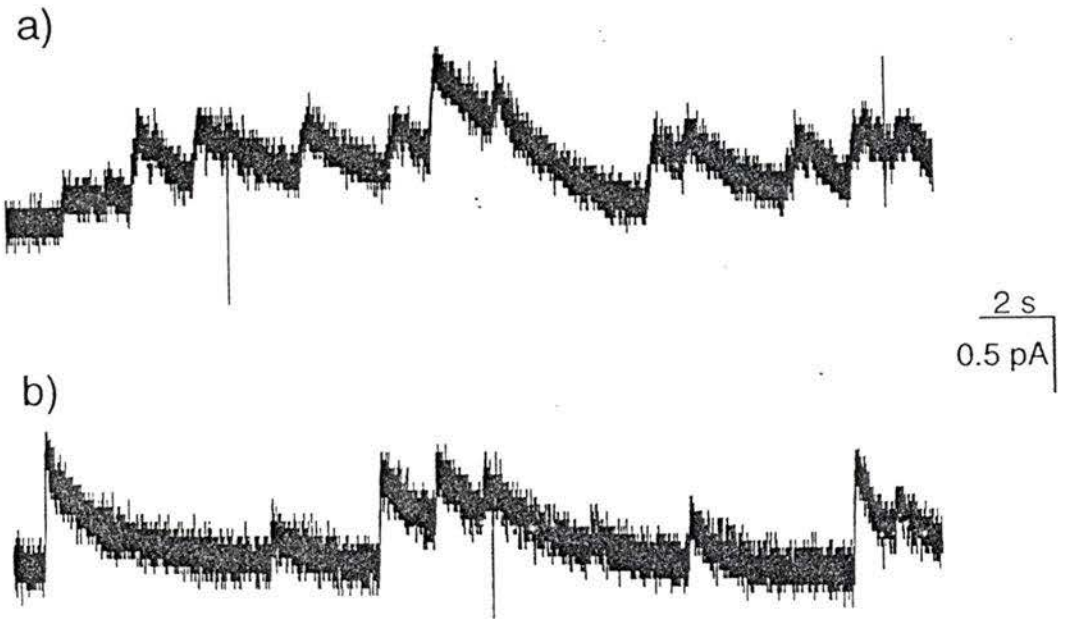

Figure 5.3: Current-time relationship for 80 nmol of Pa88PPa88Pa in diPhyPC bilayers and 1 M electrolyte. The applied transmembrane voltage was +120 mV, a) LiCl, b) KCl. Data was sampled at 10 kHz and analog filtered with a 100 Hz filter.

5.3 Effect of ionic strength

If the active aggregates are indeed stabilized by the cations than we expect that the ionic strength of the electrolyte solution will have an influence on the observed activity. The effect of replacing 1 M KCl with 0.1 M KCl is shown in Figure 5.4. A larger amount of bola-amphiphile had to be added for lower electrolyte concentrations, 120 nmol of A88PA88A at 0.1 M KCl as opposed to 80 nmol for 1 M KCl. As expected the current amplitudes were lower with the less concentrated electrolyte. Furthermore the current decayed faster at these concentrations. These effects are all consistent with the observations made for G8TrgPA8TrgA and varying ionic strength as presented in chapter

3. Upon increasing the ionic strength more bola-amphiphile will be partitioned into the bilayer hence less compound is needed to observe activity. An active aggregate will be stabilized by high ionic concentrations, therefore the openings are expected to be of shorter duration at lower ionic strength

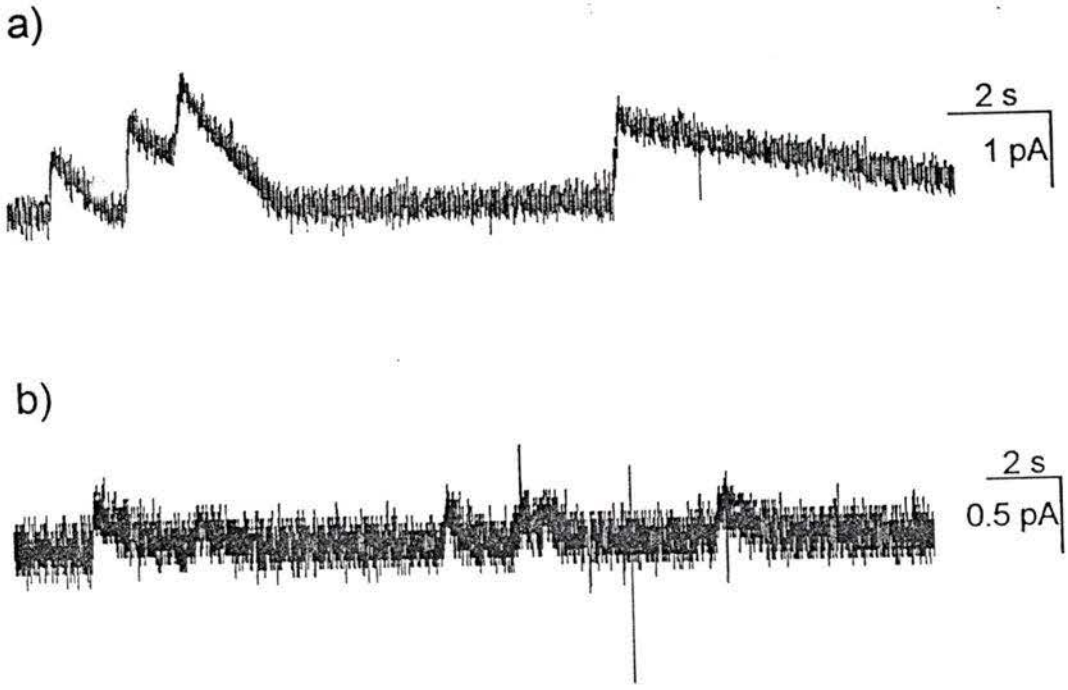

Figure 5.4: Currents induced by A88PA88A in diPhyPC bilayers at +120 mV. A) 80 nmol A88PA88A in 1 M KCl, sampling frequency was 2 kHz, 500 Hz analog filtered, b) 120 nmol A88PA88A in 0.1 M KCl Data was acquired at 20 kHz and filtered with a 100 Hz filter.

5.4 Working hypothesis

Evidently, the bola-amphiphiles with the 88 wall units transport ions across bilayer membranes with a different mechanism than the 8Trg-suite of compounds. How can the unusual signal shape for the more hydrophobic bola-amphiphiles be explained? The different time domains of the opening and closing processes indicate different underlying physical processes. The observed time scales are too long for conformational changes which normally happen in the picosecond time domain[79] or lateral diffusion processes which are believed to occur in the nano- to microsecond time domain.[79] Figure 5.5

summarizes our proposed explanation for the unusual signal shape induced by A88PA88A and Pa88PPa88Pa. Under symmetric salt conditions the transmembrane potential provides the only driving force for ions across the membrane as illustrated in a). We assume an aggregate comprised of several monomers of the bola-amphiphile as the active species. Upon formation of the aggregate a burst of cations crosses the membrane leading to the initial rise in current. Suppose that the aggregates are perfectly cation selective. Then a local Donnan potential would develop in response to the cation flux as shown in part b). This potential carries the opposite sign from the applied transmembrane voltage and therefore would lead to a decrease in current flow. Eventually both potentials would locally be of equal value and no net current would be observed. At this point we can not know whether the aggregate is still present or not. The development of the Donnan potential depends on the probability of the cations to remain near the pore after their passage through the bilayer and may be different for different cations.

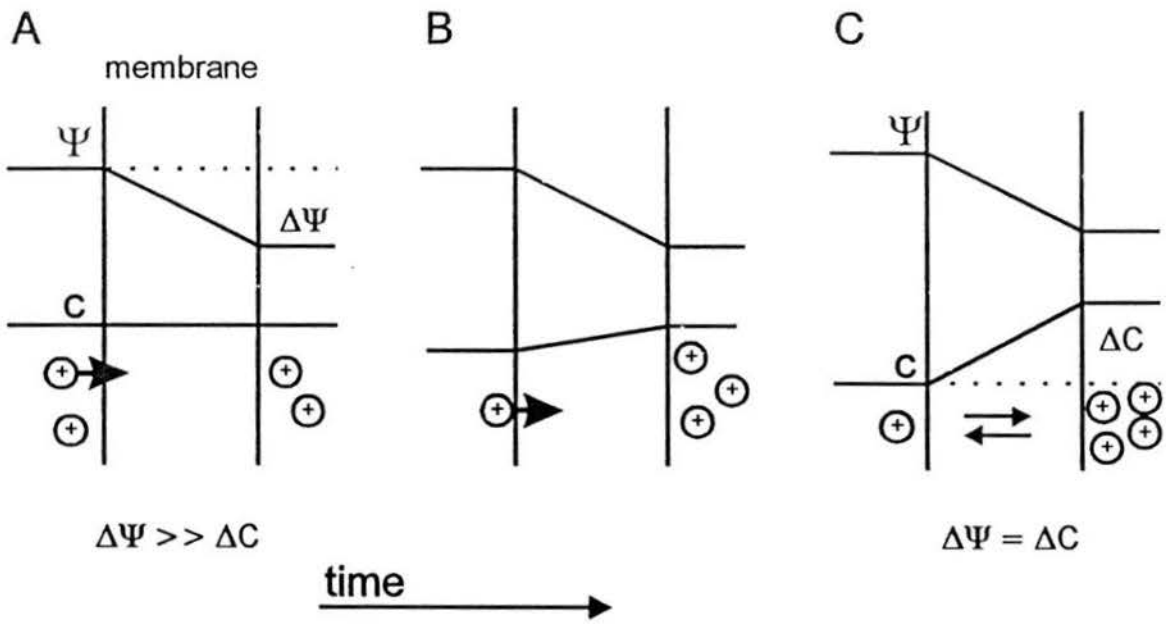

Figure 5.5: Working hypothesis for the explanation of signals with different opening and closing times. The transmembrane potential is represented by $\Delta\Psi$ and Δc represents the cation concentration gradient. Time progresses from a) to c).

Since the development of the Donnan potential requires high charge selectivity this hypothesis can be tested by measuring the reversal potentials to determine the cation:anion selectivity. In practise, the determination of the reversal potential was more difficult for these compounds than in previous cases. Typically the currents induced by the bola-amphiphiles with the 88 wall units remain of small amplitude and do not built up to macroscopic currents as was observed for the 8Trg suite. The application of the voltage ramp experiment is therefore problematic as this basic requirement cannot be met. For this section, the potential at which there was no net current was determined by changing the holding potential and monitoring the currents over periods of up to one minute per selected potential. A reversal potential of -50 mV was obtained with 0.5 M KCl on the *cis* side of the bilayer and 0.1 M KCl on the *trans* side. With the same concentration gradient for LiCl a value of -56 mV was determined for the reversal potential. For Pa88PPa88Pa a reversal potential of -36 mV was obtained for KCl using 0.5 M on the *cis* side and 0.1 M on the *trans* side of the bilayer.

These values may be compared to the equilibrium potentials for the cations; for the conditions of the experiment the values are calculated to be -37.6 mV for KCl and -39.9 mV for LiCl.[10] It is disturbing that the experimentally determined values are more negative than these limiting potentials. Using equation 2, physically unreasonable negative values for the permeability ratios P_X:P_{Cl} were obtained. An explanation for this result relates to an additional observation that in these experiments the junction potential was not stable over the course of the experiment. This was not attributed to a decline in electrode quality as no change in junction potential was observed under symmetric salt conditions. Rather we assume that some electrochemical alteration of the Ag/AgCl electrodes occurred at the electrodes leading to the observed change in junction potential and therefore to inaccurate values for the reversal potential. For example, the excess cationic charge buildup on one of the electrodes might be partly neutralized by Ag+ reduction within the electrode. This would lead to charge imbalance which would appear as a junction potential when the bilayer was ruptured. Ideally these experiments should have been performed using salt

bridges to separate the electrodes from the electrolyte solution. Since we cannot know whether the change in junction potential was linear we chose not to correct for the change in junction potential in the calculations. Nevertheless, if there were a linear correlation between the change in junction potential and the observed reversal potential, then the observed value of V_{rev} = -50 mV minus the change in junction potential (8 mV) would give V_{rev} = -42 mV, for the case of A88PA88A and KCl electrolyte. This is close to the theoretical value for a perfectly cation selective pore.

The selectivity between cations in competition was investigated for A88PA88A only. Exact values for the reversal potentials could not be determined due to low activity of the transporter; it is significant to note that the junction potentials did not change during these experiments. For 1 M $CsCl_{cis}$: 1 M KCl_{trans} the determined value was between 0 and -20 mV, leading to an upper estimate of the permeability ratio of $P_K:P_{Cs}$ = 2.2. The same estimate was obtained with 1 M LiCl instead of CsCl, indicating that there is, at best, a weak discrimination between cations. This is in contrast to the results in vesicle experiments where cation selectivity following Eisenmann III selectivity was found.[64] Again we attribute this difference to the different processes that are probed with the two experiments. The vesicle assay detects the onset of the ion transport while the planar bilayer experiment probes the ion translocation step directly.

The results summarized above imply that the pores formed by A88PA88A and Pa88PPa88Pa approach perfect charge selectivity but only weak selectivity between cations. In response to the applied transmembrane potential cations flow through the pore which leads to the development of a local Donnan potential since anions are supposed to be essentially impermeable. The Donnan potential is opposing the transmembrane potential and thereby decreasing the current flow. Eventually this would lead to a net current flow of zero. Consistent with this is the occasional observation of rapid closures of 'channels' during the decay periods. This is taken as evidence for the dissociation of the aggregate.

The increase in charge selectivity of these compounds compared to the ones described in chapters 3 and 4 must be related to the wall units. We assume that the bola-amphiphiles based on the 8Trg macrocycle have several water molecules associated with the wall units at all times whereas the 88 wall units are presumably less hydrated. Therefore the two 88 compounds would not be able to stabilize as much water in the bilayer and the pores formed will be dryer. This might lead to an increase in ion selectivity as the ions now have to interact more closely with the wall units during the translocation step. For a constant radius, anions are more highly hydrated than cations, and the hydrated radii are significantly larger.[88] Thus a drier pore will affect anions more strongly than cations and will increase cation:anion selectivity.

Due to the amphiphilic nature of the 8Trg macrocycle a specific arrangement is imposed on aggregates formed by these bola-amphiphiles. Presumably the most stable aggregate in the lipid bilayer is an aqueous pore. Here the hydrophobic parts of the wall units interact with the lipid core of the membrane while the hydrophilic polyether group points towards the aqueous lumen of the pore. In contrast to that no such structure is imposed on the bola-amphiphiles based on the 88 macrocycle. The 88 wall units are more hydrophobic and more symmetric than the 8Trg wall units. Therefore more possibilities for aggregation exist. We propose that several transporter molecules interact with each other to form a domain in the bilayer that is rich in transporter. These domains can then be composed of varying numbers of monomers.

5.5 Effect of pH

We reason that the aggregation of bola-amphiphiles based on the 8Trg macrocycle is mainly due to the incompatibility of the monomeric wall units with the lipid environment. For A88PA88A no obvious attractive interactions between the wall units are apparent while the anionic head groups will repel each other due to electrostatic interactions. Thus bola-amphiphiles based on the 88 macrocycle would tend to the monomeric state to a greater extent than the 8Trg transporters. The attractive interactions

must be of the same origins as the hydrophobic effect in aqueous solvent. The interactions between lipid-lipid and transporter-transporter molecules may be stronger than the lipid-transporter interaction thus favoring aggregation. The size of the aggregate would then be limited by the head groups. If this "balance of forces" argument is correct, then protonation of the head groups will reduce the repulsion and therefore larger aggregates may form. In addition if the pH is chosen to be close to the pK_a of the head group the potential for hydrogen bonding is given and the structures may be stabilized. These experiments were performed for A88PA88A only, since the larger currents carried made investigation easier. Figure 5.6 summarizes the effect of pH on the transport activity.

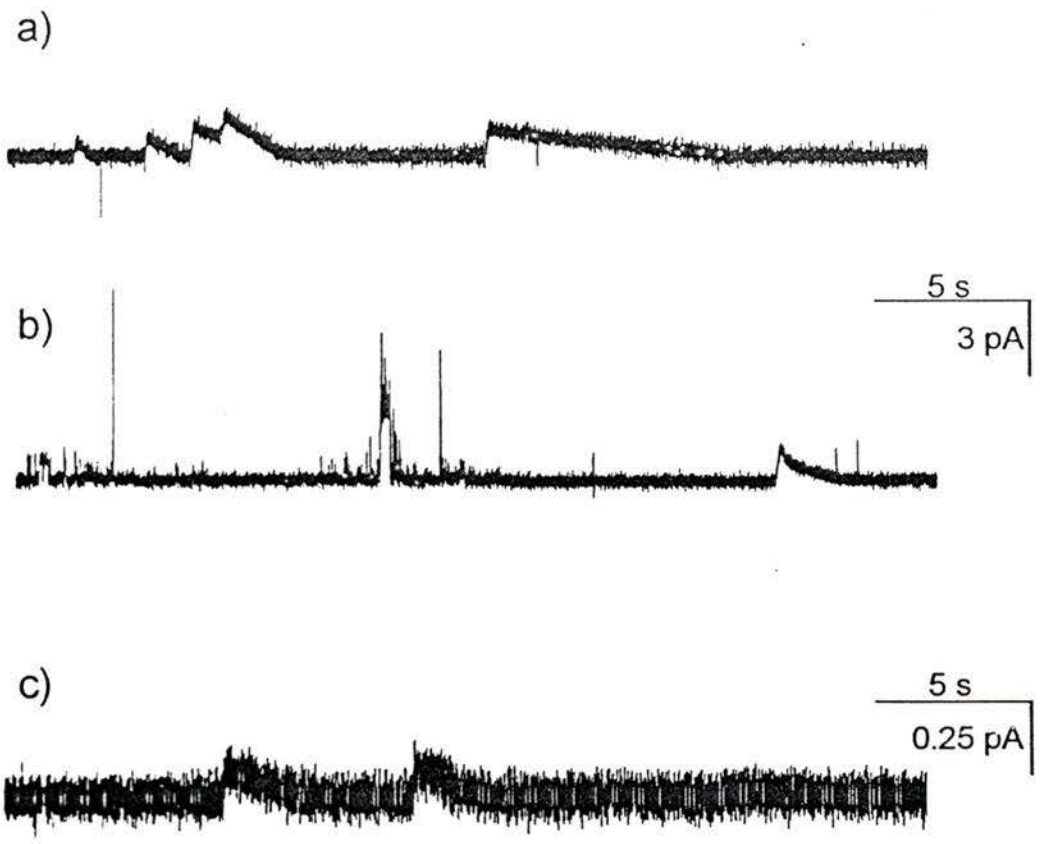

Figure 5.6: Typical currents induced by 80 nmol A88PA88A in 1 M KCl solution at the indicated pH; a) pH = 6, (2 kHz sampled, 500 Hz filtered) b) pH = 4.75 (20 kHz sampled, 2 kHz filtered), and c) pH = 4 (10 kHz sampled, 1 kHz filtered). Holding potential was +120 mV across diPhyPC bilayers.

The pK_a of the acetic acid head group is around 4.75.[86] Thus at pH 6 about 5 % of the head groups will be in their protonated form while at pH 4 about 85 % will be protonated. The pH of 1 M KCl solution was adjusted with 1 M HCl in unbuffered solutions. The qualitative behaviour at pH 6 and pH 4 is comparable. Predominantly signals with different rise and decay times are observed. However, the current amplitude is about 5 times larger at pH 6 compared to pH 4. This must be due to the stronger head group repulsion at the higher pH. Larger, more loosely structured aggregates will be formed that accomodate more water. At pH 4.75, where about 50 % of the head groups are protonated, a variety of behaviours is observed. Next to the ordinary 'sharkfin' a few single channel events and increased erratic activity was observed. This will be described below in more detail. These results show that pH can indeed control the aggregation behaviour of these compounds by reducing head group repulsions and hydrogen bond formation.

Figure 5.7 continues and expands on the behaviour of A88PA88A at pH 4.75. Erratic events such as near A occur sporadically and are observed at all pH's investigated. 'Sharkfin' events can be observed, as indicated by C. The current amplitudes were comparable to the events observed at pH 6. However, events that occur at pH 4.75 can have durations of up to 50 seconds as opposed to 2-6 seconds at pH 6. Moreover, step conductance changes appear throughout the whole experiment. Inspection of the data reveals that these channels are not of uniform current amplitude such as observed for the 8Trg suite of compounds (refer to Figure 3.2). Closer investigation of the data near A shows that several openings of the same amplitude, ~0.8 pA, occurred in succession. The amplitudes of the channels labeled B and D are comparable, ~2.7 pA The single-channel conductances observed throughout the record varied between 5 and 30 pS. This is taken as further evidence that the active structures are indeed aggregates of different monomer stoichiometry. The observation of successive openings with similar amplitude suggests that at this point a measurement on a single molecular aggregate was taken. Its activity ceases and another, larger or smaller, aggregate becomes active. Hydrogen bonding may indeed allow the formation of more structured small aggregates that display more regular

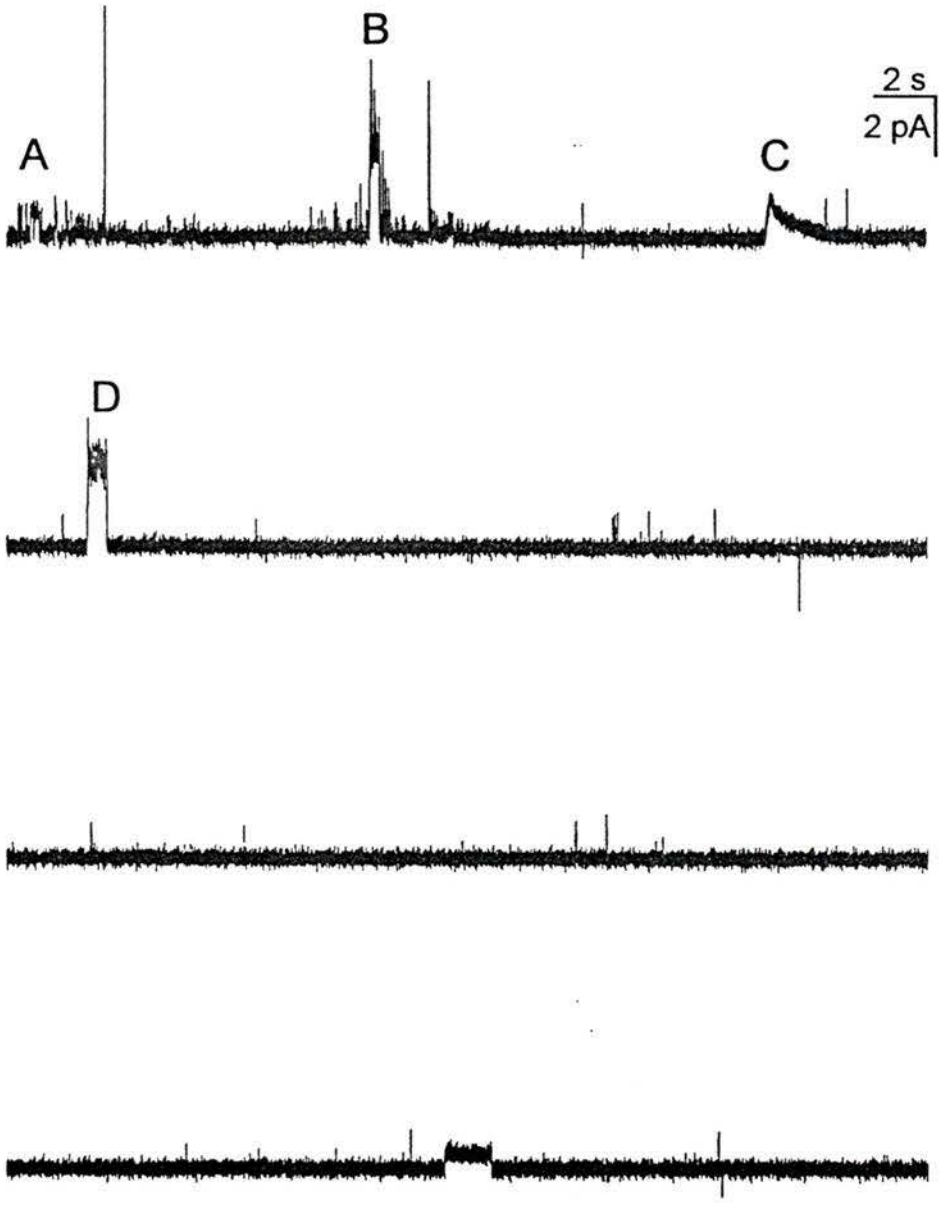

Figure 5.7: Current-time relationship of 80 nmol A88PA88A in diPhyPC membranes, +120 mV holding potential, 1 M KCl, pH 4.75. Data was acquired at 20 kHz and analog filtered at 2 kHz.

behaviour. The wide range of behaviour, from erratic over 'sharkfins' to well structured aqueous pores, suggests that this particular kind of ion transporter is very sensitive to external conditions.

5.5 Conclusions

The results presented above illustrate that a small change in structure can lead to drastically different ion transport behaviour. Replacing four oxygen atoms in the wall units of bis-macrocyclic bola-amphiphiles alters the mechanism by which ions are transported across the membrane. The more hydrophobic transporters, A88PA88A, and Pa88PPA88Pa, more closely resemble the lipid molecules in the bilayer. This offers the transporter molecules a wider possibility of stable states which is manifested in the sensitivity to external conditions. Some of these states are illustrated in Figure 5.8.

State A represents the diffusion of the transporter to the membrane. Initially an U-shaped conformation in one of the bilayer leaflets can be envisaged (state B) followed by the penetration of one of the head groups which leads to state C depicted in Figure 5.7. A second head group penetration can lead to an U-shaped conformation in the other bilayer leaflet (not shown). As mentioned in chapter 3 these states are assumed to be electrically silent. Bola-amphiphiles with the 88 wall unit can now adopt several conducting states in the bilayer. Defects, that are manifested by sporadic events of high current amplitude and short duration can be induced by monomeric transporter that undergoes major conformational rearrangement or by side-to side dimers of the U-shaped transmembrane state as illustrated in part 1 of the Figure. Part 2 describes the formation of small aggregates. Several monomers in the transmembrane conformation can come together and form an aqueous pore. Due to head group repulsion these pores can be thought of as being tighter in the membrane center than in the head group region. Aggregates of this type may not be conductive. The monomers may adopt a more cylindrical shape when head group repulsions are reduced, for example by protonation. This may lead to more stable aqueous pores that open and close with a similar mechanism as the 8Trg compounds. Aggregates of this type would lead to the step conductance changes observed at pH 4.75. Part 3 describes the formation of large aggregates in the bilayer membrane. These aggregates do not form well structured pores. Rather, they form domains that are rich in transporter molecules and are generally leaky to cations. The size of the domain is

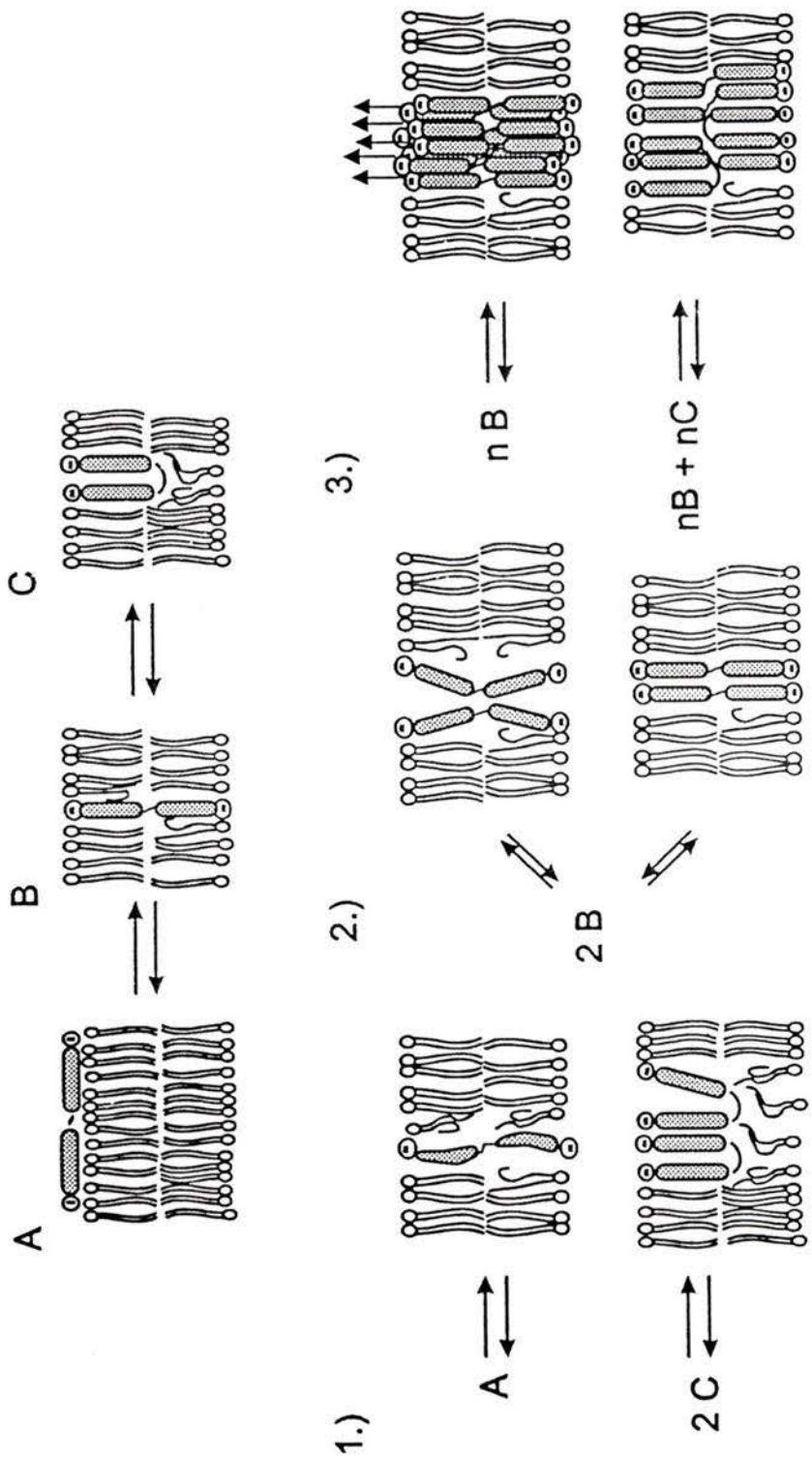

Figure 5.8: Illustration of possible membrane conformations of bola-amphiphiles with 88 wall units.

controlled by head group repulsion and is quite variable. The observed charge selectivity may be caused by electrostatic repulsion of anions from the aggregate as a high local concentration of anionic head groups would be present in the bilayer. These domains are assumed to be responsible for the signals with longer closing than opening times.

Although the general behaviour of A88PA88A and Pa88PPA88Pa is comparable, the former bola-amphiphile carries more current during each opening. Due to three additional CH_2-groups in the structure, Pa88PPA88Pa is about 2.5 Å longer than A88PA88A. These additional methylene groups give the molecule considerably more freedom of motion both in the head group part and in the central linker. Thus aggregation may be less favored for this compound as the monomers loose more entropy upon aggregation than their slightly shorter relatives. This may lead to fewer monomers per aggregate. On the other hand, the greater flexibility may allow tighter packing of the monomers in the aggregate to allow for maximum van der Waals interactions. This may lead to less water that can be stabilized in the bilayer. Taken together Pa88PPA88Pa aggregates will allow less ionic current to flow.

Results from planar bilayer experiments suggest that the bola-amphiphiles with the 88 wall units form aggregates in these membranes. This has been deduced from the open duration of several seconds which appears too long for a monomeric active species. As mentioned in chapter 3 the diffusion constant of lipids in planar bilayers is about 10^{-8}-10^{-6} $cm^2\ s^{-1}$.[79] Therefore the transporter molecules collide numerous times with lipid molecules during the lifetime of an active structure. It appears unlikely that a monomer could remain in an active conformation for several seconds under these circumstances. Furthermore, the variable maximum current amplitude of the 'sharkfin' signals suggests aggregates of variable stoichiometry. However, the apparent kinetic order in vesicle membranes was determined to be about one which implies a unimolecular rate-determining step.[64] Recall the differences between the two membrane systems: vesicle membranes are curved whereas the bilayers in the voltage clamp experiment are planar. In addition, the total

membrane area in the vesicle experiment is about a million times larger than the membrane area in a planar bilayer experiment and the aqueous phase:lipid ratio is much larger for the latter. Therefore different steps in the ion transport mechanism may dominate the behaviour in these systems.

The two experiments probe a different step in the transport process. While in planar bilayer experiments the ion translocation step is observed directly, vesicle experiments probe the initiation of ion transport. If the kinetic order in the vesicle experiment is indeed one, then a unimolecular slow step has to occur in the vesicle experiment. Two possible explanations are presented in the following paragraph.

One possibility invokes that the change from an U-shaped conformation to a linear conformation is slow in curved membranes. Thus a different kind of aggregate would form in a vesicle membrane than in a planar bilayer. The rate-determining step would then be the formation of a linear conformation which is followed by rapid aggregate formation involving one extended transporter molecule and several U-shaped molecules. The mechanism presented in Figure 5.8 illustrates a number of functional species in planar bilayers. It is conceivable that in curved vesicle membranes only one of these species can be observed. Another possibility invokes the solubility of bola-amphiphiles in water. Bola-amphiphiles based on the 88 macrocycle are presumably less water soluble than the bola-amphiphiles with the 8Trg wall units. This may lead to the formation of transporter aggregates in the aqueous phase that interact poorly with the bilayer membrane. The insertion of such an aggregate into the bilayer may not be observable in the planar bilayer experiment since it occurs only once. The observed transport activity would then be due to the activity of the bola-amphiphiles following the insertion event. On the other hand the details of the insertion in vesicle membranes may be observed as a one-molecule-at-a-time process using the pH-stat assay. However, this process would require the presence of an aggregate in equilibrium with monomer in which case the concentration of monomer would be constant and the kinetic order would be zero. Perhaps the observed kinetic order

of one is actually an average of zero and two. This hypothesis can be tested by performing light-scattering experiments to determine whether the bola-amphiphiles form aggregates in water.

It has been shown that the hydrophobic/hydrophilic balance in the structure of artificial ion transporters is an important factor in determining the aggregation behaviour of these compounds. This in turn leads to an alteration in the mechanism. Large aggregates of transporters with relatively hydrophobic wall units show a range of activities that depend on the external conditions.

6. Effect of replacing the linker of bis-macrocyclic bola-amphiphiles

Previous studies by Zojaji *et al.* indicated that the choice of the linker between the wall units can influence the transport behaviour.[62] Therefore we wanted to investigate the effect of the linker on our suite of compounds in detail. Two additional compounds in the 88 series have been synthesized by X. Zhou.[64] In these bola-amphiphiles the usual carboxyl group in the central link is replaced by sulfide. **N** and **A** have been chosen as head groups yielding bola-amphiphiles with a net 2- charge, A88Su88A, and a net 2+ charge, N88Su88N, respectively. The structures of the compounds are shown below.

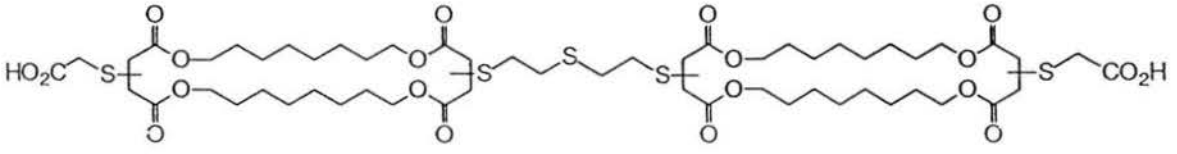

A88Su88A

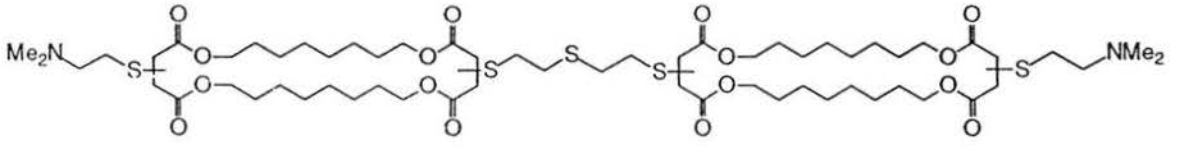

N88Su88N

Molecular dynamics and mechanics calculations using MM2 force field optimization from the CAChe Scientific program suite revealed differences in the low energy conformation of A88PA88A and A88Su88A as depicted in Figure 6.1.[64] A88PA88A adopts an extended conformation with an overall length of 30 Å. In the gas phase this is the preferred conformation for all bola-amphiphiles described so far in this thesis.[64] The sulfide linker on the other hand induces a more twisted conformation of 19 Å length as shown for A88Su88A.[64] Although the conformations in the membrane environment might be different than the ones determined by the molecular mechanics and dynamics optimization due to solvation, the results are suggestive of the preferred

orientations. Thus different transport behaviour may be expected and the importance of U-shaped conformations can be investigated. In particular the hypothesis that monomeric bola-amphiphiles in a U-shaped conformation are electrically silent, as implied in all schemes described so far in this thesis, can be tested.

a)

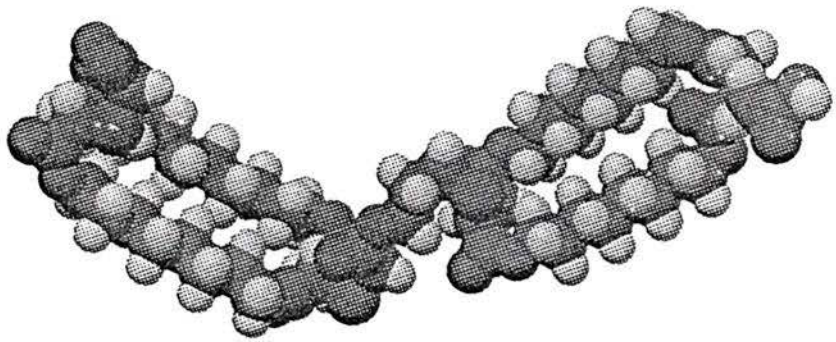

b)

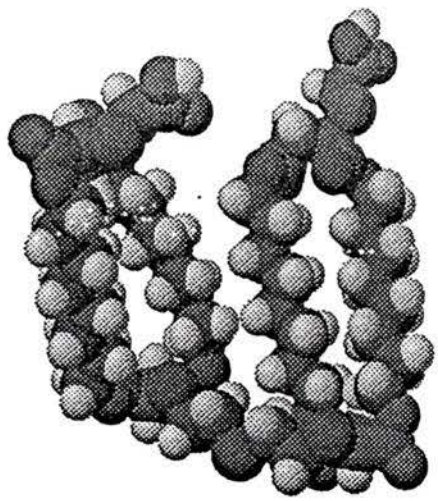

Figure 6.1: Low energy conformation of a) A88PA88A and b) A88Su88A. Data was supplied by Xin Zhou.

As usual the activity of these compounds in vesicle membranes was investigated using the pH stat assay.[64] The apparent kinetic order was about one in both cases implying that a unimolecular step initiates ion transport. The cation selectivity data is summarized in Table 7. The data for the other compounds in the 88 series is also shown for comparison.[64] Both bola-amphiphiles with the sulfide linker were significantly less active than the compounds with the carboxylate linker. Using the pH stat assay the transport rates can be determined within an uncertainty of 10 %. Taking this into consideration neither of the compounds exhibits marked discrimination between cations.

Table 7: Transport of alkali metal ions across vesicle membranes by bola-amphiphiles.[64]

Transporter	[Tr]	Rate x 10^{10}, mol H^+ s^{-1}				
	(μM)	Li^+	Na^+	K^+	Rb^+	Cs^+
A88Su88A	21	0.71	0.5	1.4	1.0	0.72
N88Su88N	21	1.1	1.2	1.6	2.1	1.3
A88PA88A	21	2.8	1.6	11	19	5.1
Pa88PPa88Pa	21	2.4	1.5	5.1	6.5	3.6

U-shaped conformations were invoked in membrane disruption by the series of compounds reported by Regen and co-workers[44,78] and in a study on bis crown ethers performed in our laboratory.[65] Therefore we were interested in whether the compounds with the sulfide linker would lead to membrane disruption or whether we would observe the unusual 'sharkfin' signal as with the related compounds. The typical activity of these compounds will be described in the following paragraph and the effect of cation type and ionic strength on the transport activity will be presented.

6.1 Typical activity in planar bilayers

In planar bilayer membranes the two sulfide-linked bola-amphiphiles behave quite differently from each other. The cationic compound, N88Su88N, acted as a membrane disrupting agent. In experiments with less than 90 nmol of transporter no activity was observed while bilayers ruptured at concentrations above this amount. Typically a few current spikes of 1-3 ms duration and amplitudes of greater than 10 pA are observed before the membrane breaks. This is illustrated in Figure 6.2. The same qualitative behaviour has been found for NaCl, KCl, and RbCl as electrolytes. Experiments were repeated 2-4 times for each electrolyte with the same qualitative result. The observed current spikes occurred very sporadically with long periods of quiescence of 5-40 seconds in between. These spikes are attributed to defects induced by N88Su88N. It is interesting that there seems to be a threshold concentration of transporter above which activity (membrane disruption) starts. This concentration dependence may reflect the formation of aggregates in the aqueous phase. This would imply that the incorporation of aggregates into the membrane leads to disruption. Alternatively, a limiting transporter density in the bilayer can be envisaged. Below this density the membrane remains stable and sealed. Once the limiting value is reached dimers or aggregates form in the bilayer that lead to disruption.

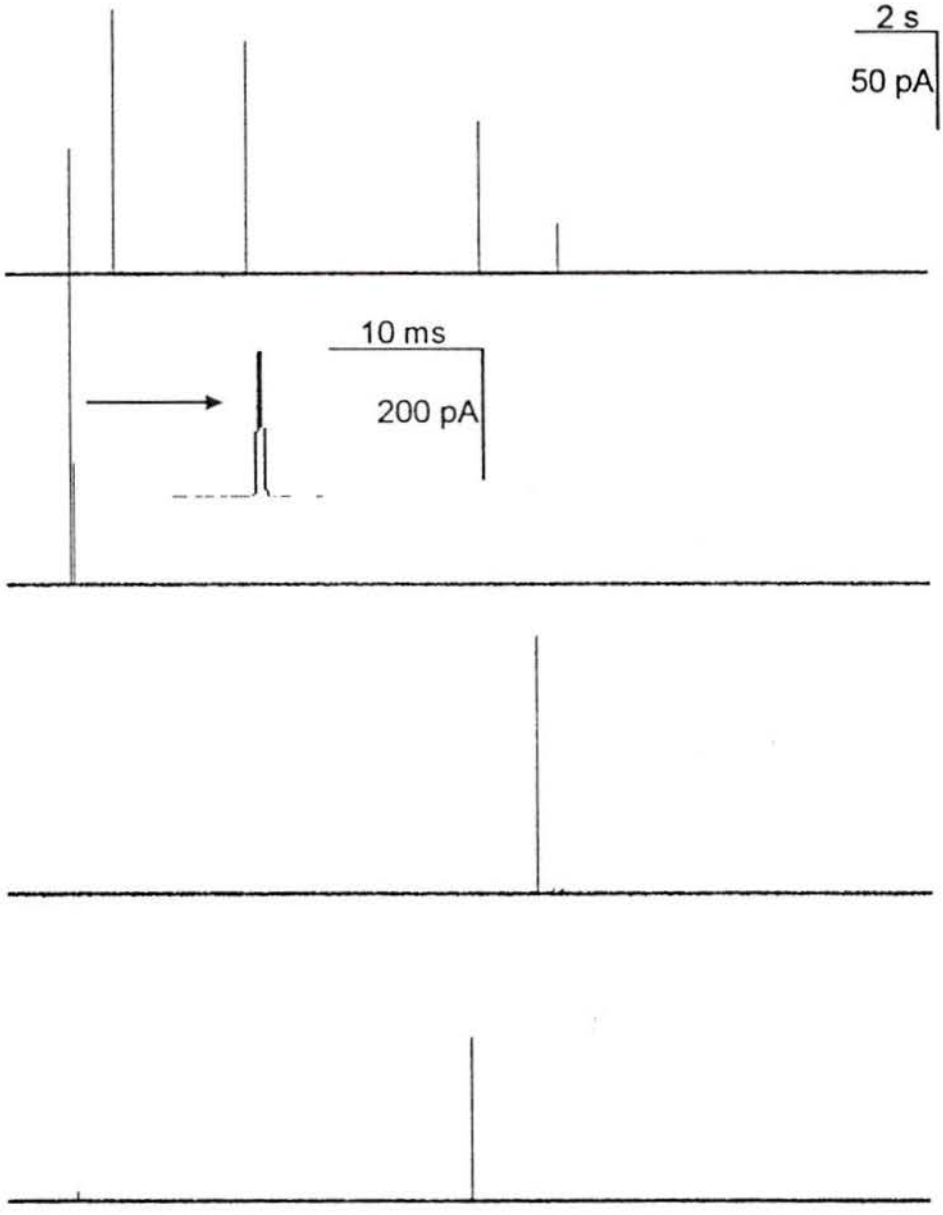

Figure 6.2: Current spikes induced by 100 nmol N88Su88N at +120 mV transmembrane potential, 1 M KCl as electrolyte, diPhyPC bilayers. Sampling frequency was 10 kHz, data was analog filtered with 1 kHz.

In contrast to the membrane disrupting activity of N88Su88N, the anionic bola-amphiphile, A88Su88A, does not destroy the membrane in all cases. Using amounts in excess of 70 nmol, the bola-amphiphile acted as a detergent in a similar fashion as N88Su88N when 1 M NaCl or 1 M CsCl were used as electrolytes. With KCl its activity more closely resembled that observed with the other compounds in the 88 series. The typical asymmetric current signal with longer decay than rise times was observed. The maximum current amplitude was much higher than for A88PA88A. As illustrated in part a) of Figure 6.3 current amplitudes of up to 15 pA in a single opening could be observed even at early stages of the experiment, while these amplitudes were rarely obtained with the other compounds. Note that the current amplitudes were variable with time implying aggregates of different stoichiometry. In addition to the dominating 'sharkfin' signals, brief (0.5-2 ms) erratic openings of varying amplitude (10-1000 pA) were observed in all records. These brief events occured more frequently throughout the experiments than for the compounds with the carboxylate linker and are indicative of the defect-inducing capability of A88Su88A. At lower ionic strength the openings were of shorter duration as illustrated by Figure 6.3 b). This is consistent with the results obtained for A88PA88A and indicates the influence of the ionic strength on the partition coefficient.

Unexpectedly, the duration of the openings was much longer at positive applied transmembrane potentials than at negative applied potentials. As illustrated in Figure 6.4 the total duration of each event became progressively shorter as the potential was changed from positive to negative. An opening duration of about 17 seconds can be seen at +120 mV, but the opening duration is only about 5 seconds at -120 mV. These events were representative of at least 10 transport events at each potential. Furthermore this voltage dependent behaviour was reproducible in three independent experiments. An additional feature is that the maximum current amplitudes varied between experiments. In one experiment maximum amplitudes of 15 pA were observed, while only 4 pA was reached in

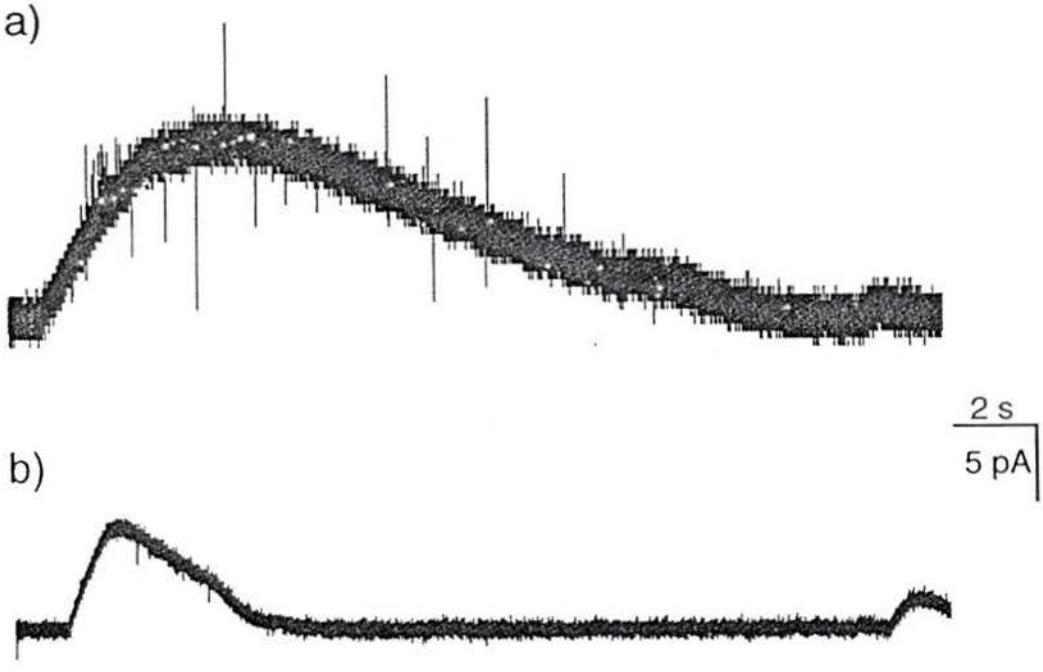

Figure 6.3 Current-time relationship of 90 nmol A88Su88A in diPhyPC bilayers at +120 mV applied potential with: a) 1 M KCl and b) 0.5 M KCl as electrolyte. Data was acquired with: a) 20 kHz; analog filtered with 2 kHz b) 10 kHz; analog filtered with 1 kHz.

the next experiment. However, the variability of the amplitude within each experiment was about ± 2 pA. The current-time traces shown are taken from an experiment where 90 nmol A88Su88A was added to the *cis* compartment of the bilayer chamber. The potential was fixed for 60 seconds and then reversed. Thus, the trace labeled -120 mV in Figure 6.4 was recorded immediately after the one labeled +120 mV. This was followed by ±80 mV, and ±40 mV applied potential.

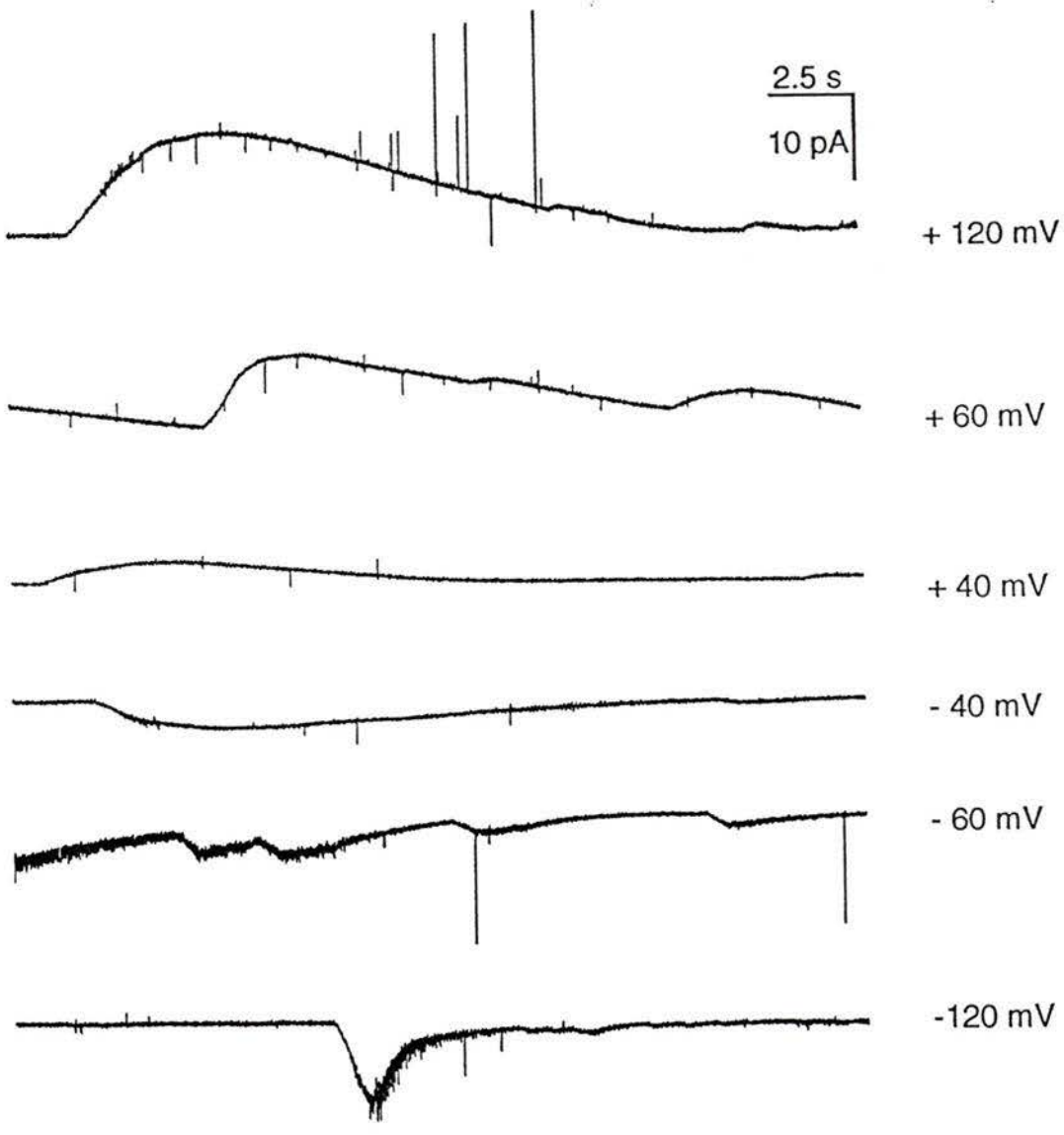

Figure 6.4: Currents induced by 80 nmol A88Su88A in a diPhyPC bilayer with 1 M KCl as electrolyte at the transmembrane potentials indicated in the Figure. All data traces have been acquired at 20 kHz and were analog filtered with a 2 kHz filter.

6.2 Working hypothesis

The transport activity of A88Su88A and N88Su88N in planar bilayer membranes is qualitatively different from that observed for the bola-amphiphiles with the carboxylate linker. This must be related to the difference in conformation between the transporters. As mentioned before, molecular modelling indicated that the sulfide linker induces a more twisted conformation while the carboxylate linker leads to a more extended conformation.[64] Although we have no direct evidence we can assume that these will be the predominant conformations in the bilayer. First the observed differences in behaviour between the two sulfide linked bola-amphiphiles will be discussed. Following that the voltage dependent behaviour of A88Su88A will be addressed.

Both sulfide linked bola-amphiphiles induce defects in planar bilayer membranes. These defects are manifested in brief openings of high current amplitude. However, while the net 2+ charged N88Su88N disrupts the membrane under all conditions investigated, the anionic A88Su88A can form stable aggregates when KCl solutions are employed as electrolytes. This difference has to be attributed to the head group charges. In general, lipid bilayer membranes are more permeable to anions than to cations.[1] It can then be envisaged that the energy barrier for head group penetration might be much higher for N88Su88N than for A88Su88A. We assume again that the transporter molecules first insert into the bilayer in a U-shaped manner. If the energy barrier for head group transfer is high for N88Su88N then the bola-amphiphile would remain in this conformation. Lateral diffusion of these U-shaped transporters in one bilayer leaflet would eventually lead to side-to-side dimers which disrupt the membrane. The energy barrier for bilayer penetration of the anionic head group is assumed to be less high and therefore the flip-flop of A88Su88A molecules from one bilayer leaflet to the other becomes feasible. The energy barriers must depend on the nature of the electrolyte employed as A88Su88A disrupted the membrane with all electrolytes except KCl. Specific interactions of the carboxylate head groups with the potassium ion may be invoked.

Since we observe the unusual signal shape with longer decay than rise times we propose that the aggregates formed by A88Su88A when KCl electrolytes were employed also approach perfect cation selectivity. However, the local Donnan potential that was invoked in the explanation of these signals must develop faster at *cis* negative potentials than at *cis* positive potentials. How can the voltage dependence of the closing process for A88Su88A be explained? Generally, mechanisms for rectifying current-voltage responses invoke that one of the steps leading to ion transport includes an asymmetry.[10,29,89,90] This asymmetry can be achieved by incorporating dipoles or charged groups into the structure.[35,83,91,92] In our previously described system this has been realized by the introduction of a dianionic head group as described in chapter 4. However, the structures of A88Su88A and N88Su88N are the most symmetric of all the bola-amphiphiles described in the previous chapters. The observed voltage dependence can therefore not be attributed to an asymmetry in the structure of the transporter. However, an overall asymmetric aggregate can easily be envisaged. Suppose that A88Su88A has a higher barrier for the change from a U-shaped conformation to a transmembrane orientation than does A88PA88A. In this case, the preferred orientation in the membrane will be a U-shaped conformation in the bilayer. Consequently flip-flop across the membrane becomes less probable and fewer transporter molecules will be found in the bilayer leaflet that is opposite to the side of addition. Thus an uneven distribution of monomers in the two bilayer leaflets exists. In analogy to the aggregation behaviour of A88PA88A (chapter 5) we assume that the active structures are large aggregates. However, these aggregates will be of asymmetric shape as depicted in Figure 6.5.a). The overall shape is assumed to be approximately conically as more transporter molecules reside in the bilayer leaflet facing the *cis* side. This also leads to an uneven distribution of negative charges at the two ends of the cone. While transporter monomers can have a maximum charge difference of two charges for N8TrgPA8TrgA, the charge difference on the two sides of the bilayer can be much greater for an aggregate composed of U-shaped monomers. The excess negative charge on the *cis*-side of the bilayer may be partially compensated by the applied transmembrane potential. To sustain a *cis* positive transmembrane potential, an excess of positive charge has to be located at the *cis* face of the bilayer which may lead to the

stabilization of the aggregate. The observation of longer open times at *cis* positive potentials than at *cis* negative potentials is consistent with this stabilizing effect as illustrated in part b) of Figure 6.5. The current amplitude, however, will be determined by the diameter of the smaller pore entrance which is consistent with the observation of roughly the same maximum current amplitude at positive and negative potentials.

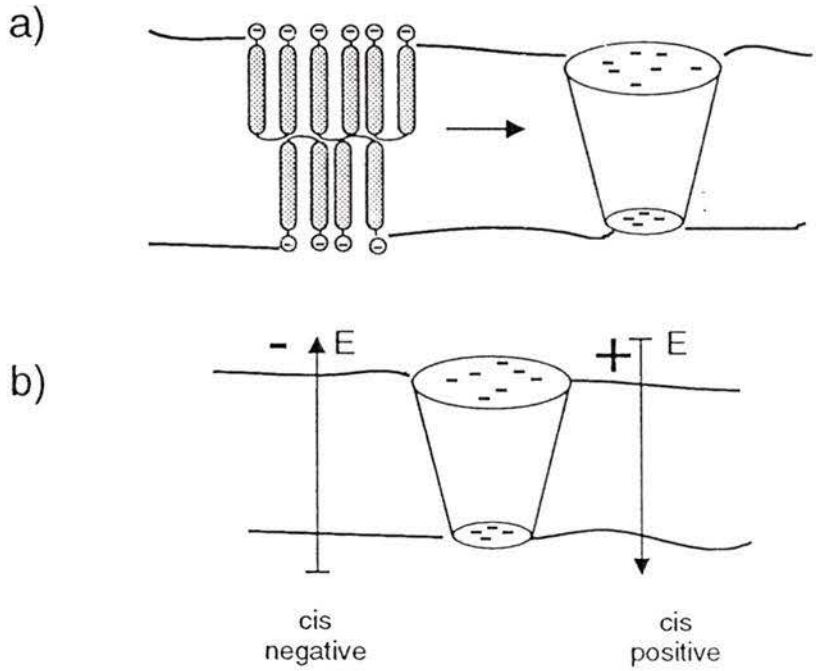

Figure 6.5: Illustration of the working hypothesis for the voltage-gated behaviour of A88Su88A.

The transmembrane electric field also directs the flow of cations across the membrane. In response to the applied transmembrane potential the cations will flow fom the *cis* side of the bilayer to the *trans* side at *cis* positive potentials. This leads to a higher concentration of cations at the wider channel entrance which stabilizes the aggregate by reducing head group repulsions and therefore leads to longer open times. As mentioned above, the local Donnan potential is proposed to develop faster at *cis* negative than at *cis* positive potentials. The local Donnan potential can be visualized as being caused by a spatially confined region at the pore entrance which is enriched in cations. At *cis* negative potential the cations, that arrive at the narrower pore mouth on the *trans* side of the bilayer, will interact with the head groups and thereby neutralize the head group charge.

An excess of positive charge, and therefore a Donnan potential, is reached faster than at positive potentials where more anionic head groups would have to be neutralized before a Donnan potential can develop.

6.3 Test of working hypothesis

6.3.1 Addition of barium ions

If the hypothesis of an asymmetric distribution of U-shaped transporter molecules is correct we would expect that the voltage-dependent behaviour can be altered by reducing the energy barriers for flip-flop. The addition of divalent cations may neutralize the anionic head groups of A88Su88A and stabilize the U-shaped conformation. This would lead to a formally neutral transporter-divalent cation complex on both sides of the membrane. Thus, the local Donnan potential would develop in the same time frame for positive and negative transmembrane potentials. Therefore upon addition of low concentrations of barium chloride we expect to be able to still observe the 'sharkfin' signal but not the voltage dependence of the closing process. This was indeed the case as illustrated in Figure 6.6.

The current-time traces shown are taken from an experiment where 100 nmol A88Su88A were added to the *cis* compartment of the bilayer chamber. As previously the potential was fixed for 60 seconds and then reversed. Thus the trace labeled -120 mV in Figure 6.6 was recorded immediately after the one labeled +120 mV. The voltage-dependence of the closing step that was evident in Figure 6.4 could not be observed in Figure 6.6. The openings were of approximately the same duration at positive and at negative transmembrane potentials, i.e. 5-7 seconds. The maximum current amplitudes in Figure 6.6 are of lower values than the maximum amplitudes observed in the experiment without barium ions. Compare ~15 pA at +120 mV applied potential in Figure 6.4 with about 4 pA at the same potential in the presence of Ba^{2+}. We do not relate this difference in amplitude to the electrolyte employed as the current amplitudes varied between 5 and 15 pA for repeat experiments with 1 M KCl as electrolyte. Rather we assume that

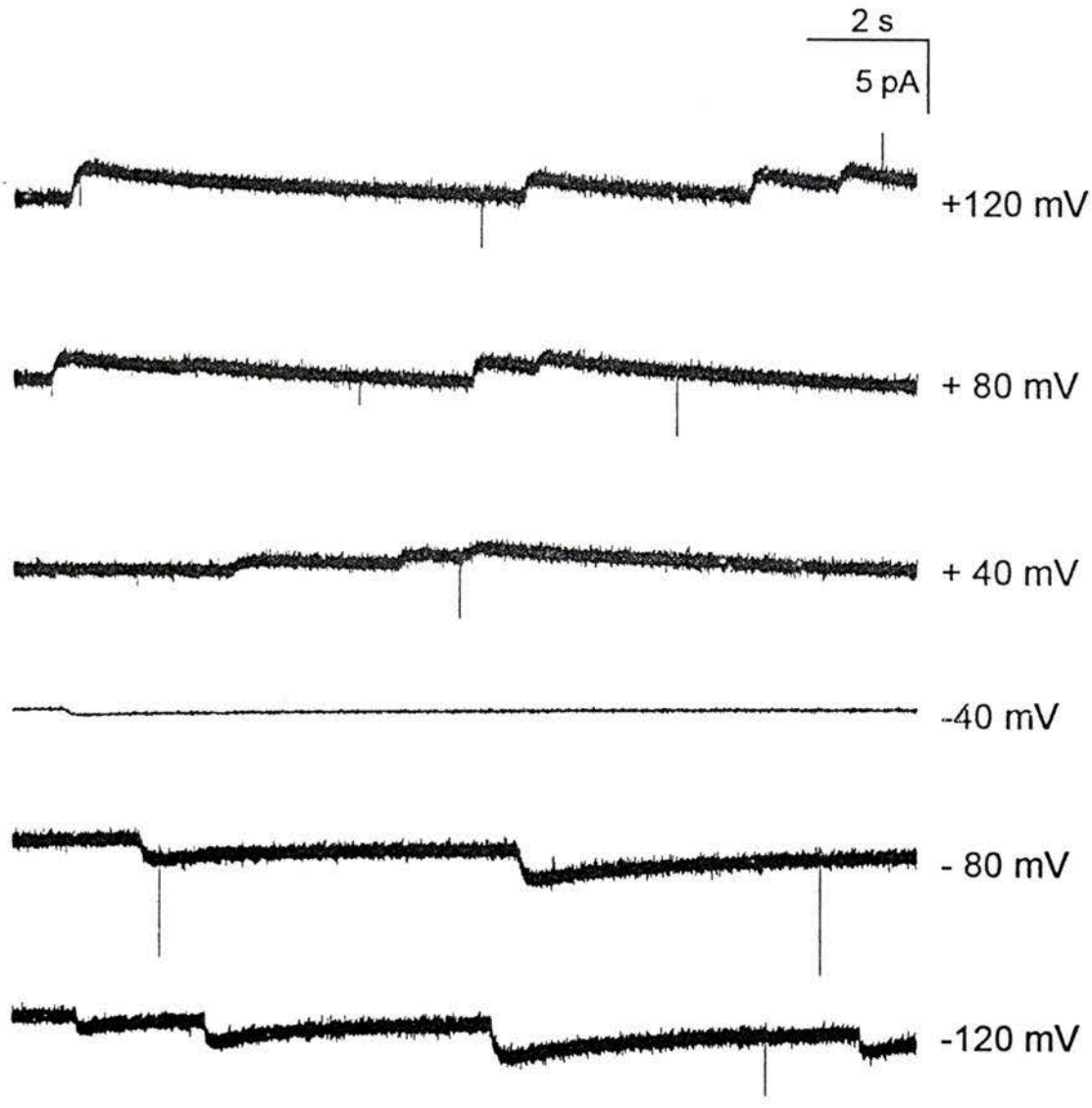

Figure 6.6: Current-time relationship for 100 nmol A88Su88A in diPhyPC bilayers with 1 M KCl, 1.6 mM $BaCl_2$ as electrolyte. Transmembrane potentials are indicated in the Figure. Data was aquired at 10 kHz, analog filtered at 1 kHz, and digitally filtered with a 200 Hz Gaussian filter.

aggregates comprised of different numbers of transporter monomers are formed in each experiment which is reflected in the maximum current amplitude. To visualize the effect of divalent barium ions on the closing time the total current in each trace recorded was integrated using the Fetchan software. The total charge that was carried across the membrane in 60 seconds is plotted as a function of transmembrane potential in Figure 6.7. In the absence of barium ions there is clearly less current carried per unit time at negative transmembrane potentials than at positive transmembrane potentials (Figure 6.7 a). Addition of Ba^{2+} leads to a more symmetric current-voltage relationship as evident in part b) of the Figure.

Barium ions may suppress the voltage dependence of the closing process by two means. The barium ions can interact with the anionic head groups and thereby neutralize the negative charge at the pore entrance. Suppose that the energy barrier for flip-flop is still high so that the distribution of transporter molecules in the bilayer leaflets remains asymmetric. Aggregation of monomers would then lead to a conical pore with pore entrances that are net neutral. The amount of current carried in each opening would be determined by the entrance with the smaller diameter. Since no formal head group charges exist the local Donnan potential would built up in a similar time frame on the two sides of the bilayer and no voltage dependent closing process would be observed.

In addition to the effect above, the negatively-charged head groups of a transporter monomer may chelate the divalent barium ion and thereby form a neutral complex. This net neutral complex can then cross the membrane and lead to a symmetric distribution of bola-amphiphiles in the two bilayer leaflets. Therefore symmetric domains that are rich in transporter can form in the bilayer leading to a lack of voltage dependent behaviour.

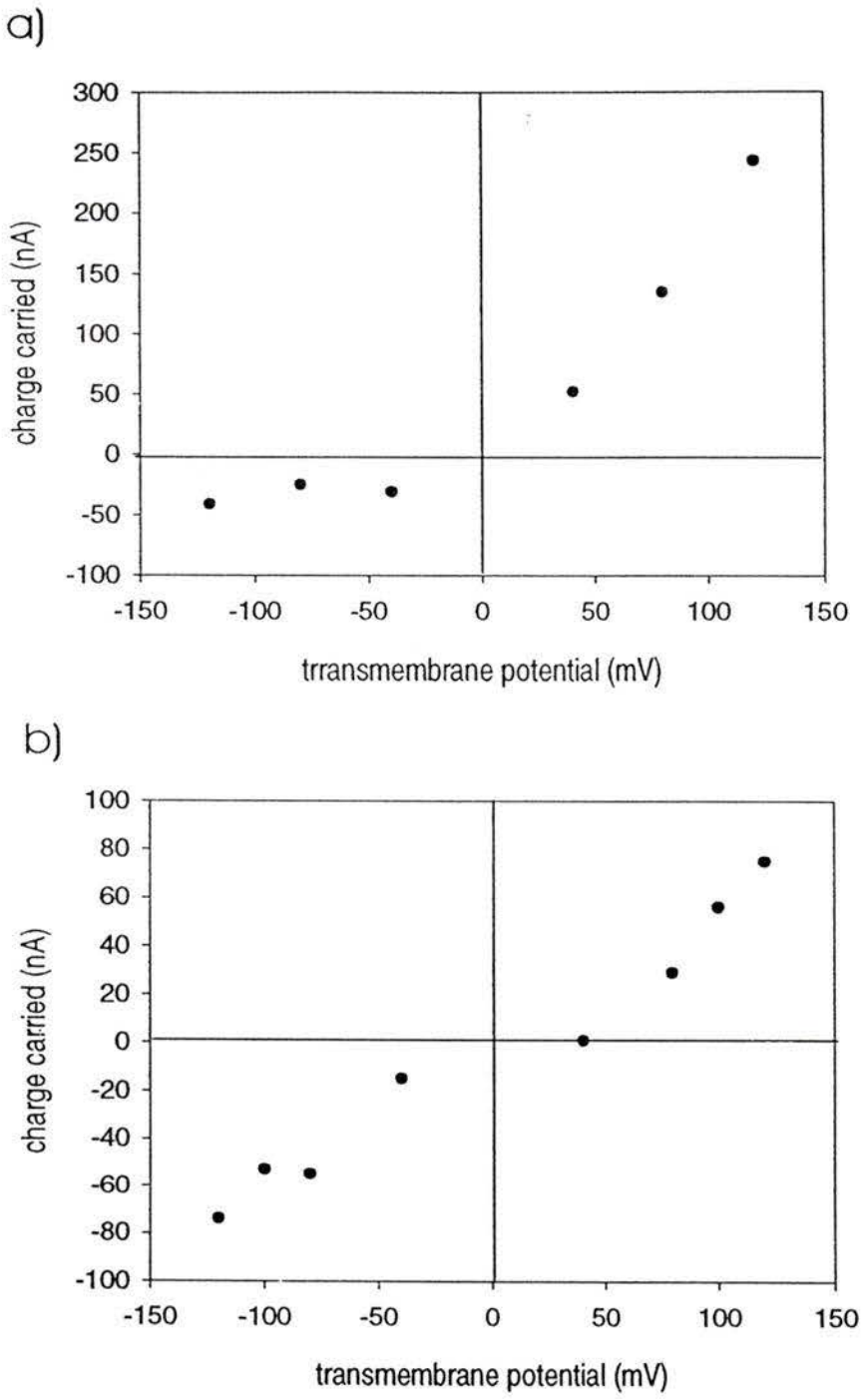

Figure 6.7: Current integrated over 60 seconds as a function of applied transmembrane potential. A) data from Figure 6.4: 80 nmol A88Su88A, diPhyPC bilayer, 1 M KCl; b) data from Figure 6.6: 100 nmol A88Su88A, diPhyPC bilayer, 1 M KCl, 1.6 mM $BaCl_2$.

6.3.2 Effect of pH

The results from the experiments with barium ions indicated that a reduction of the total head group charge in a transporter aggregate may influence the voltage dependent closing process. We propose that a similar result can be achieved by protonating the head groups. Increasing the acidity to a pH near the pK_a of the head groups ($pK_a \sim 4.75$)[86] will not only protonate 50 % of carboxylic head groups but also introduce the potential for hydrogen bond formation between the head groups. This may stabilize the aggregates and lead to longer open times. In analogy to the behaviour of A88PA88A at this pH, step conductance changes might be observed (refer to Figure 5.7, chapter 5). To investigate this possibility an experiment at pH 4.75 was conducted.

Figure 6.8: Currents induced by 130 nmol A88Su88A in a diPhyPC bilayer with 1 M KCl, pH 4.75 as electrolyte. Holding potential was +100 mV (a) and -100 mV (b). The traces were recorded with 10 kHz sampling frequency, analog filtered with 1 kHz, and digitally filtered with 200 Hz.

The two traces shown in Figure 6.8 were recorded 12 minutes after transport activity could first be observed. The typical 'sharkfin' signal was observed at all transmembrane potentials in addition to some brief openings that carried large currents.

No step conductance changes were evident at any point in the whole experiment. As shown in part b) of the Figure, at -100 mV applied potentials signals of about 15 second duration could be observed. This is comparable to the open duration at +100 mV. However, signals with faster decay times such as in the initial part of the trace shown in part b) were evident as well. These signals had open durations of about 5 seconds as opposed to about 15 seconds at +100 mV. This means that we may be observing two different populations of pores in the membrane. One population in which an asymmetric charge distribution still exists on either side of the membrane thus giving rise to the voltage-dependent closing process. A second population where a symmetric charge distribution has been achieved leading to pores that show no voltage dependence. This result shows that partial protonation of the carboxylate head groups is not as efficient in reducing the charge asymmetry across the membrane as the addition of divalent cations. However, it is expected that complete protonation of the head groups at lower pH's will lead to non-voltage dependent behaviour.

The observed step conductance changes of A88PA88A at pH 4.75 were attributed to small transmembrane oligomers that could form a structured aqueous pore. In contrast to this carboxylate-linked bola-amphiphile, A88Su88A did not induce step conductance changes at pH 4.75. We take this as evidence that the preferred conformation of this compound in the bilayer is indeed the twisted conformation that was suggested by molecular modelling.[64] The conformation is apparently not able to induce small stable aqueous pores. Therefore we can conclude that the step conductance changes that were observed for the suite of compounds based on the 8Trg wall unit (chapter 3) are also caused by transmembrane dimers rather than by the dimerization of two U-shaped monomers.

In conclusion it has been shown that the replacement of one atom in a crucial part of the structure, i.e. the linker, can alter the ion transport behaviour dramatically. Control over the conformation of the bola-amphiphile also leads to control over the ion transport behaviour. It has also been demonstrated that asymmetry is a central feature to achieve

current-voltage rectification. This asymmetry need not necessarily be located in the structure itself. Symmetric compounds such as A88Su88A can induce asymmetric current-voltage responses by forming large aggregates of overall asymmetric structure. Controlling the energy barrier for flip-flop across the membrane can also induce voltage-gating.

7. Other artificial ion transporters synthesized in the Fyles group

As mentioned in the introduction, several other bola-amphiphilic ion transporters were prepared in our group in order to gain insight on the effect of the structure on the activity. In the following paragraphs the activity of two examples in planar bilayer membranes will be presented. In the first case the compounds were designed to act as membrane disrupting agents. The second compound presented is an example for a compound that was designed as a unimolecular ion transporter. This transporter is only one out of a series of twenty-one bola-amphiphiles that were prepared mainly by T. James.[60] The behaviour of some of these compounds in vesicles was strongly suggestive of a channel-type mechanism.[58,63,93] However, the results obtained by bilayer clamp experiments show that well-behaved behaviour in vesicle experiments can be based on more erratic behaviour on the single molecule level which was too complex to be analyzed in detail. For this reason the transport behaviour of these compounds was not fully characterized.

7.1 Bis(crown ether carboxylate) bola-amphiphile

In a series of reports on membrane disrupting systems based on bis(oligoethyleneoxide) bola-amphiphiles by Regen and co-workers[44,94] U-shaped conformations were invoked in membrane disruption. This sparked the synthesis of a suite of bis(crown ether carboxylate) bola-amphiphiles in our group.[65,95] The structures of the bis(crown ethers) synthesized by B. Zeng are shown below. Only the compound with the tetradecane linker was investigated in planar bilayer membranes and will be referred to as 'bis-crown' in the reminder of this section.

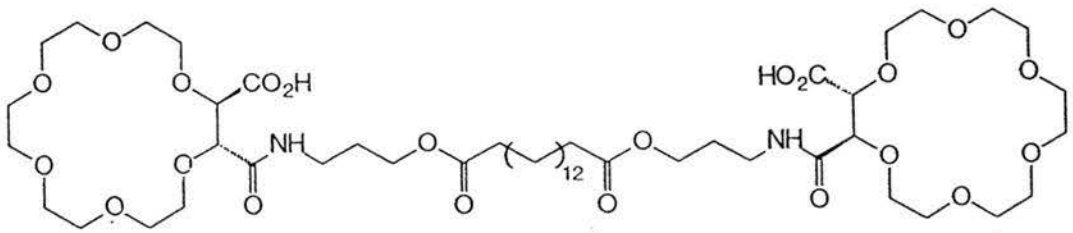

1

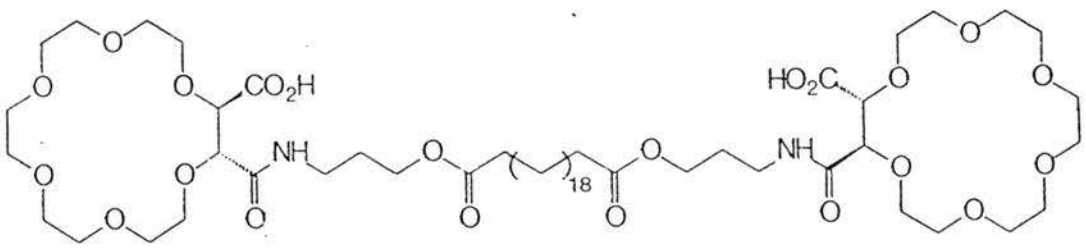

2

These compounds allow further investigation of the involvement of U-shaped states in membrane disruption. In addition, the potential for the control of the transport behaviour *via* the addition of small ligands can be explored. The crown ether carboxylate head groups repel each other sterically and electrostatically. Addition of divalent cations may overcome the electrostatic repulsion of the head groups. Therefore the binding of a divalent cation to one of the crown ethers would favor the approach of the head groups and thereby stabilize a U-shaped conformation. Membrane disruption would then be induced by these U-shaped states. Thus control of the activity may be achieved based on molecular recognition of the crown ether head groups.[96]

The activity of these compounds in vesicle membranes was studied extensively using the pH-stat assay[58,64,95] and by monitoring the release of liposome-entrapped 5[6]-carboxyfluorescein (CF).[65,95] The shorter bola-amphiphile **1** was less active than bola-amphiphile **2** in both assays indicating that the 'right' overall length is important for optimum activity. Using the pH-stat assay, qualitatively different transport behaviour was detected for the bis-crown bola-amphiphiles than for the compounds described previously in this thesis.[96] The total extent of transport increased as the transporter concentration was

increased. However, the observed rates were similar. This suggests a mechanism that involves membrane disruption rather than the controlled transport of ions. The crown ethers were cation selective in the order $K^+ > Rb^+ > Cs^+ > Na^+ > Li^+$, consistent with cation-oxygen donor interactions.[96] The effect of divalent cations was studied with the CF-assay.[65] Addition of barium ions enhanced the rate of CF release in vesicles.[65,95] The inferred mechanism involves partitioning of the bis-crown to the liposome followed by insertion in the outer bilayer leaflet. In the presence of monovalent ions alone, the two head groups repel one another which would inhibit the formation of U-shaped conformations. The addition of Ba^{2+} would then allow the formation of a neutral 1:1 complex with a U-shaped conformation which would then lead to rapid membrane disruption.

7.1.2 Planar bilayer experiments

The activity of bis-crown **1** was investigated for 1 M KCl and 1 M CsCl electrolyte. The typical current-time relationship induced by **1** in PC:PA:Chol bilayers and 1 M KCl as electrolyte is shown in Figure 7.1. A total of 8 nmol transporter was added to the *cis* compartment of the bilayer chamber. Transport activity was generally observed within 15 minutes after addition of the compound. The current-time trace shown in Figure 7.1 was recorded 10 minutes after events were first observed and is typical for an activity sustained over a period of 30 minutes. Clusters of events can be observed followed by longer periods of quiescence (5-40 seconds). The events were of 0.5-5 ms duration and the current amplitudes varied between 2-200 pA. The observed transport behaviour was qualitatively similar when 1 M CsCl was used as electrolyte. For both electrolytes transport activity could only be observed when transmembrane potentials of ±100 mV or higher were applied. This suggests that a high driving force is required to overcome the electrostatic and steric repulsion of the head groups.

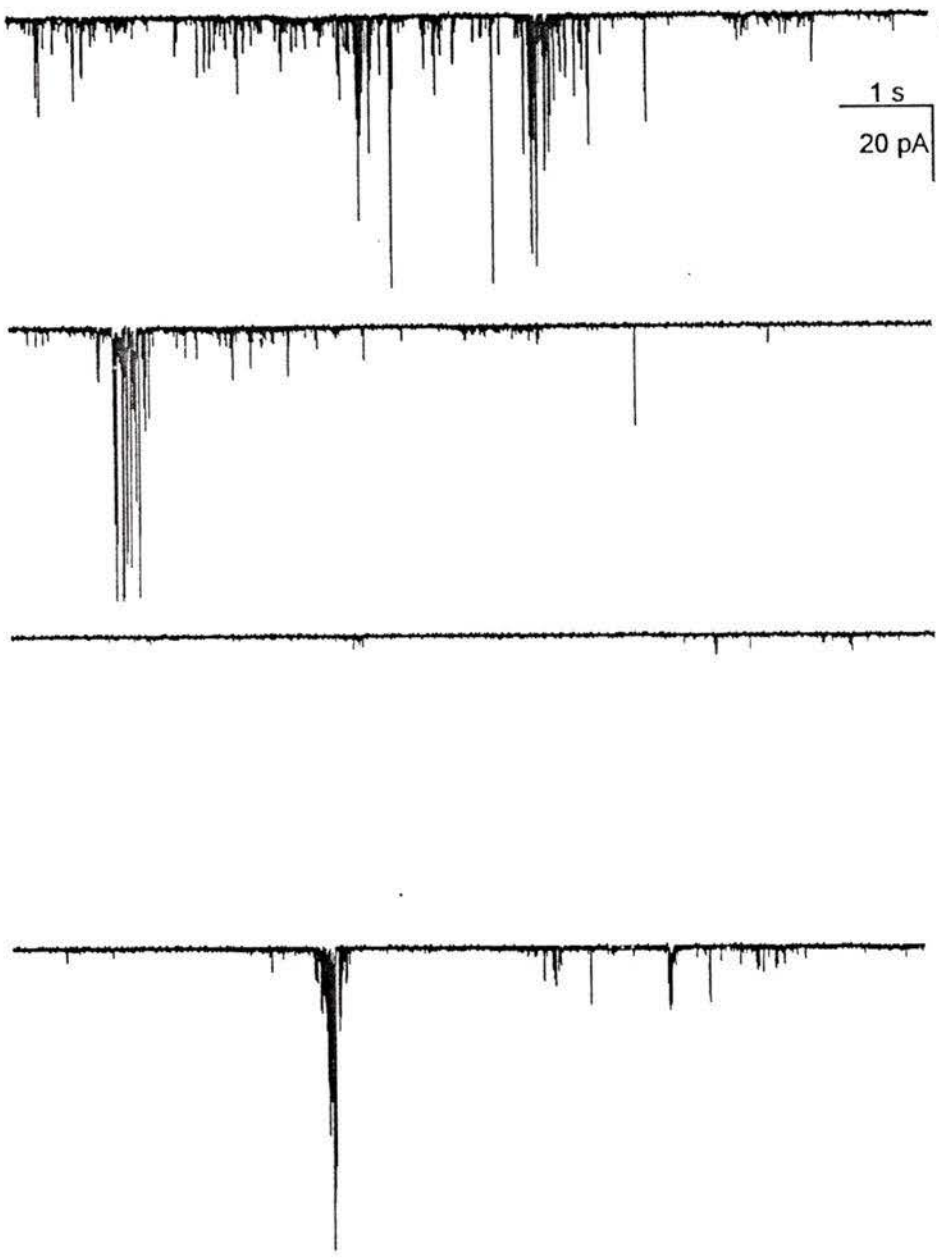

Figure 7.1: Current-time relationship for 8 nmol bis-crown **1** in a PC:PA:Chol bilayer with 1 M KCl electrolyte. Transmembrane potential was -120 mV. The data was acquired with 10 kHz sampling frequency and analog filtered with 1 kHz.

In addition to the brief erratic events, some step conductance changes of short duration could be observed as illustrated in Figure 7.2. The two events shown in the Figure had an open duration of 4-5 ms and current amplitudes of 10-11 pA. Several such step conductance changes of similar duration but with variable current amplitude were observed throughout the record. In Figure 7.2 CsCl was employed as electrolyte, however, the step conductance changes also occurred with 1 M KCl as electrolyte. The scattered values of the current amplitudes defied a comparison of the specific conductance for the two salts. The occurrence of these step conductance changes suggests the formation of transmembrane conformations of the bis-crown bola-amphiphile followed by aggregation to form transmembrane aqueous pores. The short open duration of these pores indicates that the aggregates are not very stable. This may be related to the considerable flexibility of the tetradecane linker.

Figure 7.2: Current flux across PC:PA:Chol bilayers induced by 8 nmol bis-crown **1** with 1 M CsCl as electrolyte. Applied transmembrane potential was 100 mV. Data was acquired with 100 kHz and analog filtered with 1 kHz.

The brief transport events illustrated in Figure 7.1 suggest that the bis-crown bola-amphiphile induces mainly defects in the planar bilayer membrane. This is consistent with our expectation that U-shaped conformations lead to membrane disruption. The occurrence of more regular step conductance changes of short duration indicates that transmembrane conformations can be achieved which may aggregate and thus lead to pore formation. The linker that connects the two crown ether head groups is considerably more

flexible than the macrocyclic wall units presented earlier. Therefore the extended conformation of the transporter is expected to exhibit low resistance to lipid movement which leads to the observed short open durations; compare milliseconds for the bola-amphiphile described here with several seconds for a related system that has been synthesized by Gokel and coworkers.[56,57] In their system the linker are also flexible but an additional crown ether moiety was needed in the center of the molecule to give the molecule more rigidity.[56,57]

Further studies on this set of bis crown ethers should allow more insight into the control of membrane disruption. It would have been interesting to investigate the effect of barium ions on the transport behaviour in planar bilayers. However, in a bilayer clamp experiment such as above, the activity observed is due to the non-functional part of the system, that is the disruption of the membrane is not achieved. On the other hand, as a planar bilayer experimenter, I am not interested in the disruption of the membrane. Therefore the activity of this compound was not further pursued in planar bilayers.

7.2 Unimolecular pore formers

All bola-amphiphiles described so far in this thesis were designed to form aggregates in bilayer membranes.[62,64,65,72,96] Previous graduate students in the Fyles group synthesized and characterized a suite of compounds that were designed to act as unimolecular pore formers.[58,59,61,63,63,93] These bola-amphiphiles were based on a crown ether framework. Appended to this 'core' were wall units derived from maleic acid esters and the structure was capped at either end with hydrophilic head groups, **G**, **N**, and **A**. The design assumed that the crown ether would lie near the bilayer-midplane, and would orient the wall units towards the faces of the bilayer. A total of 21 compounds based on this structure were characterized using the pH-stat assay.[58,61,63,93] One of the most active compounds that was detected in the survey was the four-armed transporter $(G8TrgP)_4Tet$ (structure below). In addition to a very high specific activity it showed a marked selectivity for Na^+ that fell outside any of the Eisenmann selectivity sequences. Instead, the

following selectivity sequence was obtained: $Na^+ > Rb^+ \approx Cs^+ > K^+ > Li^+$. The transport of Na^+ was inhibited by K^+ which strongly indicates the formation of a membrane spanning pore. The kinetic order was determined as 0.66. From the vesicle survey it was inferred that this compound is capable of forming unimolecular ion channels.[58]

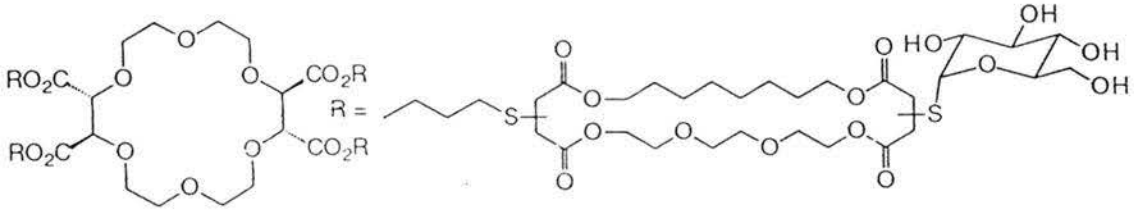

(G8TrgP)$_4$Tet

The unusual cation selectivity sequences suggests specific interactions between the transporter structure and the cation other than the electrostatic interactions normally invoked in the Eisenmann selectivity sequences.[22] Both the low kinetic order and the inhibition of sodium transport by (G8TrgP)$_4$Tet are indicative of the formation of a tunnel-like transmembrane structure that conducts ions across the membrane.[58] Following established procedures[58,59,63] (G8TrgP)$_4$Tet was re-synthesized by P. Montoya-Pelaez in order to compare the activity of this unimolecular ion transporter in planar bilayer membranes to the transport behaviour of the simpler bola-amphiphiles that form aggregates. The re-synthesized compound displayed identical behaviour in the vesicle assay to the compound synthesized earlier. Thus a full-scale replication has been achieved.

7.2.1 Planar bilayer studies of (G8TrgP)$_4$Tet

Figure 7.3 shows a portion of a single-channel record spanning about 8 seconds for (G8TrgP)$_4$Tet in an 8:1:1 PC:PA:Chol bilayer separating 0.5 M NaCl solutions, at an applied potential of +100 mV. The record was chosen to illustrate the general behaviour of the compound. This section is taken from 52-60 seconds into a record spanning 90 s, approximately 50 minutes after addition of the transporter. It is typical for an irregular

behaviour that was observed at all transmembrane potentials and with all electrolytes investigated. After addition of 25 nmol of transporter to the *cis* compartment of the bilayer chamber a variable lag-time (5-40 minutes) eventually led to sporadic openings such as those near D. These openings were of 5-10 ms duration and became more pronounced and of longer duration over the course of an experiment. Eventually major conductivity events were observed that last for 2-10 seconds such as indicated by A and B in the Figure. The current amplitude of these events sometimes exceeded 100 pA. These openings collapsed to a predominantly closed state near C. However, as the experiment progresses the quiescent states become less frequent and eventually disappear. Step conductance changes of 20-30 ms duration and current amplitudes of 15 to 60 pA could be observed intermittently. This is illustrated at the top of Figure 7.3 which shows part of the record on an expanded scale.

Although there appear to be some regularities in the records, all attempts at objective analysis of this data failed to identify any specific behaviour. The observed activity was apparently erratic at all resolution scales. This was also true for LiCl, KCl and CsCl as electrolyte and for diphytanoyl PC as lipid. The same qualitative behaviour was observed upon increasing the ionic strength to 2.5 M KCl. In addition to the brief openings of 5-10 ms duration and variable current amplitude, slightly longer step conductance changes of 20-100 ms duration were observed (data not shown). However, this type of openings occurred only sporadically and was too variable in amplitude to justify analysis.

The occurrence of step conductance changes is indicative of structured aqueous pores in the membrane some of which move significant amounts of charge across the bilayer. Thus the high activity of this transporter in the vesicles[58] is not surprising. In this brief survey we were unable to detect any pattern in the behaviours, so the ion selectivity question remains unanswered for the planar bilayers. The unusual selectivity sequences may be a result of ion-selective initiation of the erratic transport evident in the single-channel record.

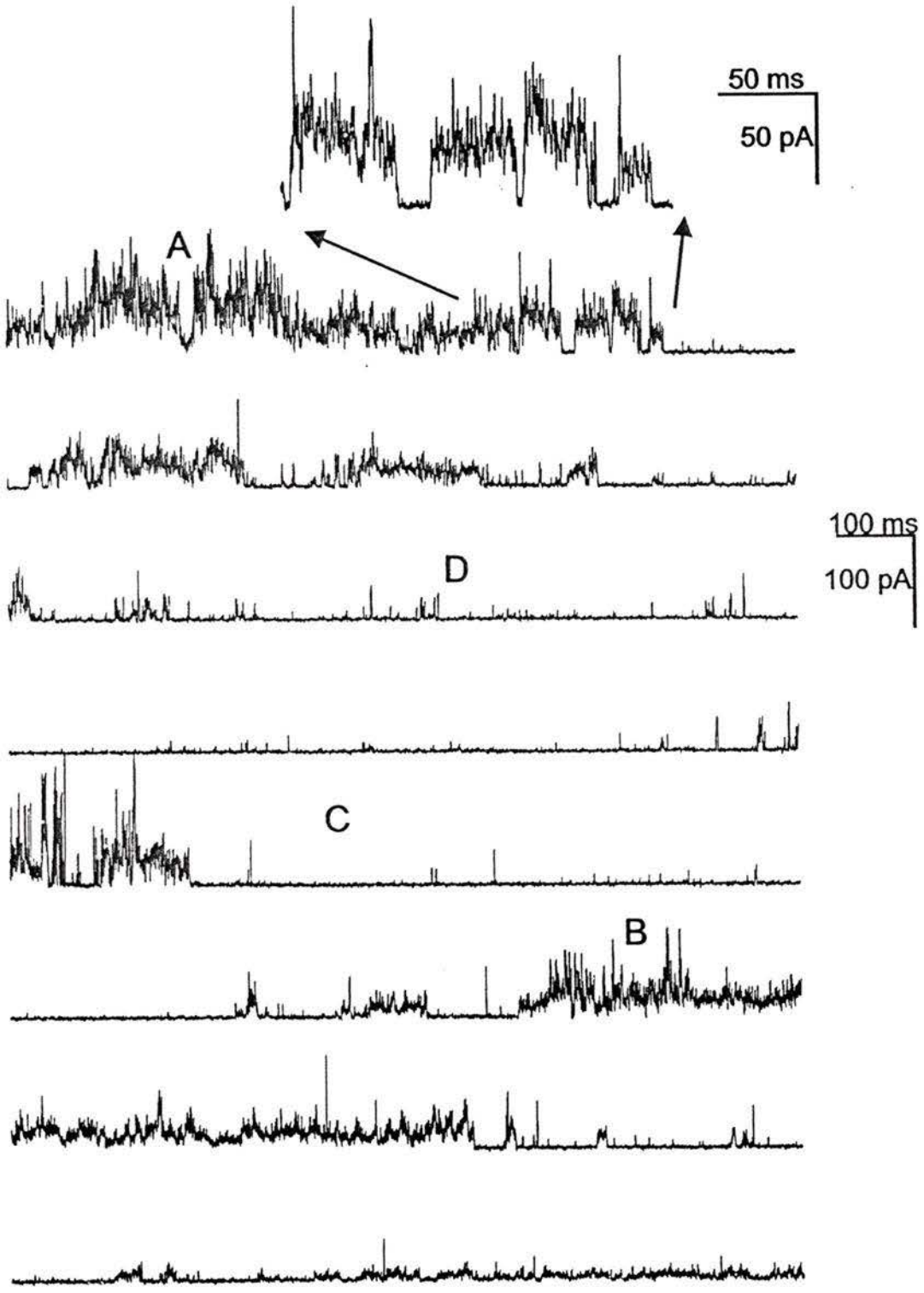

Figure 7.3: Current-time relationship of $(G8TrgP)_4Tet$ in a PC:PA:Chol bilayer, 0.5 M NaCl electrolyte, applied potential +100 mV. The top trace is an expansion of the section indicated. Data was acquired 10 kHz and analog filtered at 1 kHz.

The results presented here are another example for an apparent discrepancy of the activity of transporters in vesicle and planar bilayer membranes; active, reproducible behaviour in the vesicle experiment is seen to be based upon erratic and poorly defined molecular events as revealed by the bilayer clamp experiment. This is normal for chemical systems: gases exert an equilibrium pressure on the walls of a vessel as a result of erratic trajectories of individual molecules. What is unique about the bilayer clamp experiment is that the properties of individual molecules is observed directly.

Based on results akin to Figure 7.3, what can be deduced about the mechanism in planar bilayers? Perhaps in the early part of the experiment the activity of only one or two molecules is observed. As the experiment progresses the current rises, and the quiescent states become less frequent. This would be consistent with a slow build-up of the molecules in the membrane. One mechanistic possibility is that the observed activity is due to single molecules acting on their own. Since the structures are fairly rigid and big, insertion of the transporter into the bilayer might be disfavored, as the U-shaped conformations that were invoked earlier in this thesis can not be achieved. Thus the brief transport events observed in a single-channel record may be caused by defects due to the insertion of the transporter. Following insertion the structures may be too poorly organized to establish a pore of defined properties. Perhaps the wall units can not achieve the optimum distance from each other due to the geometry forced upon them by the crown ether core. The step conductance changes might then be caused by a transmembrane conformation of the unimolecular transporter where the wall units briefly achieve an aqueous pore structure. Alternatively, a transporter molecule may seed a transient defect in the membrane, but cannot stabilize the aqueous fjord effectively.

In conclusion the results on the unimolecular ion transporter $(G8TrgP)_4Tet$ have shown that there appears to be an optimum in flexibility that is required for efficient transport. Too rigid a structure prevents the efficient insertion of the compound in the bilayer membrane. This may be the reason for the fairly high migration ratio that was observed with the pH-stat assay.[58] The migration ratio is a measure for the ability of a

transporter to migrate between vesicles through the aqueous phase. A high migration ratio is consistent with facile transfer of transporters between vesicles, while a low migration ratio indicates that the transporter is bound to the vesicles.[58] Thus the first-order rate that was observed in the vesicle assay may be due to the monomeric transporter inserting into the vesicle membrane and seeding a transient defect.

In addition bilayer lipid molecules may be involved in the stabilization of transmembranes pores in all cases presented in this thesis. Perhaps the structurally enforced geometry of the unimolecular pores prevents the specific lipid-transporter interactions that lead to an aqueous pore.

8. Concluding discussion

The results presented in the previous chapters demonstrate that 'small' synthetic molecules can transport ions across lipid bilayer membranes with mechanisms that have not been reported for natural protein ion channels. In the natural examples ion translocation is manifested in step conductance changes in planar bilayer experiments.[10,18] Conversely, a variety of signal shapes could be observed for the compounds that were investigated in this thesis and are summarized in Figure 8.1. Thus, we have established that in principle there exist other possible pathways for ion transport than the three pathways presented in the introduction (carrier, pore, defect). This discovery makes artificial ion transporters interesting in their own right. The fact that all ion channel proteins induce only well defined step conductance changes in bilayer membranes may be related to their physiological role in the membrane. Presumably the transport of ions needs to be precisely regulated to achieve functions such as signal transduction. Therefore the irregular mechanisms might have been lost during the evolutionary process of these proteins. On the other hand, small secreted peptides such as melittin and the defensins induce more irregular behaviour in planar bilayer membranes. Again this could be related to their role in nature, namely, the lysis of the membrane of 'hostile' organisms.

All transport mechanisms presented followed a central theme. We have been able to control the overall transport behaviour by influencing specific steps in the mechanism *via* small structural alterations of the ion transporters. This approach is analogous to the introduction of point mutations in proteins. In the following paragraph a generalized transport mechanism will be described and the effect of the 'point mutations' will be summarized.

8.1 Generalized Mechanism

8.1.1 Membrane association

Usually the bola-amphiphiles were added to the aqueous phase on one side of the bilayer only. Therefore, the transporters must initially diffuse to the membrane. This step is not important for natural ion channels since the proteins are generally large and firmly anchored in the membrane.[10] For synthetic ion transporters the membrane association will be influenced by the ionic strength of the solution which affects the partition coefficient from water to the membrane bilayer. This was reflected in greater amounts of transporter molecules that had to be added to the aqueous solution for low electrolyte concentrations. All other factors that would affect the partition coefficient, such as the introduction of more hydrophobic segments in the structure, will also be important for the association step. In addition, the propensity of the transporter molecules to form aggregates in aqueous solution will alter the driving force for membrane association. Unfortunately, the bola-amphiphiles presented in this thesis lack the presence of a chromophore so we cannot gain insight into the aggregation behaviour of these transporters. However, light-scattering experiments would allow us to detect the formation of large aggregates in the aqueous phase. Finally, the nature of the lipid membrane used is expected to be important. Negatively charged lipid membranes would presumably repel negatively charged ion transporters.

8.1.2 Insertion

Following association to the bilayer the transporter molecules have to insert into the membrane. Several possibilities exist as discussed in chapter 3. A U-shaped insertion of the compound into one leaflet of the bilayer can be envisaged, followed by the penetration of one of the head groups. Alternatively this extended transmembrane conformation can be achieved by direct insertion. A second head group penetration can then generate another U-shaped conformation in the opposite bilayer leaflet.

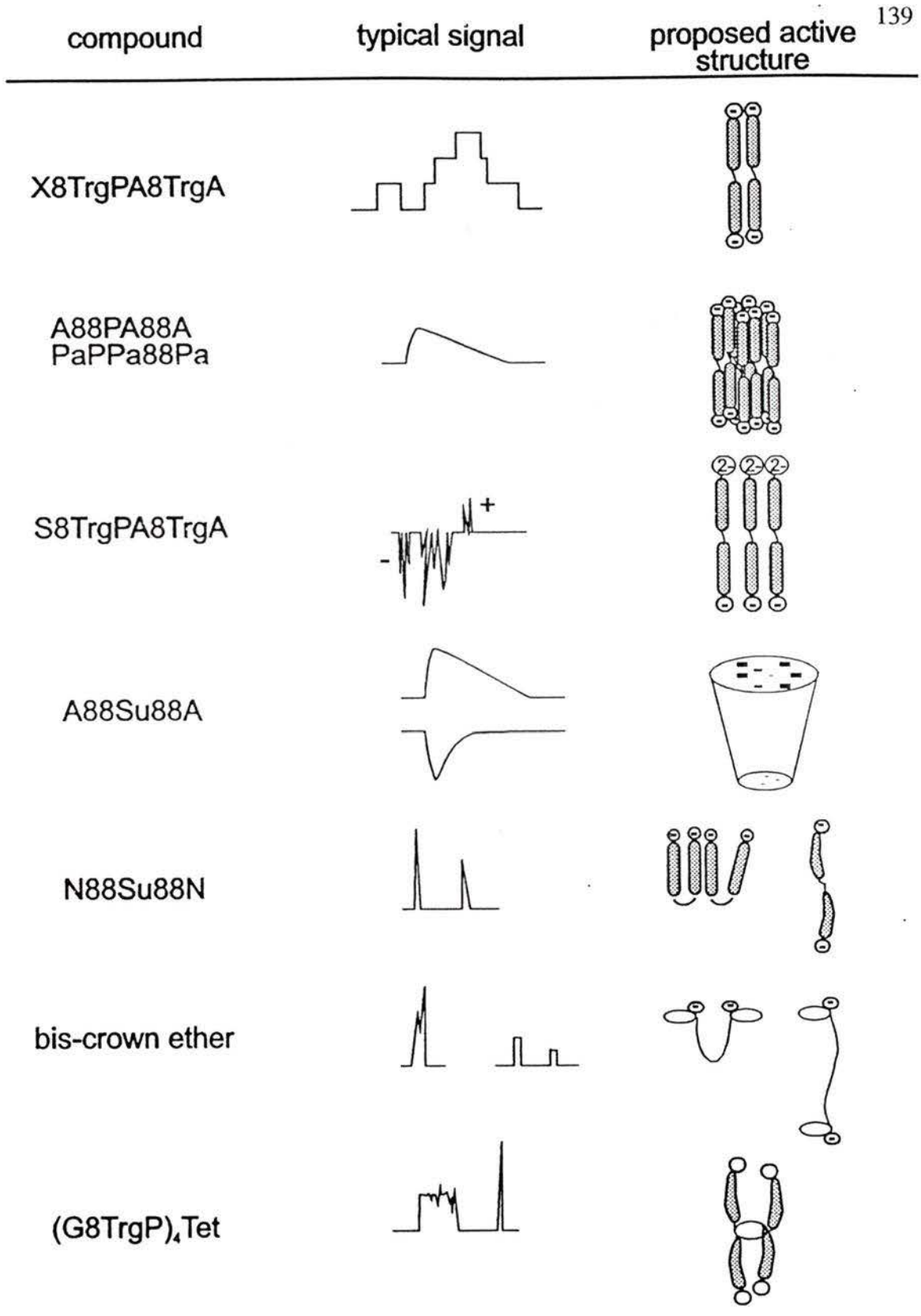

Figure 8.1: Summary of the observed ion transport signals and proposed active structures.

Our results show that control over the insertion and penetration step can lead to alteration of the observed transport behaviour. A flexible structure is required to achieve the U-shaped conformation. The unimolecular transporter $(G8TrgP)_4Tet$ is presumably too rigid to insert into in the bilayer in a non-destructive way. The conformation change from U-shaped to linear has been shown to be also important. This step will obviously be dependent on the transporter length. The size and charge of the head groups will determine whether bilayer penetration is feasible. The dianionic succinate head group of S8TrgPA8TrgA is assumed to remain on the bilayer side of addition due to its high charge. Thus an asymmetric distribution of transmembrane conformations results which leads to voltage gating as shown in Figure 8.1. The positively charged ammonium head group, **N**, presumably does not penetrate the bilayer well. In cases were penetration does occur membrane disruption follows for bola-amphiphiles with two such head groups (N88Su88N).

Reducing the flexibility in the central linker has a profound impact on the change from a U-shaped to an extended conformation as was evident in the activity of A88PA88A and A88Su88A. The structures of these molecules differ by only two atoms in the central linker, i.e. an ester group was replaced by a sulfide bond in A88Su88A. The preferred conformation for the sulfide-linked bola-amphiphile has been calculated to be the U-shaped state while the ester-linked bola-amphiphiles adopt an extended conformation. This leads to an asymmetric distribution of U-shaped transporters in the two bilayer leaflets with only very few linear conformers. The active structures that form from these monomers displayed voltage-gated behaviour.

Other compounds that remain preferentially in the U-shaped conformation induce defects due to the formation of side-to-side dimers. Representative cases were N88Su88N and the bis(crown ether) shown in Figure 8.1.

8.1.3 Aggregation

Except for the presumed unimolecular pore former $(G8TrgP)_4Tet$, all conducting structures presented in this thesis are assumed to be aggregates. Thus, controlling the forces that lead to the stabilization and destabilization of aggregates will lead to control of the observed ion transport mechanism which is reflected in the signal shapes observed (Figure 8.1). The size of aggregates will be limited by head group repulsion, the hydrophilic/hydrophobic balance in the wall units, and the flexibility of the molecule.

An extensive study on the influence of the head group charge and size has been performed on the linear transporters that are based on the 8Trg wall unit. While a singly charged head group does not appear to influence the activity of the aggregate, the introduction of a dianionic head group led to voltage-gated behaviour (chapter 4). For this transporter (S8TrgPA8TrgA) the head group repulsion controls the aggregation behaviour which has been tested *via* the addition of divalent cations and an increase in pH. A similar effect was observed for the bis-crown ether where the head groups are electrostatically and sterically repelling.

The hydrophilic/hydrophobic balance in the structure of the wall units determines whether the aqueous pores are small, of defined stoichiometry, and well structured, or whether larger aggregates of less defined structure and stoichiometry are formed. Thus, all linear bola-amphiphiles that are based on the more hydrophilic wall unit 8Trg exhibit step conductance changes (chapter 3). Conversely, the linear bola-amphiphiles with the more hydrophobic 88 wall unit display a range of activities as discussed in chapter 5.

The overall flexibility of the transporter monomers will also have an influence on the size of the aggregates formed. A monomer that has many conformational degrees of freedom would have to pay more entropy upon aggregation than monomers that are more rigid from the outset. Thus, smaller aggregates may form for more flexible compounds

which was evident in the signals of smaller current amplitude for Pa88PPa88Pa compared to A88PA88A.

It is unfortunate that the compounds investigated do not possess a chromophore. The investigation of the aggregation behaviour of these transporters in the bilayer environment would be extremely interesting. To my knowledge, only one study on the aggregation behaviour and the location of synthetic, non-peptidic ion transporters in vesicles has been performed to date. Gokel *et al.* introduced fluorescent probes in the head group region of tris-macrocyclic ion channels. Dansyl and N-methylindole terminated tris-macrocycles were active transporters in vesicles as evaluated by a ^{23}Na-NMR technique. Fluorescence and fluorescence quenching experiments were consistent with an interfacial location of the head groups. In addition, the transporter appears to be incorporated in the membrane as monomers.[97]

8.1.4 Closing process

For the compounds that gave rise to signals with symmetric opening and closing times, the closing process is presumably the reverse of the aggregation process. An alternative closing process exists for the compounds that display 'sharkfin' signals. In these cases (chapters 5 and 6) a local Donnan potential develops due to the high charge selectivity of the transporters. This potential would eventually be of the same magnitude as the applied transmembrane potential and no net current flux can be observed; note, that at this point we do not know whether the aggregate still persists.

8.2 Voltage-gating

In most synthetic systems that display voltage-gated behaviour, the re-orientation of molecular dipoles in response to the applied transmembrane potential is invoked in the proposed mechanism.[19,34,35,48,83,84] Our results of chapter 3 and 4 indicate, however, that rather than a large molecular dipole moment, it is the introduction of asymmetry into the

mechanism that leads to voltage gating. This can be achieved by the introduction of an asymmetry in the molecular structure which then controls the membrane penetration step as discussed in chapter 4 and reported in the literature for oligo-THF peptides.[52] As shown in chapter 6, it is not required that the asymmetry is located in the structure of the bola-amphiphile itself. Voltage-gated behaviour can also be achieved *via* an unequal distribution of transporter molecules in the two bilayer leaflets. Therefore, an asymmetric step in the mechanism appears to be a requirement for voltage-gating.

8.3 Ion selectivity

It is not immediately obvious why aqueous pores that are assembled from a number of monomers should exhibit any selectivity for ions. However, the results presented in this thesis demonstrate that charge selectivity can be achieved by two means. Choosing predominantly anionic head groups will lead to an attraction of counterions to the channel mouth while anions will be repelled. Therefore, transporters with negatively charged head groups should be cation selective, which was observed in all cases investigated. In addition, hydration of the monomeric wall units will control the total amount of water that can be stabilized in the pore lumen. For a constant radius, anions are more highly hydrated than cations. Therefore anions would be more strongly affected than cations by a 'drier' pore. A greater cation:anion selectivity was indeed observed for the compounds with the 88 wall units than for the compounds with the more highly hydrated 8Trg wall unit. Conversely, the selectivity between cations was modest in all cases.

8.4 Conclusions

It has been shown that the bilayer clamp technique is a powerful tool for the investigation of ion transport across lipid bilayer membranes. Transport behaviour that has not been reported previously was thus observed (chapters 5 and 6). Artificial transporters possess mechanistic avenues that are apparently not available to natural ion channel proteins. However, the large experimental expenditure involved in bilayer clamp experiments renders them unsuitable for extensive structure-activity studies. Vesicle

experiments on the other hand are well suited for this kind of survey. However, one should always be aware of the differences between the two methods and use them to compliment each other. Several times throughout this thesis it has been pointed out that different results were observed for the two experiments. The observed ion selectivity was generally different, and the apparent kinetic order that was determined by pH-stat experiments did not match the proposed mechanism in planar bilayer membrane in all cases. These differences are not specific for the pH-stat vesicle assay used in our group, but were also observed for a dynamic ^{23}Na -NMR method employed by Gokel and co-workers.[56]

The bilayer clamp technique can not only be used as a diagnostic tool for the transport mechanism of ion channels but it can also be used as a controlling element. Thus, control of the ion conducting properties of a transmembrane pore *via* the applied transmembrane potential was demonstrated for two compounds, S8TrgPA8TrgA and A88Su88A. We have shown that the overall transport behaviour can be controlled by influencing specific steps in the mechanism *via* small structural alterations of the ion transporters.

Potential applications based on the elements of this dissertation are in the construction of highly sensitive biosensors. The advantage of incorporating ion channels in these devices is the high amplification of a single molecular interaction. Thus, the flux of 10^7 ions s^{-1} can be achieved as the result of a single transport event. A biosensor based on gramicidin has recently been reported.[98] The creation of a stable bioamplifier with high gain will also have implications for the development of molecular electronic devices.[99]

Appendix 1

Below the data acquisition part of the ai.VB program is shown:

```
Private Sub SR_AI_BufferFilled(task As Integer, device As Integer, subsystem As Integer, mode As Integer, bufindex As Integer)

'This DriverLINX event procedure can be called recursively during buffer
'processing and plotting due to the multi-tasking,event-driven nature of Windows.
'The "UpdatingGraph" flag prevents recursion from causing stack overflow
'because DoEvents would otherwise be called again before control had returned.
'Buffer overwrite will occur if time to convert exceeds time to fill buffer.

If UpdatingGraph Then Exit Sub
   UpdatingGraph = True    'ok to process data while UpdatingGraph = True

dummy = VBArrayBufferConvert(SR_AI, bufindex, 0, NumSamples, VBDataArray2(0), DL_tSINGLE, 0, 0)

dummy = VBArrayBufferXfer(SR_AI, bufindex, VBDataArray1(0), DL_BufferToVBArray)

For buf_fill_index = 0 To NumSamples - 1
 If VBDataArray1(buf_fill_index) And &O1 Then
   'tag
   If changestate = -1 Then
    changestate = buf_fill_index
    bufferstart = buffnum
   End If
 ElseIf changestate > -1 Then

     acalc = CSng((CSng(buffnum) - CSng(bufferstart)) * CSng(NumSamples) + CSng(buf_fill_index) - CSng(changestate)) / CSng(SampleRate)

     If buf_fill_index > 1 Then
```

```
    If VBDataArray2(buf_fill_index - 1) > VBDataArray2(buf_fill_index - 2) Then
      bcalc = VBDataArray2(buf_fill_index - 1)
    Else
      bcalc = VBDataArray2(buf_fill_index - 2)
    End If
  Else
    bcalc = bpre
  End If

  '3. elapsed time is calculated as:
  ccalc = (CSng(buffnum) * CSng(NumSamples) + CSng(buf_fill_index)) / CSng(SampleRate)

  '4. time since last completion
  dcalc = ccalc - precalc
  precalc = ccalc

  Print #1, drindex, CSng(CLng(ccalc * 10000)) / 10#, CSng(CLng(acalc * 10000)) / 10#,
CSng(CLng(bcalc * 10000)) / 10000#, CSng(CLng(dcalc * 10000)) / 10#
  drindex = drindex + 1
  changestate = -1
 End If


Next buf_fill_index
If VBDataArray2(NumSamples - 1) > VBDataArray2(NumSamples - 2) Then
 bpre = VBDataArray2(NumSamples - 1)
Else
 bpre = VBDataArray2(NumSamples - 2)
End If

buffnum = (buffnum + 1) Mod 10000

DoEvents   'get unprocessed Windows event messages (mouse or keyboard)
UpdatingGraph = False      ' next buffer may now be processed
End Sub
```

Appendix 2

List of experimentally determined reversal potentials.

8TrgPA8TrgA:

1 M NaCl:1M CsCl	89 ± 0.7 mV
1 M NaCl: 1 M KCl	81.2 ± 0.2 mV
0.1 M KCl:0.5 M KCl	31.1 ± 3.4 mV

A8TrgPA8TrgA:

1 M NaCl:1M CsCl	54.4 ± 1.1 mV
0.1 M KCl:0.5 M KCl	36.8 ± 0.6 mV

N8TrgPA8TrgA:

1 M CsCl:1M NaCl	-44 ± 2 mV
1 M KCl: 1 M NaCl	-21 ± 2 mV
0.1 M KCl:0.5 M KCl	31.1 ± 0.6 mV

G8TrgPA8TrgA:

1 M NaCl:1M CsCl	48 ± 2 mV
1 M NaCl: 1 M KCl	35 ± 2 mV
0.1 M KCl:0.5 M KCl	30 ± 6 mV

S8TrgPA8TrgA:

0.5 M KCl:0.1 M KCl	-31 ± 2 mV

A88PA88A;

1 M KCl:1M LiCl	$0 > V_{rev} > -14$ mV
1 M KCl: 1 M CsCl	$0 > V_{rev} > -20$ mV
0.5 M KCl:0.1 M KCl*	-50 ± 2 mV
0.5 M LiCl:0.1 M LiCl*	-56 mV

Pa88PPA88Pa:

0.5 M KCl:0.1 M KCl*	-32 ± 4 mV

* Junction potentials were not stable over the course of the experiment

Activity coefficients used for the calculation of reversal potentials:

salt	activity coefficient
0.1 M KCl	0.770
0.5 M KCl	0.666
1 M KCl	0.604
1 M NaCl	0.657
0.1 M CsCl	0.756
0.5 M CsCl	0.606
1 M CsCl	0.544
0.1 M LiCl	0.790
0.5 M LiCl	0.740
1 M LiCl	0.774

References

1. L. Stryer, *Biochemistry*, W.H. Freeman and Company, New York, (1988).

2. H. Luecke, B. T. Chang, W. S. Mailliard, D. D. Schlaepfer and H. T. Haigler, *Nature*, (1995), **378**, 512.

3. G. McDermott, S. M. Prince, A. A. Freer, A. M. Hawthornthwaite-Lawless, M. Z. Papiz, R. J. Cogdell and N. W. Isaacs, *Nature*, (1995), **374**, 517.

4. B. Kadenbach, *Ang. Chem. Int. Ed. Engl.*, (1995), **34**, 2635.

5. D. Xia, C.-A. Yu, H. Kim, J.-Z. Xia, A. M. Kachurin, L. Zhang, L. Yu and J. Deisenhofer, *Science*, (1997), **277**, 60.

6. K. A. Ketchum and C. W. Slayman, *FEBS Lett.*, (1996), **378**, 19.

7. C. L. S. Grossou, S. C. Cannon and J. F. Gusella, *Mol. Brain Res.*, (1996), **42**, 222.

8. P. J. G. Kormelink and W. H. M. L. Luyten, *FEBS Lett.*, (1997), **400**, 309.

9. P. Mueller and D. O. Rudin, *Nature*, (1968), **217**, 713.

10. B. Hille, *Ionic Channels of Excitable Membranes*, Sinauer Assoc., Sunderland, (1984).

11. G. R. Marshall and D. D. Beusen, In *'Advances in chemistry series: Biomembrane Electrochemistry'*, Eds.: M. Blank, I. Vodyanoy, American Chemical Society, Washington, D.C., (1994), **10**, 259.

12. K. S. Akerfeldt, P. K. Kienker, J. D. Lear and W. F. Degrado, In *'Comprehensive Supramolecular Chemistry'*, Ed. D. N. Rheinhoudt, Elsevier Science Ltd., Oxford, (1996), **10**, 659.

13. E. Bamberg and P. Lauger, *J. Membr. Biol.,* (1977), **35**, 351.

14. B. Bechinger, *J. Membr. Biol.,* (1997), **156**, 197.

15. T. M. Fyles and W. F. Van Straaten-Nijenhuis, In *'Comprehensive Supramolecular Chemistry'*, Ed. D. N. Rheinhoudt, Elsevier Science Ltd., Oxford, (1996), **10**, 53.

16. G. W. Gokel and O. Murillo, *Acc. Chem. Res.,* (1996), **29**, 425.

17. R. R. C. New, *Liposomes: a Practical Approach*, Oxford University Press, Oxford, England, (1991).

18. G. A. Woolley and B. A. Wallace, *J. Membr. Biol.,* (1992), **129**, 109.

19. M. S. P. Sansom, *Prog. Biophys. Molec. Biol.,* (1991), **55**, 139.

20. A. Finkelstein and O. S. Andersen, *J. Membr. Biol.*, (1981), **59**, 155.

21. V. B. Myers and D. A. Haydon, *Biochim. Biophys. Acta,* (1972), **274**, 313.

22. G. Eisenmann and R. Horn, *J. Membr. Biol.,* (1983), **76**, 197.

23. R. E. Koeppe II, J.-L. Mazet and O. S. Andersen, *Biochemistry,* (1990), **29**, 512.

24. E. W. B. Russel, L. B. Weiss, F. I. Navetta, R. E. Koeppe II and O. S. Andersen, *Biophys. J.,* (1986), **49**, 673.

25. R. E. Koeppe II and O. S. Andersen, *Annual Review of Biophysics and Biomolecular Structure,* (1996), **25**, 231.

26. G. A. Woolley, A. S. I. Jaikaran, Z. Zhang and S. Peng, *J. Am. Chem. Soc.,* (1995), **117**, 4448.

27. D. C. J. Jaikaran and G. A. Woolley, *J. Phys. Chem.,* (1995), **99**, 13352.

28. L. Lien, D. C. J. Jaikaran, Z. Zhang and G. A. Woolley, *J. Am. Chem. Soc.*, (1996), **118**, 12222.

29. D. S. Cafiso, *Annual Review of Biophysics and Biomolecular Structure,* (1994), **23**, 141.

30. M. A. Montal, M. S. Montal and J. M. Tomich, *Proc. Natl. Acad. Sci. USA,* (1990), **87**, 6929.

31. A. Grove, M. Mutter, J. E. Rivier and M. Montal, *J. Am. Chem. Soc.*, (1993), **115**, 5919.

32. M. Montal, M. S. Montal and J. M. Tomich, *Soc. Neurosci. Abstr.*, (1989), **15**, 970.

33. K. S. Akerfeld, J. D. Lear, Z. R. Wasserman, L. A. Chung and W. F. DeGrado, *Acc. Chem. Res.*, (1993), **26**, 191.

34. J. D. Lear, Z. R. Wasserman and W. F. DeGrado, *Science,* (1988), **240**, 1177.

35. J. D. Lear, J. P. Schneider, P. K. Kienker and W. F. DeGrado, *J. Am. Chem. Soc.*, (1997), **119**, 3212.

36. S. C. Hartsel, C. Hatch and W. Ayenew, *Journal of Liposome Research.* (1993), **3**, 377.
review.

37. M. E. Kleinberg and A. Finkelstein, *J. Membr. Biol.*, (1984), **80**.

38. M. P. Borisova, R. A. Brutyan and L. N. Ermishkin, *J. Membr. Biol.*, (1986), **90**, 13.

39. R. A. Brutyan and P. McPhie, *J. Gen. Physiol.*, (1996), **107**, 69.

40. D. W. Urry, *Top. Curr. Chem.*, (1985), **128**, 175.

41. M. T. Tosteson and D. C. Tosteson, *Biophys. J.*, (1981), **36**, 109.

42. M. A. J. Pregel, L. Jullien, J. Canceill, L. Lacombe and J.-M. A. Lehn,*J. Chem. Soc., Perkin Transactions,* (1995), **2**, 417.

43. M. J. Pregel, L. Jullien and J.-M. Lehn,*Ang. Chem. Int. Ed. Engl.*, (1992), **31**, 1637.

44. N. Jayasuriya, S. Bosak and S. L. Regen, *J. Am. Chem. Soc.*, (1990), **112**, 5844.

45. E. Stadler, P. Dedek, K. Yamashita and S. L. Regen, *J. Am. Chem. Soc.*, (1994), **116**, 6677.

46. Y. Tanaka, Y. Kobuke and M. Sokabe, *Ang. Chem. Int. Ed. Engl.*, (1995), **34**, 693.

47. Y. Kobuke, K. Ueda and M. Sokabe, *J. Am. Chem. Soc.*, (1992), **114**, 7618.

48. Y. Kobuke, K. Ueda and M. Sokabe, *Chem. Lett.*, (1995), 435.

49. D. Seebach, A. Brunner, M. H. Burger, R. N. Reusch and L. L. Bramble, *Helv. Chim. Acta*, (1996), **79**, 507.

50. J.-C. Meillon and N. Voyer,*Ang. Chem. Int. Ed. Engl.*, (1997), **36**, 967.

51. S. Cincotti, M. Parodi and M. A. Storace, *Journal of Electrostatics*, (1996), **37**, 95.

52. H. Wagner, K. Harms, U. Koert, S. Meder and G. Boheim, *Ang. Chem. Int. Ed. Engl.*, (1996), **35**, 2643.

53. M. R. Ghadiri, J. R. Granja and L. K. Buehler,*Nature*, (1994), **369**, 301.

54. O. Murillo, S. Watanabe, A. Nakano and G. W. Gokel, *J. Am. Chem. Soc.*, (1995), **117**, 7665.

55. A. Nakano, Q. Xie, J. V. Mallen, L. Echegoyen and G. W. Gokel, *J. Am. Chem. Soc.*, (1990), **112**, 1287.

56. O. Murillo, I. Suzuki, E. Abel, C. L. Murray, E. S. Meadows, T. Jin and G. W. Gokel, *J. Am. Chem. Soc.*, (1997), **119**, 5540.

57. E. Abel, E. S. Meadows, I. Suzuki, T. Jin and G. W. Gokel, *J. Chem. Soc. Chem. Comm.*, (1997), 1145.

58. T. M. Fyles, T. D. James and K. C. Kaye, *J. Am. Chem. Soc.*, (1993), **115**, 12315.

59. T. M. Fyles, T. D. James, A. Pryhitka and M. Zojaji, *J. Org. Chem.*, (1993), **58**, 7456.

60. T. D. James, *Ph.D. Dissertation*, University of Victoria, (1991).

61. T. M. Fyles, T. D. James and K. C. Kaye, *Can. J. Chem.*, (1990), **68**, 976.

62. T. M. Fyles, K. C. Kaye, A. Pryhitka, J. Tweddell and M. Zojaji, *Supramolecular Chemistry*, (1993), **3**, 197.

63. G. G. Cross, T. M. Fyles, T. D. James and M. Zojaji, *Synlett*, (1993), 449.

64. X. Zhou, *Ph.D. Dissertation*, University of Victoria, (1997).

65. T. M. Fyles and B. Zeng, *J. Chem. Soc. Chem. Comm.*, (1996), 2295.

66. S. H. White, In '*Ion Channel Reconstitution*', Ed. C. Miller, plenum Press, New York, (1986), 3.

67. D. Colquhoun and F. J. Sigworth, In '*Single-Channel Recording*', Eds. B. Sakmann, E. Neher, Plenum Press, New York, (1983), 191.

68. F. Jahnig and K. Dornmair, In '*Biologically Inspired Physics*', Ed. L. Peliti, Plenum Press, New York, (1991), 149.

69. P. Labarca, J. Lindstrom and M. Montal, *J. Gen. Physiol.*, (1984), **83**, 473.

70. K. A. F. Gration, R. L. Ramsey and P. N. R. Usherwood, In '*Single-Channel Recording*', Eds. B. Sakmann, E. Neher, Plenum Press, New York, (1983), 377.

71. D. Colquhoun and A. G. Hawkes, In '*Single-Channel Recording*', Eds. B. Sakmann, E. Neher, Plenum Press, New York, (1983), 135.

72. T. M. Fyles, D. Loock, W. F. Van Straaten-Nijenhuis and X. Zhou, *J. Org. Chem.*, (1996), **61**, 8866.

73. W. F. Nijenhuis, (1994) personal communication.

74. M. Hervé, B. Cybulska and C. M. Gary-Bobo, *Europ. Biophysics J.*, (1985), **12**, 121.

75. R. A. Moss and J.-M. Li, *J. Am. Chem. Soc.*, (1992), **114**, 9227.

76. R. A. Moss, G. Li and J.-M. Li, *J. Am. Chem. Soc.*, (1994), **116**, 805.

77. R. A. Moss, T. Fukita and Y. Okumura, *Langmuir*, (1991), **7**, 2415.

78. Y. Liu and S. L. Regen, *J. Am. Chem. Soc.*, (1993), **115**, 708.

79. S. Konig and E. Sackmann, *Curr. Opin. Coll. & Interf. Sci.*, (1996), **1**, 78.

80. S. J. Ludtke, K. He and H. Hung, *Biochemistry*, (1995), **34**, 16764.

81. B. Bechinger, *J. Mol. Biol.*, (1996), **263**, 768.

82. D. Chen, J. A. Lear and B. Eisenberg, *Biophys. J.*, (1997), **72**, 97.

83. A. G. Woolley, R. M. Epand, I. D. Kerr, M. S. P. Sansom and B. A. Wallace, *Biochemistry*, (1994), **33**, 6850.

84. A. Matsubara, A. Asami, A. Akagi and A. Nishino,*J. Chem. Soc. Chem. Comm.*, (1996), 2069.

85. O. S. Andersen, *Biophys. J.*, (1983), **41**, 135.

86. *CRC Handbook of Chemistry and Physics*, 46th Ed., Eds. R. D. Weast, S. M. Selby, The Chemical Rubber Co., Cleveland, Ohio, (1964).

87. C. Hansch, A. Leo, In '*Substituent Constants for Correlation Analysis in Chemistry and Biology*', Wiley-Interscience, New York, (1979).

88. *Ionic Hydration in Chemistry and Biophysics*, Elsevier Scientific Publishing company, Amsterdam, 1981.

89. F. Bezanilla and E. Stefani,*Annual Review of Biophysics and Biomolecular Structure*, (1994), **23**, 819.

90. M. Blank, In '*Advances in chemistry series: Biomembrane Electrochemistry*', Eds.: M. Blank, I. Vodyanoy, American Chemical Society, Washington, D.C., (1994), **10**, 429.

91. S. Oiki, R. E. Koeppe II and O. S. Andersen, *Proc. Natl. Acad. Sci. USA*, (1995), **92**, 2121.

92. G. Menestrina, K.-P. Voges, G. Jung and G. Boheim, *J. Membr. Biol.*, (1986), **93**, 111.

93. V. E. Carmichael, P. J. Dutton, T. M. Fyles, T. D. James, J. A. Swan and M. Zojaji, *J. Am. Chem. Soc.*, (1989), **111**, 767.

94. S. L. Regen, N. Jayasuria and W. Fabionowski,*Biochem. Biophys. Res. Commun.*, (1989), **159** , 566.

95. B. Zeng, *Ph.D. Dissertation*, University of Victoria, (1997).

96. T. M. Fyles, D. Heberle, B. Zeng and X. Zhou, *Chemically Modified Surfaces: Recent Developments*, Eds. J. J. Pesek, M. T. Matyska, R. R. Abuelafyia, The Royal Society of Chemistry, (1996), 125.

97. E. Abel, G. E. M. Maguire, E. S. Meadows, O. Murillo and G. W. Gokel, *In Press*, (1997).

98. B. A. Cornell, V. L. B. Braach-Maksvytis, L. G. King, P. D. J. Osman, B. Raguse, L. Wieczorek and R. J. Pace, *Nature*, (1997), **387**, 580.

99. A. P. F. Turner, *Nature*, (1997), **387**, 555.

VITA

Surname: Loock Given Names: Daniela

Nee: Heberle

Place of Birth: Darmstadt, Germany

Educational Institutions Attended:

University of Victoria 1994 to 1997

Technische Hochschule Darmstadt

(Technical University of Darmstadt) 1987 to 1993

Degrees Awarded:

Diplom-Ingenieurin Technische Hochschule Darmstadt 1993

Honours and Awards:

Dr. E. And Mrs. M. Von Rudloff Award 1996

Publications:

Synthetic ion transporters in bilayer membranes

T.M. Fyles, D. Heberle, W.F. Van Straaten-Nijenhuis and X. Zhou; Supramolecular Chemistry (1995) **6**, 71.

Pores Formed by Bis-macrocyclic Bola-amphiphiles in Vesicle and Planar Bilayer Membranes

T.M. Fyles, D. Loock, W.F. Van Straaten-Nijenhuis and X. Zhou; J. Organic Chemistry (1996) **61**, 8866.

A Voltage-gated Ion Channel Based on a Bis-macrocyclic Bolaamphiphile

T.M. Fyles, D. Loock, and X. Zhou; submitted

Bolaamphiphiles and the Creation of Pores in Bilayer Membranes

T.M. Fyles, D. Heberle, B. Zeng, and X.Zhou; In JJ. Pesek, M.T. Matyska, R.R. Abuelafyia (Eds.); 'Chemically Modified Surfaces: recent Developments', The Royal Society of Chemistry 1996, 125.

Conference Presentations:

T.M. Fyles, D. Heberle, *Single-channel activity of bis-macrocyclic bola-amphiphiles*, 1995 International Chemical Congress of Pacific Basin Societies, Honolulu, Hawaii, December 17-22, 1995.

T.M. Fyles, D. Loock, *Single-channel activity of bis-macrocyclic bola-amphiphiles*, Gordon Research Conference 'Chemistry at Interfaces', Meriden, N.H., July 19-24, 1996.

PARTIAL COPYRIGHT LICENSE

I hereby grant the right to lend my dissertation to users of the University of Victoria Library, and to make single copies only for such users or in response to a request from the Library of any other university, or similar institution, on its behalf or for one of its users. I further agree that permission for extensive copying of this thesis for scholarly purposes may be granted by me or a member of the University designated by me. It is understood that copying or publication of this thesis for financial gain shall not be allowed without my written permission.

Title of Dissertation:

Ion Transport Mechanisms of Bola-Amphiphiles in Planar Bilayer Membranes

Author 

Daniela Loock

September, 1997